

STABILITY OF SINGLE-LAYER CUBES ON LEE-SIDE OF BREAKWATERS

Quantative Research on the Stability of a Single Cubic Armour Layer on the Lee-side of
Breakwaters using a Wave Overtopping Simulator

Master's Thesis
Author: N.A.T. Drouen
Date: March 7, 2018



Stability of Single-layer Cubes on Lee-side of Breakwaters

Quantative Research on the Stability of a Single Cubic Armour Layer on the
Lee-side of Breakwaters using a Wave Overtopping Simulator

by
Niels Drouen
Student number: 4064216

Graduation Committee

Prof. Dr. Ir. W.S.J. Uijttewaal	Delft University of Technology
Dr. Ir. B. Hofland	Delft University of Technology
Ing. C. Kuiper	Delft University of Technology
Dr. Ir. M.R.A. van Gent	Deltares
Ir. B. van den Berg	Witteveen+Bos

A thesis presented for the degree of
Master of Science in Coastal Engineering



Faculty of Civil Engineering and Geosciences
Department of Hydraulic Engineering
Delft University of Technology

Preface

This research contributes to a longer line of studies that have been done at the Delft University of Technology in combination with engineering firm Witteveen+Bos. Preceding this research, two students have already written reports on the stability of a single armour layer of cubes on the lee-side of breakwaters. The first was research was done by Hellinga (2016) and was titled: *Stability of Single Layer Cubes on Breakwater Rear Slopes*. Subsequently Rietmeijer (2017) wrote a report titled: *Rear-Slope Revetment Stability Approached by the Wave Overtopping Simulator*. Both reports have been very helpful for the current research. The long-term goal of the subject is to develop a design formula which tells engineers the dimensions of cubes that need to be placed on the rear-slope of a breakwater, given a certain sea state. Ideally the design formula should be linked with the front-slope of a breakwater and result in a rule of thumb which relates the dimensions of the outer-slope armour layer to the dimensions of the inner-slope armour layer.

During the writing of this thesis I was guided by my graduation committee: Wim Uijtewaald (Professor at the Delft University of Technology), Marcel van Gent (Head of department Coastal Structures & Waves at Deltares), Bas Hofland (Assistant Professor of Coastal Structures at the Delft University of Technology), Coen Kuiper (Part-time lecturer at the Delft University of Technology) and Bert van den Berg (Project Engineer at Witteveen+Bos). I would like to thank them for their useful input during the meetings.

I would like to thank the employees of the Fluid Mechanics Laboratory for their help during the build of the test set-up. Also all the employees at Witteveen+Bos and especially the group Kust, Rivieren en Land-aanwinning for their interest and ideas. And my family for their support during my studies and the writing of this report.

Niels Drouen, February 26, 2018

Summary

Breakwaters are hydraulic structures used to create calm and steady environments for moored ships in harbors. They dampen the wave by dissipating the energy through wave breaking. Most studies of breakwaters have only been carried out on the seaward slope of the structure. However, few have conducted research on the landward-, inner-, slope of breakwaters. The existing accounts are all empirical design formulae, commonly denoted as applicable for conceptual design. Improvement of the design of the armour layer of the inner slope leads to economical advantages. This research focused on three main goals: (1) Presenting a theoretical methodology for the waves tested, (2) It verified the Wave Overtopping Simulator as built by Rietmeijer (2017) and (3) Performed stability tests for the inner slope by conducting physical model tests in the Fluid Mechanics Laboratory of Delft University of Technology.

The first goal of this research has been to develop a theoretical approach to overtopping waves in combination with a simulator. This has been done by linking certain storm characteristics, being the significant wave height H_s and peak period T_p to wave characteristics; water volume, water layer thickness and the front velocity of the water body. These three combined lead to an impinging wave on the rear slope causing damage. Subsequently the storms have been filtered to only select the highest percentage of waves, since these were marked as extreme storm conditions. This resulted in different significant wave heights which were tested.

To verify the Wave Overtopping Simulator tests have been performed and specific elements have been measured and analyzed. This has resulted in relationships between theoretical wave characteristics and simulator settings. The relationships are the required water level in the reservoir to obtain a certain front velocity of the water body. To adjust the water layer thickness the valve settings have been changed. For a specific volume the overtopping period has been altered. These three elements have been measured using wave gauges and a high speed camera after which the data was carefully analyzed.

The stability tests have been executed using a model of a breakwater in the Fluid Mechanics Laboratory of Delft University of Technology. Results of the preparatory calculations together with results obtained from former research have led to the design of the test set-up. A single armour layer of 20 mm cubes with an porosity of nearly 40% was built with an unfixed toe. This configuration was tested with increasing storm intensities until failure. Subsequently the damage has been measured using photo camera's and laser technique.

This research has successfully verified the wave overtopping simulator by measuring individual waves and their specific discharge, water layer thickness and velocity. These measurements have been compared to an other method, using a high speed camera. The found values have been checked with found literature and it has been concluded that the Wave Overtopping Simulator together with the test set-up as built in the Fluid Mechanics Laboratory is useful for this research. By measuring the displacement of cubes by means of video camera and laser technique, the research has been able to identify damage and failure cases. The horizontal displacement has been divided into several classes ranging from settlement of the armour layer, to instant failure. In addition, this research has presented a possible link between the stability of a single cubic armour layer and the number of rows beneath the waterline.

Contents

1	Introduction	8
1.1	Problem description	8
1.2	Methodology	9
1.2.1	Theoretical approach: characteristics of sea states	9
1.2.2	Verification of Wave Overtopping Simulator	9
1.2.3	Stability research	9
1.3	Outline of report	9
2	Theoretical Approach	11
2.1	Breakwater Crest	14
2.2	Input in model	15
2.3	Wave calculations	16
3	Verification of the Wave Overtopping Simulator	21
3.1	Design of Wave Overtopping Simulator	21
3.1.1	Plunge machine van Dijk (2001)	22
3.1.2	Dutch Overtopping Simulator by van der Meer et al. (2006)	23
3.2	Results of previous research	24
3.3	Methodology	25
3.4	Results	29
3.4.1	High-speed video measurements	29
3.4.2	Wave gauge measurements	33
3.4.3	Combined results of the two measuring methods	38
3.5	Conclusions	39
3.5.1	High-speed video measurements	39
3.5.2	Wave gauge measurements	40
3.5.3	Conclusion on verification of Wave Overtopping Simulator	40
4	Stability research	42
4.1	Methodology	42
4.2	Breakwater geometry	43
4.3	Instruments and measurements	45
4.4	Recommendations from previous research	48
4.5	Scaling laws	49
4.6	Test Program Stability Research	51
4.6.1	Fixed Toe	51
4.6.2	Non-fixed Toe	51
4.6.3	Crest Freeboard	52
4.7	Data Analysis	52
4.7.1	Wave characteristics	52
4.7.2	Rear slope damage	53
4.8	Results	53
4.8.1	Fixed toe	53
4.8.2	Non-Fixed Toe	55
4.8.3	Crest Freeboard	58
4.9	Conclusions	60
4.9.1	Fixed Toe	60

4.9.2	Non-fixed Toe	61
4.9.3	Crest Freeboard	61
5	Conclusions	63
5.1	Theoretical Approach	63
5.2	Verification of the Wave Overtopping Simulator	63
5.3	Stability Research	63
5.4	Overall Conclusion	64
6	Recommendations	66
A	Theoretical Approach	70
A.1	Crest freeboard $R_c = 0,10\text{m}$	70
A.2	Crest freeboard $R_c = 0,20\text{m}$	71
B	Results of Verification Wave Overtopping Simulator	73
B.1	Wave gauge measurements	73
B.2	Video measurements	74
C	Technical drawings WOS	77
D	Stability research	80
D.1	Overview test series	80
D.2	Failure overviews per test	82
D.3	Transect side-views	83
E	Matlab codes	85
E.1	Wave gauge meters	85
E.2	Framestack plotting	87
E.3	3d profile plotter	87
F	Specifications of Linear Motor	90

List of Figures

2.1	Diagram of the theoretical approach	11
2.2	Overview of used parameters	12
2.3	Two-parameter Weibull distribution for crest height of 15 cm with increasing wave heights	18
3.1	Sketch of experimental set-up used by van Dijk (2001)	22
3.2	Experimental set-up van Dijk (2001) as built.	22
3.3	Discretization of the two parameter Weibull distribution of a storm. van der Meer et al. (2006)	23
3.4	Calibration set-up as built by van der Meer et al. (2006)	24
3.5	Discharge in time	25
3.6	Velocity in time	25
3.7	Placement of simulator in a water basin	26
3.8	Idealized simulated overtopping flow parameters in time	27
3.9	Row of pixels observed	29
3.10	Frame stack of 100% coverage, 100mm opening and 30cm head difference.	30
3.11	Frame stack of 50% coverage, 100mm opening and 30cm head difference.	31
3.12	Zoom-in on the front velocity of the overtopping wave event over the rest	31
3.16	Overview of results obtained with wave gauges. 50% coverage, valve opening of 100mm and reservoir level of 30cm	34
3.17	Overview of results obtained with wave gauges. 100% coverage, valve opening of 100mm and reservoir level of 30cm	35
3.18	Measured wave steepness compared with theoretical wave steepness	36
3.21	50% and 100% coverage results of wave gauges combined	38
3.22	Velocity results of Video Analysis (VA) and Wave Gauges (WG) for both 50% and 100% coverage.	39
4.1	Design of the test set-up as built in the Fluid Mechanics Laboratory of Delft University of Technology	43
4.2	Set-up as built in Waterlab	44
4.3	Transect of breakwater configuration, Rietmeijer (2017)	45
4.4	Transects made of a river bed at 0 hours and after 96 hours of flow	47
4.5	Difference for several time intervals of one transect	47
4.6	Positioning of measuring instruments	48
4.7	2 degrees of freedom of the cubes	53
4.8	Test set-up built with a fixed toe	54
4.9	Photo's of the hollow space under the armour layer of the configuration with a fixed toe	54
4.10	Example A	55
4.11	Example B	55
4.12	Analysis of failure R30C15_43	56
4.13	Analysis of failure R30C15_43, before and after storm	57
4.14	Analysis of R30C15_39, after same storm conditions as figure 4.13 during test R30C15_43	57
4.15	Overview of the correlation between dimensionless stability parameter and number of rows beneath the waterline	58
4.16	Settlement of the slope with a freeboard of 10 cm quantified	58
4.17	Settlement of the slope with a freeboard of 15 cm quantified	59

4.18	Stability parameter over settlement observed	59
4.19	Overview of the relation between dimensionless stability parameter and the dimensionless crest height	60
A.1	Two-parameter Weibull distribution for crest height of 10 cm with increasing wave heights	70
A.2	Two-parameter Weibull distribution for crest height of 20 cm with increasing wave heights	71
D.1	15 rows beneath water line	82
D.2	17 rows beneath waterline	82
D.3	11 rows beneath the waterline	82
D.4	Test R30C15_34 and 35. Configuration with 15 rows beneath the water line	83
D.5	Test R30C15_36, 37 and 38. Configuration with 15 rows beneath the water line . .	84

List of Tables

2.1	Explanation parameters as used by Schüttrumpf and Oumeraci (2005)	14
2.2	Overview of studies concerning the development of the wave tongue, Rietmeijer (2017)	14
2.3	Important parameters for research	16
2.4	Overview of the wave groups which correspond to storm conditions for $R_c = 15$ cm	20
3.1	Overview of studies concerning the development of the wave tongue, Rietmeijer (2017)	28
4.1	Overview of the wave groups which correspond to storm conditions for $R_c = 15$ cm	51
4.2	Overview of the wave groups which correspond to storm conditions for $R_c = 10$ cm	51
4.3	Overview of the wave groups which correspond to storm conditions for $R_c = 20$ cm	51
4.4	Wave series applied for $R_c = 15$ cm	52
A.1	Overview of the wave groups which correspond to storm conditions for $R_c = 10$ cm	71
A.2	Overview of the wave groups which correspond to storm conditions for $R_c = 20$ cm	72
B.1	hres = 30 cm	73
B.2	hres = 40 cm	73
B.3	hres = 50 cm	73
B.4	hres = 60 cm	74
B.5	hres = 70 cm	74
B.6	Porosity of 50%	75
B.7	Porosity of 0%	76
D.1	Overview of dimensionless stability parameters at which failure occurs	81

Chapter 1

Introduction

1.1 Problem description

A breakwater is an hydraulic structure which is used all over the world to create a calm and safe environment for ships in harbours and to minimize sand infiltration in ports. This is done by dampening waves created offshore either by wind or by storm. Different types of breakwaters exist and they can be categorized into three main groups being: Loose grains, coherent materials and impervious. In this research a combination of the first and second group is used and the breakwater consists of a rubble core with a protective outer layer. For this outer layer several options are available such as Xbloccs, Accropodes, Tetrapods and concrete cubes. This report is specifically interested in the stability of a single layer of cubes as an armour layer of a breakwater. Cubes are chosen due to their simple geometry. Construction of the cubes can happen on-site and does not require certified companies to deliver formworks. The terms inner- or rear-slope refer to the landward side of the construction.

Waves created offshore hit the outer slope of the breakwater. The energy of these waves is dissipated by wave breaking and so they are dampened. A combination of structure slope and wave steepness gives a certain type of wave breaking. After breaking, the waves '*climb*' up the slope in a process called 'run-up'. When the significant wave height of the waves increases, so does the run-up until it is higher than the crest height of the structure. In this case a volume of water will go over the crest and hit the rear-slope. This is called wave overtopping and it is an essential part of this research.

Numerous empirical formulae have been developed as design guidelines for the outer armour layer of breakwaters and most of the research was restricted to impermeable structures. There is ad demonstrable lack of knowledge of the stability of cubes which are placed at the rear-side of the construction. The inner-slope has a different load than the outer-slope. The outer-slope is loaded by waves directly from the sea whereas the inner-slope is loaded by the overtopping waves. Since the overtopping wave load is believed to be smaller, smaller dimensions of armour layer material can be applied on the rear slope. In addition, research on the subject has been mostly restricted to impermeable structures in full scale. These research are mostly expensive and can only be done in specific locations. The problem which arises is that there is a lack of knowledge on the rear slope stability for single armour layer of cubes. Until now, no clear relation has been posed between the offshore wave characteristics and the size, position and placement of cubes. Research executed by Hellinga (2016) has shown that it is difficult to produce a good model of an overtopping wave to study rear slope stability. It is thought that unclear influencing factors in front of the outer crest lead to deviations in the hydraulic parameters which are involved in the project scope. To decrease these influencing factors, Rietmeijer (2017) has designed and developed a Wave Overtopping Simulator, WOS, to remove the need of a wave flume. This simulator is used in this research to asses the stability of the rear-slope.

The lack of knowledge which is presented leads to the following research question posed in this report:

Research question

How can the stability of a single cubic armour layer on the rear-slope of breakwaters quantitatively be assessed using a Wave Overtopping Simulator?

1.2 Methodology

To guide the work and help answer the research question three main goals of this research are introduced. These three goals have individual chapters in which the approach, methodology and results are discussed. Each main goal has its own sub-questions which need to be answered in order to answer the main research question step-by-step.

1.2.1 Theoretical approach: characteristics of sea states

In this research use has been made of a simulator. The input parameters of this simulator have to be defined in such a manner that the produced water body corresponds to a given sea state being significant wave height H_s and peak period T_p . Calculations have to be made to define which characteristics belong to which sea state and sea states are of interest for this research. The following sub-questions are posed:

- What elements of an overtopping wave characterize the flow of the water body?
- What percentage of overtopping waves is defined as extreme?
- What are the input parameters of the Wave Overtopping Simulator?

1.2.2 Verification of Wave Overtopping Simulator

The Wave Overtopping Simulator, or WOS, has been designed and constructed by Rietmeijer (2017). It is believed to be a good alternative to executing tests in a wave flume. Unfortunately, no clear data is available to define if this simulator is suitable for research and if the equipment available at the Fluid Mechanics Laboratory of the Technical University of Delft is able to measure the required data. Therefore the following sub-questions need to be answered:

- Does the newly developed wave overtopping simulator provide reliable results compared to theoretical values with regard to front wave velocity, water layer thickness and overtopping period?
- How does the velocity of an overtopping wave develop over the crest of a rubble mound breakwater?

1.2.3 Stability research

For the stability research a methodology is used in which the gained knowledge from chapter 2 and chapter 3 is applied and tests are executed. Before and after each test the slope will be measured using different techniques to assess the damage. In order to be able to pose a conclusion on the stability of a single layer of cubes on the rear slope, the following sub-question needs to be answered:

- What failure mechanisms play a significant role in the quantitative description of the stability of a single armour layer of cubes on the rear slope of breakwaters?
- Can the failure mechanisms be quantitatively assessed?

1.3 Outline of report

As stated previously, the report is built up of three main goals. These three goals can be found in the structure of the report and will gradually build up to answering the research question posed in this introduction. Chapter 2 will elaborate on the theoretical approach and is used to set-up a test

program. It gives some theoretical background as well to explain how waves are formed and how they propagate towards the coastline. Chapter 3 will discuss the verification of the simulator used and determine to what extent the simulator is suitable for this research. Chapter 4 will discuss the stability research executed for this research. Information is given on the criteria which are defined to be 'settlement', 'damage' or 'failure'. in addition the build of the test set-up will be explained in this chapter.

Chapter 2

Theoretical Approach

In this chapter a summary is given of the literature study which has been done at the start of this masters thesis. It describes the whole theoretical background of a wave which is created offshore, approaches a breakwater, breaks on the outer slope, runs-up onto the crest, flows over the crest and impinges the inner slope. This step-wise refinement of the theory gives a clear overview and a logical structure. A result of this literature study is a new approach to the problem which is a step forward compared to other studies. A direct link is made between settings of the simulator and offshore wave conditions. The diagram below gives an overview of the elements which result in the theoretical approach of this report

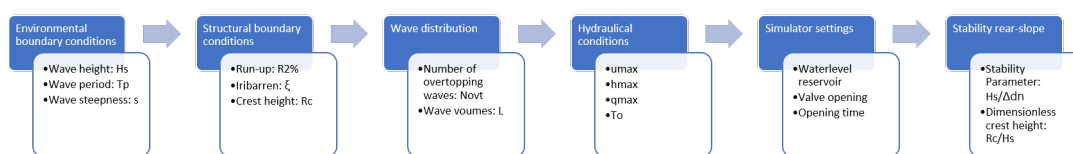


Figure 2.1: Diagram of the theoretical approach

Waves created during a storm far out in the ocean propagate towards the land and reach the coastline. At the coastline they reach either a beach, or an hydraulic structure called a breakwater. The loads on the seawards side of a breakwater and on the landward side differ from each other. These loads are given by the environmental boundary conditions such as significant wave height H_s , mean wave period $T_{m-1,0}$, wave steepness s and the bathymetry in front of the structure. When the mean wave height is taken from the highest third of the waves from an observation, it is defined as the significant wave height H_s . When it is taken from a statistical wave energy density spectrum, not from an actual measurement, it is defined as the zeroth-order moment H_{m0} . Since the difference in magnitude between the two is small, a few percent, in this research they are equal. The seaward side of the breakwater is directly loaded by waves coming from deep sea. These wave are generated by wind and when making the transition from deep water to shallow water, the energy spectrum of the waves changes. This change is due to waves breaking and energy dissipating. The amount of energy that is dissipated depends on the relation between the steepness of the wave and the steepness of the shore it reaches; the Iribarren number. This is defined as the tangens of the slope angle divided by the square root of the steepness of the wave.

$$\xi = \frac{\tan(\alpha)}{\sqrt{\frac{2\pi}{g} \frac{H_s^3}{T_p^2}}} \quad (2.1)$$

With,

α	Slope of outer angle	$[deg]$
g	Gravitational acceleration	$[m/s^2]$
H_s	Incident wave height at the toe of the structure	$[m]$
T_p	Wave period	$[s]$

This dimensionless breaker parameter actually can be seen as the relation between the fore shore slope steepness and the wave steepness. And it contains several different classes being: surging, collapsing, plunging and spilling. There is a transition between breaking and non-breaking around $\xi \approx 2.5 - 3$. For higher values the wave surges up and down the slope with minor air entrapment Schiereck and Verhagen (2012). In this research an Iribarren value of 3.03 is applied which corresponds to plunging waves. An overview of the used parameters is shown in the following figure:

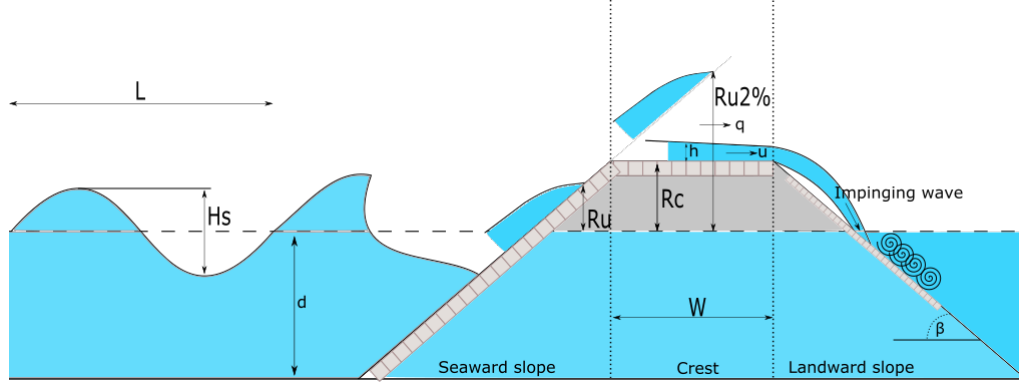


Figure 2.2: Overview of used parameters

The landward side of the breakwater is loaded by a hydraulic response of the construction, waves break on the seaward side, run-up occurs onto the breakwater, and depending on the crest-height, some waves, called overtopping waves, will run over the breakwater. Because of this difference in loading, a different design can be applied in both locations. When the forces on the seaward side of a breakwater are decomposed in horizontal and vertical direction, on the seaward side the horizontal force works in the direction of the wave whereas the vertical force is directed opposite of the gravitational force. On the landward side however, the horizontal force is away from the slope and the vertical force directed downward. Because of a lack of research in landward side stability of concrete units, additional research can help to increase the knowledge on this subject and possibly gain insight in the stability of these elements when linking them to offshore sea states.

To decide whether an incoming wave will become an overtopping wave depends on the structural parameters of the breakwater. Two important parameters are the crest height R_c and the front slope angle α . Together they influence the wave run-up. Wave run-up is defined as the maximum height a wave can run-up the slope of a structure measured from still water level. When this fictive height exceeds the height of the crest, overtopping will occur and a water body will flow over the crest. Previous studies and literature often use the 2% run-up level: $Ru_{2\%}$. This is the run-up level which is exceeded by 2% of the incoming waves. The number of waves exceeding this level is accordingly related to the number of incoming waves and not the number that runs up the slope. Together with the iribarren number, the significant wave height, the presence of a berm, wave period and friction, a general formula, developed by van der Meer et al (2002), can be applied to calculate the fictional run-up height:

$$\frac{R_{u,n\%}}{H_{m0}} = A \cdot \gamma_b \cdot \gamma_f \cdot \gamma_{beta} \cdot \epsilon_{m-1,0} \quad (2.2)$$

With a maximum value of;

$$\frac{R_{u,n\%}}{H_{m0}} = \gamma_b \cdot \gamma_{f,surging} \cdot \gamma_{\beta} \left(B - \frac{C}{\sqrt{\epsilon_{m-1,0}}} \right) \quad (2.3)$$

With,

$R_{u,n\%}$	Maximum run-up height exceeded by n% of the incident waves	[m]
H_{m0}	significant wave height	[m]
γ_b	Berm reduction factor	[-]
γ_f	Roughness reduction factor	[-]
γ_β	Angle of attack reduction factor	[-]
ϵ	Iribarren number	[-]

Due to the irregularity of the sea, a certain percentage of the waves is used to describe the fictive wave run-up defined as the extreme loads. This is the n percent of waves that exceed a certain height. When, for example, $n = 2\%$ is used, it is called the 2% wave run-up height, $R_{u,2\%}$. The coefficient A used is determined deterministic and in this research it is set to $A = 1.75$: van der Meer et al (2002)

As can be seen in equation 2.2 different factors have an influence on the wave run-up. The friction of the slope is of great importance. A breakwater with a smooth surface has higher run-up heights compared to a breakwater with a very rough slope. In the formula this is included in the parameter γ_f . For smooth slopes like asphalt, concrete and grass a factor of 1.0 is used. For concrete blocks a factor of $\gamma_f = 0.5$ is used, van der Meer et al. (2016). The roughness factor can be described by:

$$\gamma_{f,surg\text{ing}} = \gamma_f + (\epsilon_{m-1,0} - 1.8) \cdot \frac{1 - \gamma_f}{8.2} \quad (2.4)$$

$$\gamma_{f,surg\text{ing}} = 1; \epsilon_{m-1,0} > 10$$

A maximum dimensionless run-up, as described by 2.3, for a permeable core is $\frac{R_{u,2\%}}{H_{m0}} = 1.97$ for a deterministic approach.

Next to these formulas, another formula for the wave run-up is proposed by van Gent (2002):

$$\frac{R_{u,n\%}}{\gamma H_{m0}} = c_0 \cdot \epsilon_{m-1,0}; \epsilon_{m-1,0} < p \quad (2.5)$$

$$\frac{R_{u,n\%}}{\gamma H_{m0}} = c_1 - \frac{c_2}{\epsilon_{m-1,0}}; \epsilon_{m-1,0} > p \quad (2.6)$$

Where $c_2 = 0.25 \cdot \frac{c_1^2}{c_0}$ and $p = 0.5 \cdot \frac{c_1}{c_0}$. For the 2% run-up height the coefficients are given by: $c_0 = 1.35$ and $c_1 = 4.7$.

The wave run-up leads to a boundary condition of the scope of this research. It gives us information on the layer thickness, velocity, discharge and period of the wave tongue at the seaward side of the crest. This is a starting point of our area of interest. Schüttrumpf and Oumeraci (2005) describes these parameters as follows:

$$\frac{h_{n\%}(x_c = 0)}{H_{m0}} = c'_{h,n\%} \cdot \left(\frac{R_{u,n\%} - R_c}{\gamma_f H_{m0}} \right) \quad (2.7)$$

$$\frac{u_{n\%}(x_c = 0)}{\sqrt{g \cdot H_{m0}}} = c'_{u,n\%} \cdot \left(\frac{R_{u,n\%} - R_c}{\gamma_f H_{m0}} \right)^{0.5} \quad (2.8)$$

$$\frac{q_{n\%}(x_c = 0)}{\sqrt{g \cdot H_{m0}^3}} = c'_{q,n\%} \cdot \left(\frac{R_{u,n\%} - R_c}{\gamma_f H_{m0}} \right)^{1.5} \quad (2.9)$$

$$\frac{T_{ovt,n\%}(x_c = 0)}{T_{m-1,0}} = c'_{T,n\%} \cdot \left(\frac{R_{u,n\%} - R_c}{\gamma_f H_{m0}} \right)^{0.5} \quad (2.10)$$

Where,

$h_{n\%}$	=	Maximum layer thickness exceeded by n% of the incident waves	[m]
$u_{n\%}$	=	Maximum velocity exceeded by n% of the incident waves	[m/s]
$q_{n\%}$	=	Maximum flow exceeded by n% of the incident waves	[m ² /s]
$T_{ovt,n\%}$	=	Duration of overtopping volume	[s]
R_c	=	Crest height	[m]
$c'_{h,n\%}$	=	empirical coefficient	[-]
$c'_{u,n\%}$	=	empirical coefficient	[-]
$c'_{q,n\%}$	=	empirical coefficient	[-]

Table 2.1: Explanation parameters as used by Schüttrumpf and Oumeraci (2005)

At this point the theory has arrived at the point of interest for this research; the seaward side of the crest. The environmental boundary conditions combined with the structural parameters have led to the hydraulic parameters. Subsequently the hydraulic parameters have led to the Hydraulic loads encompassing the overtopping time and the maximum layer thickness, velocity and discharge. These parameters should play a significant role in the stability of the inner slope.

2.1 Breakwater Crest

After the wave passes the seaward side of the crest, it develops over the width of the crest. Several processes influence the hydraulic loads in these elements. The width of the crest, the amount of infiltrating water and the roughness of the surface play an essential role in the development of the wave tongue over the crest, Verhagen (2005). The parameters that describe this wave tongue are the layer-thickness, the velocity and the discharge. A review of all the research done in these fields, and their resulting formulas to describe the development of the layer thickness and velocity, can be found in the following table:

	Schüttrumpf (2001)	van Gent (2002)	Bosman et. al. (2008)	van der Meer et. al. (2010)	Trung (2014)
Dataset	Schüttrumpf (2001)	van Gent (2002)	Schüttrumpf (2001) + van Gent (2002)	Schüttrumpf (2001) + van Gent (2002) + Flowdike, lorke et. al.	van Gent (2002)
Slope	1:6	1:4	1:4 - 1:6	1:3 - 1:6	1:4
γ_f	1	1 and 0.5	1	1	1 and 0.5
$\frac{h_{2\%}(z_c=0)}{H_s}$			$c'_{h,2\%} \cdot \left(\frac{z_{2\%} - R_c}{\gamma_f H_s} \right)$		$c'_{h,2\%} \cdot \frac{V_{2\%} \cdot \sin \alpha}{R_{u,2\%} - R_c}$
$\frac{u_{2\%}(z_c=0)}{\sqrt{gH_s}}$			$c'_{u,2\%} \cdot \left(\frac{z_{2\%} - R_c}{\gamma_f H_s} \right)^{0.5}$		$c'_{u,2\%} \cdot \cos \alpha \sqrt{\frac{gV_{2\%}}{\sin \alpha H_{m0}}}$
$c'_{h,2\%}$	0.33	0.15	$9 \cdot 10^{-3} / \sin^2 \alpha$	0.13	1.1
$c'_{u,2\%}$	1.37	1.3	$0.30 / \sin \alpha$	$0.35 \cot \alpha$	0.88

Table 2.2: Overview of studies concerning the development of the wave tongue, Rietmeijer (2017)

When linking the discharge and velocity to a single volume, as is done in Hughes (2015), one obtains:

$$q_{peak} = 7.405 \cdot \frac{V \sqrt{\tan \alpha}}{T_{m-1,0}} \quad (2.11)$$

$$u_{@peak} = 25,99 \cdot \frac{\sqrt{V \tan \alpha}}{T_{m-1,0}} \quad (2.12)$$

It is also possible to only look at one position on the crest, in this case the seaward side, and evaluate its progress in time, as is done in Hughes (2012):

$$h(t) = h_p \left(1 - \frac{t}{T_o} \right)^a ; o < t < T_o \quad (2.13)$$

$$u(t) = u_p \left(1 - \frac{t}{T_o} \right)^b ; o < t < T_o \quad (2.14)$$

It is said that when the values of a and b have values of unity, the decrease in flow thickness and velocity are linear, which turns out to be a reasonable assumption, according to Hughes (2001).

Combining equations 2.13 and 2.14 will lead to the individual wave volumetric discharge per unit length:

$$q = h_p u_p \left(1 - \frac{t}{T_0}\right)^{a+b} = q_p \left(1 - \frac{t}{T_o}\right)^m ; o < t < T_o \quad (2.15)$$

A lot of research has been done on the overtopping waves on impermeable grass covered dikes and levees. The first reports on a wave overtopping simulator are written by van Dijk (2001) after which this small scale set-up has been extended to a full scale prototype made by van der Meer et al. (2006). Tests have been conducted on both small and large scale prototypes and have resulted in several equations and formulas to describe the propagation of an overtopping wave tongue over the crest of a breakwater. The next step in this research would be to transform these equations from impermeable to permeable structures as is the case with breakwaters made up out of rubble stone. The equations of van Gent and Pozueta (2004), Bosman et al. (2008), van der Meer (1992) and Hai (2014) are all based on the principal of the continuity equation and the fact that the volume of the wave tongue over the crest is constant. Infiltration is not taken into account. This is not possible when permeable structures are considered. In this case infiltration will occur all over the breakwater and the volume will decrease until the water hits the rear slope of the structure.

And these studies have not dealt with a simulator which releases a volume of water in a certain time frame. This means that the simulator used in this study deviates from the former mentioned studies. When a closer look is taken at the released water body, instead of looking at the wave run-up, one could also look at other hydraulic phenomena which contain the same element. A sudden release of a water body with an elevated water level compared to a reference level, is also seen at a dam-break. In Ritter (1892) the first solution was derived for the propagation of a sudden release of a waterbody. It studies the effects of dam failure and it's complicated physics with many uncertainties involved. The uncertainties are mainly from the fact that it is difficult to predict the hydrograph of the outflow of such an event. The solution was for a wave structure of an idealized fluid which, during dam failure, was propagating over an initially dry horizontal bed. In his paper he states that the velocity is a turbulent motion of water with a front propagating at:

$$u = 2 \cdot \sqrt{g\Delta h} \quad (2.16)$$

The hydraulic event can be compared to the sudden opening of a valve or gate in a canal. Additional research by Castro-Orgaz and Chanson (2017) points out that the positive front of the wave propagates slower than the solution presented in 2.16. This could be the result of bulging of the front of the wave where interaction takes place with the dry-bed. In this present research the solution as presented in 2.16 is applied as a maximum boundary for the velocity of a wave front after sudden release by a valve over an horizontal dry terrain.

2.2 Input in model

The significant wave height combined with the peak period represent a certain storm event. Combined with the Irribaren number and a given crest height leads to a distribution of the volume at the outer crest line. This gives the wave volume V , layer thickness h and velocity of the wave front u_f . These three parameters are the boundary conditions of the whole set-up. They describe the waves which are present during storm conditions and which will cause damage and failure to the rear slope. An overview of the parameters which are used in the model can be found in the following table:

Symbol	Variable	Range
H_s	Significant wave height	8 - 32 <i>cm</i>
s	Wave steepness	0,04 [-]
T_p	Wave period	1.1 - 2.5 <i>s</i>
R_c	Freeboard	10 - 20 <i>cm</i>
D_n	Cube size	20 <i>mm</i>
ρ_n	Cube density	2120 <i>kg/m</i> ³
V	Volume	5-120 <i>L</i>
T_{ovt}	Time	0 - 3 <i>s</i>
q	Specific discharge	0 - 0.5 <i>m</i> ² / <i>s/m</i>
u_f	Front velocity	0 - 5 <i>m/s</i>
$h(x, t)$	Layer thickness	0 - 10 <i>cm</i>
W_c	Crest width	40 <i>cm</i>
n	Porosity	0.4 [-]
β	Rear slope angle	1:1,5
γ_f	Friction on crest	0.5

Table 2.3: Important parameters for research

A list of dimensionless parameters that best characterize the research:

- Dimensionless stability parameter $H_s/(\Delta d_n)$
- Dimensionless crest height R_c/H_s
- Dimensionless instantaneous overtopping discharge $q/(g \cdot H^3)^{0.5}$
- Dimensionless time duration t/T_{ovt}

2.3 Wave calculations

A wave in the end should result in the wave characteristics front velocity u_{max} , water layer thickness h_{max} , overtopping time T_{ovt} and a wave volume. As stated in van der Meer et al. (2006) a wave steepness of $s_{op} = 0.04$, 4% is observed in the Waddensea in the Northern part of the Netherlands. This is also taken as a constant in this report. The seaward slope of the structure will be kept constant at 1:1.5 and the configuration of the cubes is not changed between the tests. This to ensure that time and energy is spent on looking at the hydraulic parameters in stead of the structural parameters.

The configuration of the rear slope is subjected to increasing wave loads until failure of the rear slope occurs. During the tests, the significant wave height and peak period are step wise increased, meaning bigger storms, as each storm has it's own Weibull distributed volume as stated in van der Meer et al (2002). From the Weibull distribution the highest 0.1% of the waves is chosen, as this is the theoretical maximum overtopping volume. The extreme waves occur very seldom but have the highest velocity and volume. This makes them the waves which are most likely to initiate damage or failure on the rear slope. Failure in this sense is defined as either the stability parameter: $H_s/(\Delta D)$. Or the damage number defined as:

$$N_{od} = \frac{\text{Number of displaced units}}{\text{Armour layer width}/D} \quad (2.17)$$

In van der Meer et al. (2016) it is stated that failure of the revetment occurs at $N_{od} = 2$. As a single layer revetment behaves brittle, initial damage quickly leads to total collapse and will expose an under-layer. Hence, the start of the damage will be the leading value of $N_{od} = 0.2$.

For the determination of the wave volume corresponding to certain significant wave heights use has been made of van der Meer et al. (2016), Hughes (2012), Zanuttigh et al. (2013) and Hughes (2015).

The significant wave height in combination with the wave steepness of 4% results in a relating wave peak period which are the hydraulic parameters for a certain storm. This leads to a certain overtopping discharge, probability of overtopping, a shape factor and a scale factor. With the help of a theoretical storm duration of 3 hours the volume of water that will overtop the

structure can be determined.

For the determination of the wave steepness and irribarren number, with outer slope angle of 1:1,5:

$$s_0 = \frac{2\pi H}{g T^2} \quad (2.18)$$

$$\xi = \frac{\tan \alpha}{\sqrt{s_0}} \quad (2.19)$$

Subsequently the run-up is calculated with $A = 1,75$, $\gamma_b = 1,0$, $\gamma_f = 0,5$, $\gamma_\beta = 1,0$:

$$\frac{R_{u,2\%}}{H_{m0}} = 1,75 \cdot \gamma_b \cdot \gamma_f \cdot \gamma_\beta \cdot \xi_{m-1,0} \quad (2.20)$$

After which the instantaneous specific discharge is calculated using:

$$\frac{q}{\sqrt{g \cdot H_{m0}^3}} = \frac{0.026}{\sqrt{\tan \alpha}} \cdot \gamma_b \cdot \xi_{m-1,0} \cdot \exp \left[- \left(2.5 \frac{R_c}{\xi_{m-1,0} \cdot H_{m0} \cdot \gamma_b \cdot \gamma_f \cdot \gamma_\beta \cdot \gamma_v} \right)^{1.3} \right] \quad (2.21)$$

In the following steps the formulas for the scale factor a and shape factor b are taken from Zanuttigh et al. (2013) being:

$$a = \left(\frac{1}{\gamma \left(1 + \frac{1}{b} \right)} \right) \left(\frac{q T_m}{P_{ov}} \right) \quad (2.22)$$

$$b = 0.73 + 55 \cdot \left(\frac{q}{g \cdot H_{m0} \cdot T_{m-1,0}} \right)^{0.8} \quad (2.23)$$

After which the percentage of overtopping waves is calculated by means of:

$$P_{ov} = \exp \left[- \left(\sqrt{-\ln 0.02} \frac{R_c}{R_{u,2\%}} \right)^2 \right] \quad (2.24)$$

From equations 2.21, 2.22, 2.23 and 2.24 we obtain the necessary parameters to compute the two parameter Weibull distribution for the overtopping wave volume. To make an estimation of the discharge of the overtopping wave event, several methods have been developed in the last couple of years. The most significant is data based on approximately 10.000 tests executed during the CLASH project by de Rouck (2005). Subsequently a neural network is developed for estimating the average discharge. This neural network has been presented by van Gent et al. (2007). The probability of a certain volume exceeding a set volume is found using:

$$P_v = \exp \left[- \left(\frac{V}{a} \right)^{1/b} \right] \quad (2.25)$$

This can be rewritten in:

$$V = a \cdot \left[-\ln \left(\frac{P_v}{100\%} \right) \right]^{1/b} \quad (2.26)$$

With a maximum of

$$V_{max} = a \cdot [\ln(N_{ow})]^{1/b} \quad (2.27)$$

In which V_{max} is a first estimation of the predicted value for the maximum volume of one wave that can be expected in a storm duration of 3 hours. An example of this volume distribution is given in the following figure:

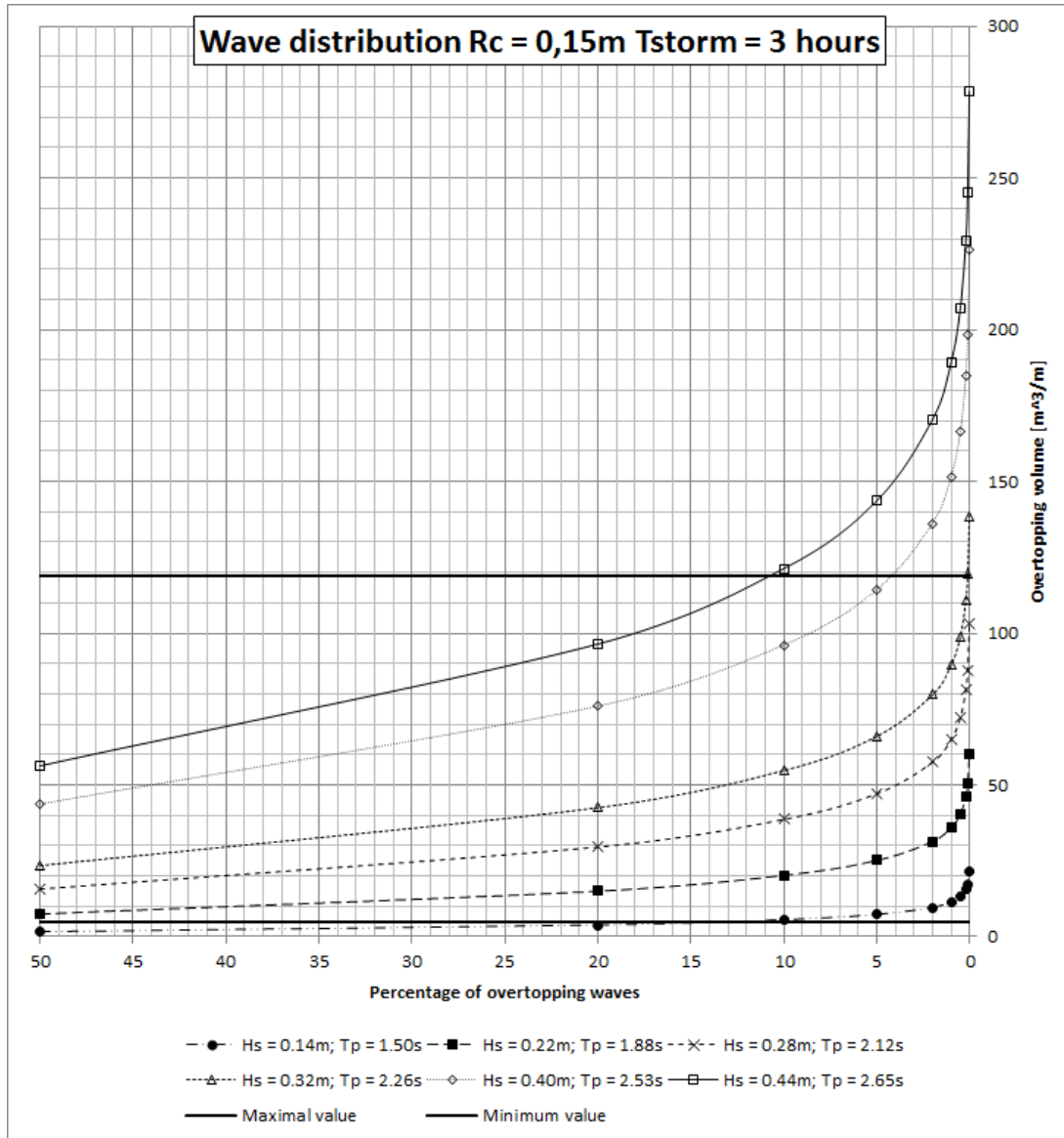


Figure 2.3: Two-parameter Weibull distribution for crest height of 15 cm with increasing wave heights

In figure 2.3 is shown how the distributions of a significant wave height ranging from 0.10m - 0.30m relate to each other. The differences in volume of the different wave height for high percentages of occurrence are small. These differences increase for very low percentages of occurrence. The percentages of occurrence correspond to an amount of waves. In this research the percentage of occurrence is set to 1 in a thousand: 0.01%. In this manner the amount of waves is low which is practical for tests being executed in a laboratory and the differences between the waves are large. In this stage this is necessary due to the fact that not sufficient information is available on the stability of the wave overtopping simulator and the stability of a single cubic armour layer.

Calculation of wave layer thickness and velocities

These calculations lead to a volume which can be linked to a certain sea state, such as a significant wave Height H_s and a peak period T_p as can be observed in deeper waters. However for the measurements on top of the slope, and to actually give a visual representation of the wave tongue one needs to know the layer thickness and velocity at which the volume travels over the crest. The velocity can be controlled by the water level in the simulator's reservoir, the layer thickness can be steered by the opening height of the valve, and the volume and duration of the overtopping wave

can be regulated by adjusting the flume axial width of the reservoir. To quantify these parameters and link them to specific overtopping volumes Hughes (2015) has developed the following empirical equations:

$$u_{max} = 27.67 \frac{\sqrt{V \cdot \tan \alpha}}{T_{m-1,0}} \quad (2.28)$$

$$h_{max} = 0.324 \sqrt{V} \quad (2.29)$$

$$q_{max} = 7.405 \frac{V \cdot \sqrt{\tan \alpha}}{T_{m-1,0}} \quad (2.30)$$

$$u_{@qmax} = 25.99 \frac{\sqrt{V \cdot \tan \alpha}}{T_{m-1,0}} \quad (2.31)$$

$$h_{@qmax} = 0.299 \sqrt{V} \quad (2.32)$$

$$T_0 = 15.56 \left(\frac{\sqrt{V}}{g} \right)^{0.5} \quad (2.33)$$

An overview of the layer thicknesses, flow velocities and discharges is given as well as the required Δz for the flow velocity and the Δh for the volume. This to check whether these values lie within the range of the simulator.

This can also be calculated by solving the following differential equation, which has a solution for the area of the reservoir. This means that by adjusting the reservoir width the velocity of the wave front can be determined:

$$u(t) = \sqrt{2g\Delta z(t)} \quad (2.34)$$

$$\frac{\delta z}{\delta t} = \frac{Q(t)}{A(z)} \quad (2.35)$$

$$Q(t) = u(t) \cdot h_{opening}(t) \cdot \mu \quad (2.36)$$

Solving equations 2.34, 2.35 and 2.36 for $A(z)$ leads to the development of the area over time. This is necessary to adjust the area of the reservoir per wave which is to be simulated. The maximal and minimal values have been derived using Kudale and Kobayashi (1996). The maximum value stands for waves which have a velocity on the crest which exceeds the maximum because the horizontal displacement is too large for the wave to inflict damage or failure on the inner-slope of the structure. The minimal value is for waves which are too small and do not reach the water level at the rear side of the breakwater. One can calculate the expected horizontal and vertical displacement of the wave front. This is done with the following formulas:

$$V_x = u \quad (2.37)$$

$$\Delta x = \frac{1}{g} \left[u^2 \tan \theta_l + \sqrt{u^4 \tan^2 \theta_l + gh u^2} \right] \quad (2.38)$$

$$\Delta y = \Delta x \tan \theta_l + \frac{h}{2} \quad (2.39)$$

$$V_y = \frac{g\Delta x}{u} \quad (2.40)$$

$$V_R = \sqrt{V_x^2 + V_y^2} \quad (2.41)$$

$$\alpha = \tan^{-1} \left(\frac{V_y}{V_x} \right) \quad (2.42)$$

In this way boundary conditions are found for the test facilities as built in the Fluid Mechanics Laboratory at Delft University of Technology. For a relative crest height of 0,15 m the maximum value is 119 liters and a minimal value of 24 liters per overtopping wave.

When taking the 1 in thousandth wave from Figure 2.3 the following wave groups are found:

Rc = 0.15m										
Hs [m]	Tp [s]	$q/(g * Hs^3)^{0.5}$	Waves	Volume [L]	umax [m]	hmax [m]	qmax [m2/s/m]	To [s]	Hres [m]	Valve [m]
0.14	1.50	0.012	5	17	2.18	0.04	0.08	1.8	0.168	0.07
0.22	1.88	0.030	5	50	2.97	0.07	0.18	2.35	0.311	0.12
0.28	2.12	0.041	5	88	3.48	0.10	0.28	2.70	0.427	0.15
0.32	2.26	0.047	5	119	3.79	0.11	0.35	2.92	0.501	0.18
0.40	2.53	0.057	5	198	4.37	0.14	0.52	3.31	0.674	0.23
0.44	2.65	0.060	5	245	4.64	0.16	0.62	3.5	0.759	0.26

Table 2.4: Overview of the wave groups which correspond to storm conditions for Rc = 15 cm

Figure 4.1 shows an overview of the 1 in thousand waves, 0, 1% of the overtopping waves which occur, according to a two-parameter Weibull distribution, 5 times during a three hour storm. When the storm length increases the amount of waves present in the spectrum will increase as well. A storm with a duration of 2 - 6 hours is frequent in the North-Sea. In addition the number of 5 waves to be tested is practical for experimental tests done in a laboratory. These calculations have been made for three heights of the crest freeboard being Rc = 0,10, 0,15 and 0,20 meter. Figures as Figure 2.3 and Figure 4.1 for the other crest free boards can be found in Appendix A.

Chapter 3

Verification of the Wave Overtopping Simulator

In this chapter the overtopping simulator as designed and constructed by Rietmeijer (2017) will be verified. It is believed that the simulator has the potential to reproduce overtopping waves on a scale level, this assumption is however not yet confirmed by convincing physical test results. In section 3.1 the theory which is used for the design of the simulator is explained. In section 3.2 the results which have been found by previous research is mentioned, and this gives a starting point for the current research. What is already known and where is there room for improvement? Section 3.3 discusses the approach used to validate the simulator. This approach is a combination of the used theory and the approach used in former research. Because of the empirical nature of the system an big amount of data is help full to determine whether or not the simulator is applicable. Section 3.4 presents the results obtained by the current research. In section 3.5 the conclusion which follows from the results will be presented. This conclusion will contain the statement whether or not the simulator is useful for the research of overtopping waves and furthermore for the research in the stability of the rear armour layer.

3.1 Design of Wave Overtopping Simulator

Hellinga (2016) has demonstrated that there is the potential to find a link between the hydraulic parameters and the stability of the armour layer at the rear slope of a breakwater. This research has, however, also shown that tests executed in a flume are difficult and time-consuming. More research is needed to collect useful data which can be used to describe rear slope damage. Another discovery was that the accuracy of the answers is low. Simulating waves using a full-length wave flume is considered to be so difficult that other options were reviewed.

To decrease the amount of unclear influencing factors in front of the outer crest which lead to deviations in the hydraulic parameters, a simulator was designed and been built at the Fluid Mechanics Laboratory of Delft University of Technology. This simulator was based on research executed by van Dijk (2001). and van der Meer et al. (2006). These researches describe the design and the construction of simulators now used in stability studies on both impermeable dykes and permeable breakwaters. In the next subsection these reference projects are reviewed. Overall it can be said that a wave overtopping simulator has several advantages being used for physical model testing. It also has certain advantages over the use of a full-length wave flume. Firstly one has exact knowledge of the magnitude of hydraulic parameters which describe the overtopping wave. When using a flume, every spatial step, from offshore wave conditions to breaking on the breakwater, introduces new influencing factors on the propagating wave. It is extremely difficult to quantify these influences, especially at the transition from the seaward slope to the crest where the scatter in simulated waves is big. By using a simulator the amount of deviation in the hydraulic parameters is minimized by excluding the factors before the start of the crest. In addition, it is possible to test larger test scales without the requirement of a real wave. Real waves need 3-5 times the wavelength to adapt to the bathymetry. Hence, only small waves can be tested. With a simulator this is not the case and the total dimensions of the set-up can be reduced, while increasing the maximum wave height which can be simulated. By increasing the scale of the waves scaling

errors are decreased as well. A disadvantage of using a simulator is that the link to an actual sea state is always solely based on theory and that the actual offshore wave conditions are merely an estimation of the real situation. For a flume the same holds, the waves are solely based on theory, however this theory is developed more than the theory used for overtopping waves. In the stage the research and knowledge on the subject is now, a simulator is believed to be suitable to gain insight on the matter and make a big step in gathering data on overtopping waves.

3.1.1 Plunge machine van Dijk (2001)

In 2001 Bas van Dijk performed research in the Fluid Mechanics Laboratory at Delft University of Technology for his master's thesis. The focus of this research was on the rear slope stability of rubble mound breakwaters as a whole. In this research the first idea was to use a certain 'plunge' as a starting point to represent the hydraulic behaviour of an overtopping wave. The wave itself is considered as a black box and the hydraulic processes on top of the breakwater are simulated by plunges. For the generation of this plunge several conceptual designs of the simulator were discussed after which one design was used resulting in a reservoir with a valve. In this way the size of the reservoir and the size of the orifice are easily adaptable. The features of the 'plunge' are thought to have the following characteristics. The layer thickness of the water body which travels over the crest can increase from zero to maximum in a short period of time and subsequently it decreases from maximum to zero in a time frame which is longer. For the velocity of the water body the same occurs because the discharge is a multiplication of the two and it also holds for the discharge. Additionally, it is thought that the maximum layer thickness and the maximum velocity usually occur simultaneously. The four characteristics of a 'plunge' are: maximum layer thickness; maximum velocity; peak period; and, the total period. The discharge and volume of the water body can be derived from these characteristics.

The experimental set-up used by van Dijk (2001) is shown in the following figure:

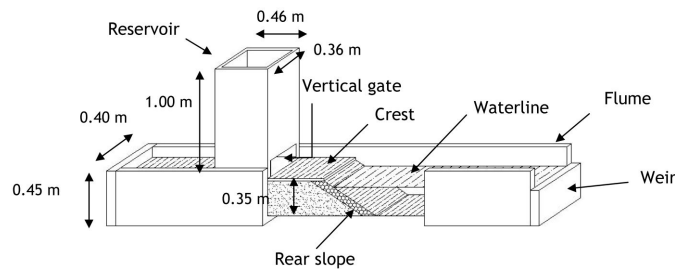


Figure 3.1: Sketch of experimental set-up used by van Dijk (2001)

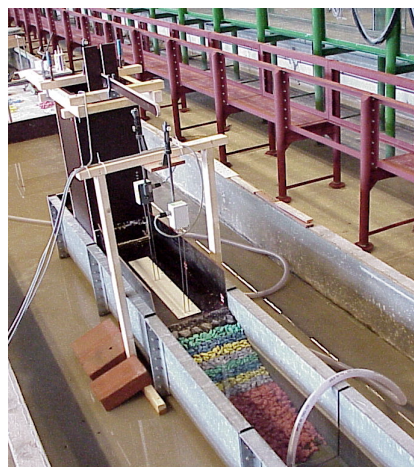


Figure 3.2: Experimental set-up van Dijk (2001) as built.

The measuring equipment used is wave height meters to measure wave layer thickness and the velocity of the wave front. In addition, the meter is used to measure the volume which

leaves the reservoir. The velocity which results from these measurements is not a velocity as a function of time but a velocity at a certain moment in time.

3.1.2 Dutch Overtopping Simulator by van der Meer et al. (2006)

To come up with overtopping resistant solutions for dikes without increasing the dike geometry it was necessary to design and construct a simulator which can reproduce the largest wave in a normative storm of the Dutch coast and be transportable. The starting point of the dimensions used was the calculation of the discharge using van der Meer et al (2002). The concept of the overtopping simulator is based on:

- Everything on wave breaking on slopes and generating overtopping waves is known
- Everything on individual overtopping waves is known as volumes, distributions, velocities and flow depth of overtopping water on the crest; and,
- Actual waves that are not really required to simulate wave overtopping.

The possible failure mechanisms of infiltration and sliding can only be tested on an actual dyke and for a sufficient width, for example around 30m. In this research the attention was more focused on the stability of grass covered dykes. As grass and clay cannot be scaled, only large scale facilities can be used. In this research it was also proposed not to simulate the fully distribution as calculated but to discretize this distribution for simulation. This is done because it was assumed that it was not necessary to mimic every volume exactly. A visualization of this is given in figure 3.3.

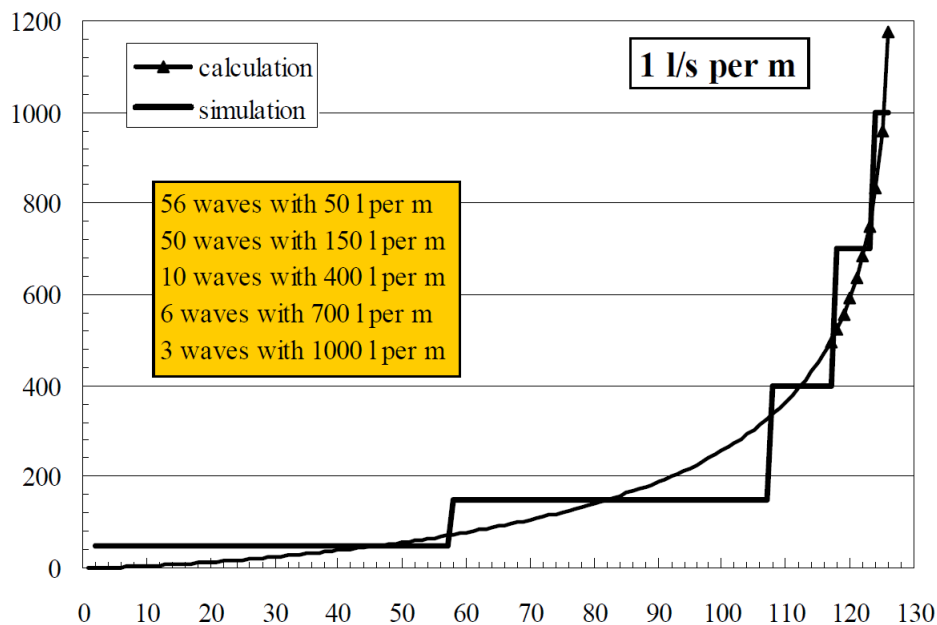


Figure 3.3: Discretization of the two parameter Weibull distribution of a storm. van der Meer et al. (2006)

The volume of overtopping water flows fast and in a limited time over the crest and inner side of the dike. For the overtopping simulator only the behaviour at the crest is important, as the behaviour on the inner slope will follow automatically. The overtopping simulator should simulate the right velocity and flow depth in time at the crest of the dike, for a given overtopping volume. The following aspects were considered for the technical design of the device:

- Maximum volume of $3.5m^3/m$ (4m wide)
- Shape of the box: as high and slender as possible, in order to reach the large velocities for large volumes.
- Opening of the valve: $0.5m$, to be adjusted during calibration.

- Possibility to place the device at different heights with respect to the crest

The pressure height above the valve determines the flow velocity at the valve. Because there is quite a difference between the predicted layer thicknesses between Möller et al. (2003) and van Gent (2002) this parameter is not well-known. The velocity parameter is more similar and therefore the only well-known parameter at the crest. The flow velocity and flow depth in time give also a good idea of the overtopping volume, just by integration. A quick way is to assume a triangular shape and calculate the overtopping volume. The instruments used in this set-up are acoustic flow depth meters and electromagnetic velocity meters. In figure 3.4.



Figure 3.4: Calibration set-up as built by van der Meer et al. (2006)

3.2 Results of previous research

van Dijk (2001) concludes that the built set-up is able to produce a 'plunge' with a shape that resembles the schematized plunge. The decrease of the layer thickness after the maximum is reached is somewhat longer than desired. This is not a problem because it is thought that the front part of the wave inflicts the most damage.

The conclusions given by van der Meer et al. (2006) are that based on the research good reliable requirements are only available for the maximum flow velocity of each overtopping wave volume. The flow depth is not easily measured and this research shows large deviations. However, the research concludes that the overtopping simulator is useful for further research. In addition, it is possible to simulate the triangular shape as discussed before. Therefore it is justifiable to calculate the volume of the calculated using:

$$V = 1/3 \cdot v_{max} \cdot d_{max} \cdot t_1 \quad (3.1)$$

Rietmeijer (2017) conducted preliminary tests for the calibration of the simulator. The results can be found in the figures 3.5 and 3.6:

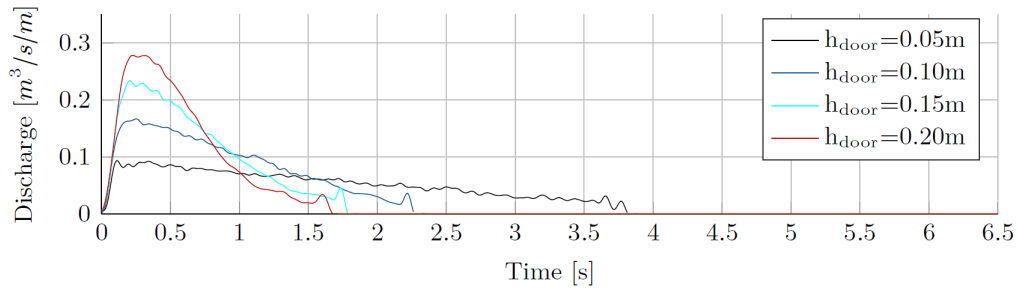


Figure 3.5: Discharge in time

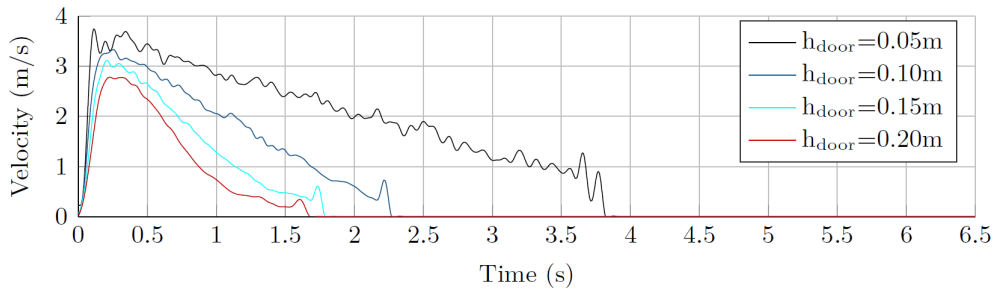


Figure 3.6: Velocity in time

In both figures more or less a triangular shape can be seen representing the characteristics of an overtopping wave. However, the length of the event is rather long. This is because there is no sequence of motion. This means that in these tests only an opening action is performed by the linear actuator. In this way the reservoir is completely emptied and the volume which leaves the reservoir is too big to correspond with the desired overtopping event. Because of this, it is difficult to justify this wave as being a steep wave front and the opening as being quasi-instantaneous. Furthermore, the velocity appears to be between 3 and 3.5 m/s. This is a good reference value to see if in the tests which are conducted in the current research values of the same magnitude occur.

3.3 Methodology

The placement of the Wave Overtopping Simulator (WOS) will be at the Fluid Mechanics Laboratory at the Delft University of Technology in a flume containing a see-through window on one side of the flume. This is done to collect visual data which can later be analyzed. One important aspect of the set-up is that a crest can be constructed with small cubes, after which a slope is situated. At the end a collection basin should be created in which the water level can be controlled. It should also be possible to drain excess water from this basin when it increases too much. Subsequently the linear actuator should be placed and the software installed on the computer. The software used is SoMove 2.6.2. connected to a Lexium 32 M-S. The used DTM version is 1.16.00.03. First calibration of the linear actuator must be performed to determine its accuracy. In the following figure the placement of the simulator in the basin is shown:

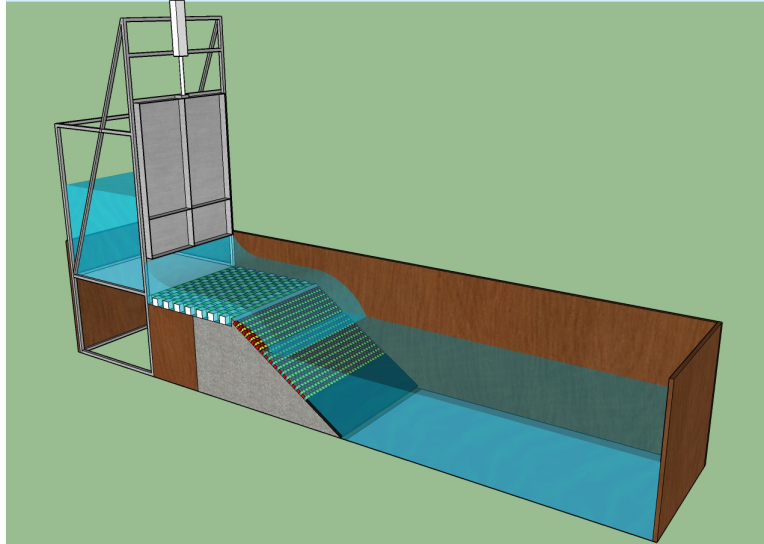


Figure 3.7: Placement of simulator in a water basin

The placement of the simulator should be done carefully in order to decrease negative side effects such as leakage. To determine the negative side effects a couple of pre-tests will be done with the set-up to determine the following:

- By measuring the decrease in water level for a given time period in the reservoir tank the leakage can be determined. A reference value of 0.1 L/s is observed.
- At a former test-up the simulator did not have a tight fit within the flume. Eddies occurred which could influence measurements. The length of these eddies needs to be measured in order to determine the re-circulation area. Former research gives a value of: 31cm. In the current set-up the simulator is fixed more accurate in the flume and it is expected that this length has decreased.
- Preparatory calculations of the water level after opening the valve must have to be compared to measured values in order to be able to say something about the wall roughness. This must be small so that it does not influence the instantaneous release of the water body. In addition tests have been done with a impermeable layer, 0% porosity, and a maximum permeable layer, 50% porosity. Where porosity is a measure of the empty space in a material or on a slope. The term coverage is also applied. In this case coverage equals: $coverage = 1 - porosity$.

When the simulator is installed and the valve is working properly, the opening and closing time can be controlled and adjusted. One can then check if its flow characteristics can be validated with preparatory made calculations. The calculations are applied in reference literature and follow from the continuity equation. To measure some hydraulic parameters of the wave tongue wave gauges will be used to measure the height of the overtopping wave. The wave gauges will be applied in the reservoir, halfway to the crest and just before the transition from crest to inner slope. The three will be used to measure the following:

Reservoir outflow: Torricelli provided the equation $U = \sqrt{2g(\Delta z)}$ with ΔZ being the head difference for stationer flow. Stationer flow is not the case when talking about an instantaneous release of a waterbody of a dry-bed, however it is a good indication of the magnitude of the flow. The dam-break solution of Ritter (1892) for a friction-less 1d flow of an instantaneous released waterbody over a horizontal dry bed: $u = 2\sqrt{g(\Delta z)}$ will be used as a maximum value. The outflow can be used to calculate the discharge through $Q = \mu \cdot A_{opening} \cdot U$ in which $A_{opening}$ is the width of the simulator multiplied with the opened valve height. This theoretical discharge can be checked using the wave gauge in the reservoir by:

$$Q = A_{res} \cdot \frac{dh}{dt}$$

in which the dh is measured by the wave gauge and the dt is stated by the frequency at which the wave gauge measures the water height.

Maximum layer thickness: the maximum layer thickness will be found by measuring water level heights on top of the crest using two wave gauges which will be compared to find the maximum value over the crest.

Maximum front velocity: to measure the front velocity of the wave tongue use is made of two wave gauges positioned x cm's apart. In this way we have two reference points of the position of the front of the wave. One can use

$$u_f = \frac{\Delta s}{\Delta t_{d=x}}$$

In this equation the Δs can be manually chosen by positioning the two measuring points, the wave gauges, a certain distance from each other. The $\Delta t_{d=x}$ is the point where the wave height has reached a certain reference height x so that a good distinction is made of a certain point of the wave front. It is also possible to fit a smooth line through many $x_t(t)$ measurements which have been made by the video camera. This measurement should be repeated sufficiently though, to obtain representative values.

Characteristic velocity: as stated in literature it is possible that the maximum velocity may not be the governing parameters that defines the stability of the cubes on the rear slope. In van Dijk (2001) the characteristic velocity is mentioned to be more important. It is defined as:

$$u_{char} = \frac{Q_{max}}{B \cdot d_{max}}$$

The expected results of these measurements will be the typical triangular shapes as illustrated in figure 3.8

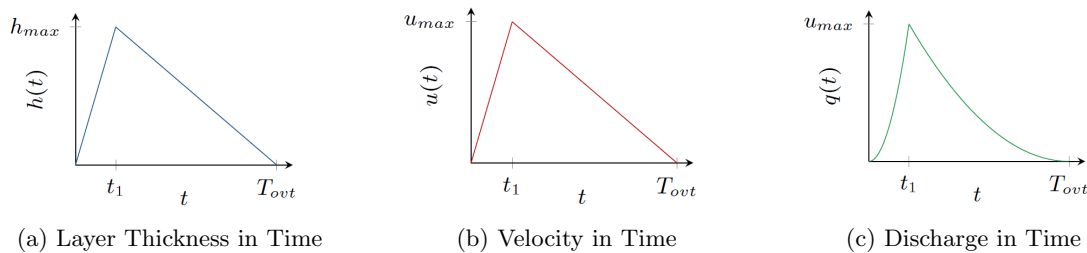


Figure 3.8: Idealized simulated overtopping flow parameters in time

As described in Hughes (2012) a single overtopping wave can be simulated as a triangle when considering h_{max} , u_{max} or q_{max} over time, with a steep increase to its maximum and a less steep decrease to zero again. In the test set-up of this research the opening width of the gate influences the layer thickness in time as seen in (a) of figure 3.8. The velocity in time however is governed by $U = \sqrt{2g\Delta z}$ or $U = 2\sqrt{g\Delta z}$ which can be tuned by the head difference between the opening valve and the water level in the reservoir. The quotient of the t_1 over T_{ovt} should be small. Hughes (2015) mentions a threshold value of:

$$\frac{t_1}{T_{ovt}} < 0.2$$

for all released volumes. Hughes (2015) derives the duration of the overtopping wave event as follows:

$$T_{ovt,theory} = \frac{w_{res}}{d_{valve} \cdot \mu} \cdot \sqrt{h_{res}(t=0)} \cdot \sqrt{\frac{2}{g}} \quad (3.2)$$

In addition, results obtained with the WOS can be validated by looking at table 3.1.

	Schuttrumpf (2001)	van Gent (2002)	Bosman et. al. (2008)	van der Meer et. al. (2010)	Trung (2014)
Dataset	Schuttrumpf (2001)	van Gent (2002)	Schuttrumpf (2001) + van Gent (2002)	Schuttrumpf (2001) + van Gent (2002) + Flowdike, lorke et. al.	van Gent (2002)
Slope	1:6	1:4	1:4 - 1:6	1:3 - 1:6	1:4
γ_f	1	1 and 0.5	1	1	1 and 0.5
$\frac{h_{2\%}(z_c=0)}{H_s}$			$c'_{h,2\%} \cdot \left(\frac{z_{2\%}-R_c}{\gamma_f H_s}\right)$		$c'_{h,2\%} \cdot \frac{V_{2\%} \cdot \sin \alpha}{R_{u,2\%} - R_c}$
$\frac{u_{2\%}(z_c=0)}{\sqrt{gH_s}}$			$c'_{u,2\%} \cdot \left(\frac{z_{2\%}-R_c}{\gamma_f H_s}\right)^{0.5}$		$c'_{u,2\%} \cdot \cos \alpha \sqrt{\frac{gV_{2\%}}{\sin \alpha H_{m0}}}$
$c_{h,2\%}$	0.33	0.15	$9 \cdot 10^{-3} / \sin^2 \alpha$	0.13	1.1
$c_{u,2\%}$	1.37	1.3	$0.30 / \sin \alpha$	$0.35 \cot \alpha$	0.88

Table 3.1: Overview of studies concerning the development of the wave tongue, Rietmeijer (2017)

Here one can see that several equations have been developed over the years. Some only differ by a certain coefficient while others differ a bit more. Because there is a lot of research done in this area and a lot of these equations are empirical and are computed for mostly different structures such as smooth, gentle and impermeable slopes, it is doubtful if it is relevant to check all the theories with the obtained data. It is expected that a good correlation will not occur and if there even is a resemblance it will only result in a slight modification of the coefficient. These formulas can however be useful when comparing the results between permeable and impermeable structure. One can then see if abnormal differences occur when this transition is made.

In addition to the formulas of table 3.1 the wave front can also be validated by looking at the formulas developed by van Gent and Pozueta (2004). This formula describes the development of the wave tongue over the full crest width. In this research, however, wave gauges will only be installed on certain positions so only on these points can the values be compared. The formulas used for this validation are:

$$\frac{R_{u,2\%}}{\gamma H_s} = c_0 \cdot \xi_{s-1,0} \quad (3.3)$$

$$\frac{R_{u,2\%}}{\gamma H_s} = c_1 - \frac{c_2}{\xi_{s-1,0}} \quad (3.4)$$

Where 3.3 is for $\xi_{s-1,0} < p$ and 3.4 is for $\xi_{s-1,0} > p$ with $p = 0,5 \frac{c_1}{c_0}$. Subsequently the velocity of the wave front and the layer thickness can be calculated using:

$$\frac{u_{2\%}}{\sqrt{gH_s}} = c'_{a,u} \left(\frac{R_{u,2\%} - z}{\gamma_f H_s} \right) \quad (3.5)$$

$$\frac{h_{2\%}}{H_s} = c'_{a,h} \left(\frac{R_{u,2\%} - z}{\gamma_f H_s} \right) \quad (3.6)$$

Further validation of the WOS is possible depending on the results of the above mentioned tests. In this research special interest is in the development of the velocity over the crest. To get more detailed data for this parameter Particle Imagery Velocimetries can be applied as was done by Coticone (2015) and Vitulli (2017). This was not considered during this research due to the restriction in time and the priority to gain knowledge in rear slope stability first.

The velocities are also measured using the video camera which shoots a video from every single overtopping wave from the side. This footage is analyzed using matlab which splits the video in separate, single frames. To illustrate this, the figure 3.9 shows the row of pixels which is observed for every separate frame. These rows are subsequently plotted in time to show the propagation of the wave. This plot gives a time over distance plot and the slope indicates the velocity of the wave front.



Figure 3.9: Row of pixels observed

The distance between the two wave gauges is chosen as area of interest in order to compare the results obtained with the method used in the previous section of this paper. The green area in the figure is pixel row 256 counted from above and the horizontal distance is 1263 pixels. Using a ruler taped to the glass the amount of pixels per cm is obtained and so it is found that the horizontal distance is 40.74 cm. The frames are stacked to obtain a time-distance figure in which the slope of the figure gives the velocity of the wave front. In the figure the y-axis represent each individual frame taken from the wave video. The stack consists in this case of 400 frames. The results are compared to the results obtained by the wave gauges. The video camera settings is set to shoot at 100 frames per second. So 400 frames gives 4 seconds of film.

3.4 Results

In the following sections the results of the tests for the validation of the wave overtopping simulator are discussed. First, the results obtained by video analysis will be presented after which they are plotted in graphs to present visual relations. Secondly the measurements of the wave gauges are presented. These results will also be plotted after which they will be combined with the results obtained by the video analysis and the calculated values to see what the results are compared to one another and compared to theoretical values.

3.4.1 High-speed video measurements

For the video analysis I use a high speed camera that can capture up to 100 frames within a single second. To capture the front of the wave as single row of frames just above the crest is observed as indicated in figure 3.9 The frames have been 'stacked' so that a video can be transferred into a single image to obtain relevant information. In this case the relevant information is the velocity of the wave front. It has been observed that due to turbulence of the water, it is difficult to differentiate the wave front from the main wave body, and especially both velocities. By means of color values of the outer wave contour this distinction has been made and a clear wave front is visible. For a single wave video translated into a frame stack the following image is obtained for a 100% coverage, opening width of vale of 100mm and a reservoir height of 30 cm. Comparing this to values calculated in chapter 2 this represents a wave of $H_s = 0.22\text{m}$:

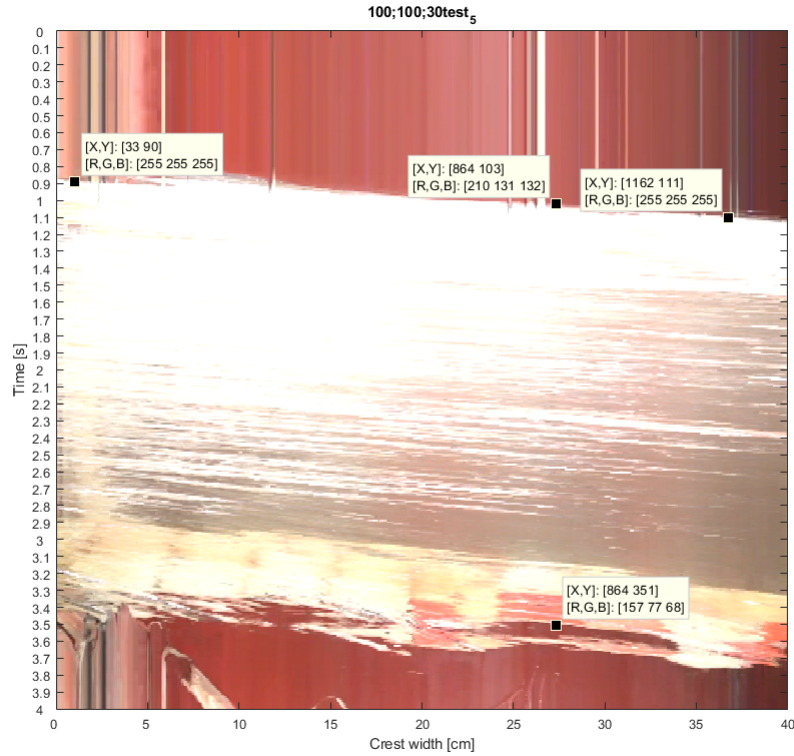


Figure 3.10: Frame stack of 100% coverage, 100mm opening and 30cm head difference.

In this time over distance graph, the slope gives us the velocity of the wave front: $v = \frac{\Delta x}{\Delta y}$. In the example in Figure 3.10 the first data point is 33 pixels horizontally and 90 pixels vertically. The second data point to calculate the slope is: 1162 pixels horizontally and 11 vertically. This gives a horizontal difference of 1129 pixels and a vertical displacement of 21 pixels. By knowing the amount of frames per second, being 100, and the amount of pixels in 1 cm, being 3100, one obtains a velocity of: 1.73 m/s. This is the velocity of the water body which has been identified by the white values of each pixel. Furthermore the image gives an overtopping period, a time indication of the overtopping event. To obtain this value the first data point of 864 horizontally and 103 vertically, is taken. The second data point is 864 horizontally and 351 vertically. In this case it is important to take the same horizontal data point for both cases as one wants to know the period in one exact position on the crest. The difference between the vertical data points indicates the duration of the event. In this case: $((351 - 103)/100) = 2.48$ seconds. The same measurement has been executed for a crest with a coverage of only 50%. Only the configuration of the tested object has been altered, the same camera and codes has been applied.

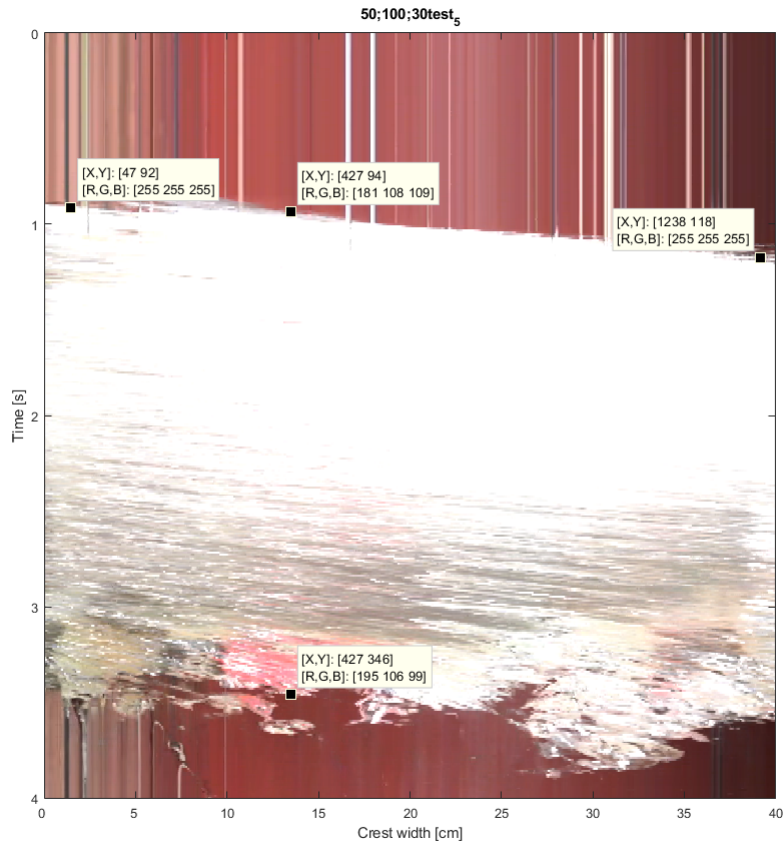


Figure 3.11: Frame stack of 50% coverage, 100mm opening and 30cm head difference.

By applying the same calculations as the example above, one obtains a velocity of 1.36 m/s and a period of 2.34 seconds. From the framestack overview it seems as if the velocity over the crest can be assumed to be a constant. This is further analyzed by zooming in on the slope of the wave:

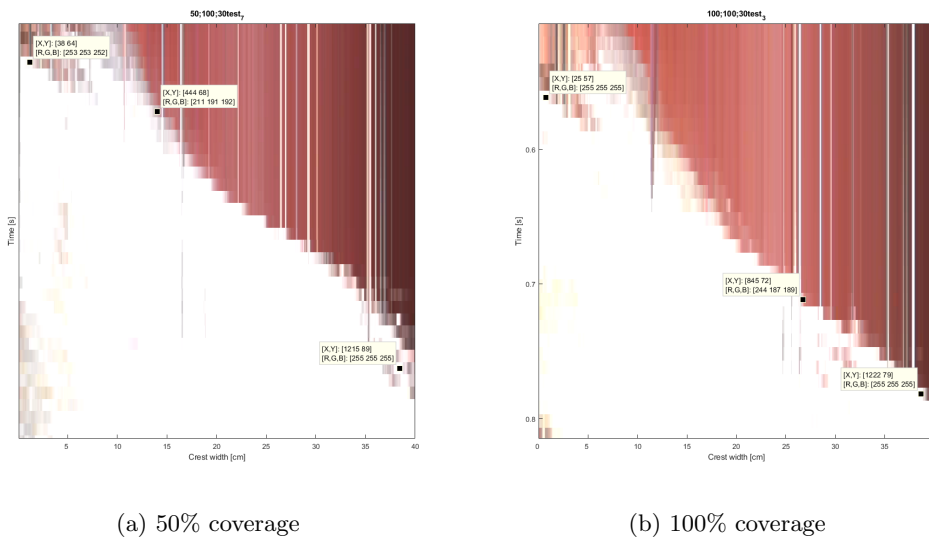
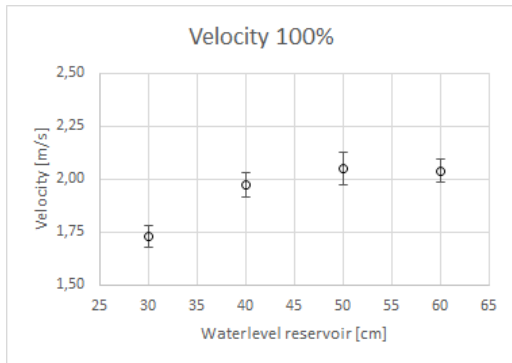


Figure 3.12: Zoom-in on the front velocity of the overtopping wave event over the rest

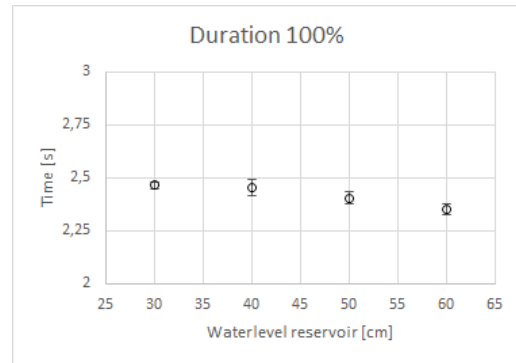
As can be seen in both images it is difficult to tell which pixels represent the outer layer

of the wave front. Both pictures do have a 'splash' which is observed in the upper left corner. This is neglected for the determination of the front velocity. When a linear line is drawn between the most outer data point it seems to be fair average velocity. Both pictures show a white spot in the upper left corner. This spot is observed in all tests and corresponds to a splash which preceding the main wave body. In the lower right corner differences are visible. The slope of the wave over the 50% seems to increase. This means the wave takes more time to propagate over a smaller distance. This does not happen for the 100% coverage. It seems as if the friction part only plays a significant role for crest widths bigger than 35 cm and for a packing density of 50%.

This example is repeated 10 times for water levels in the reservoir of 30, 40, 50 and 60 cm. These values were chosen because the theoretical values of the waves are situated within this range. For the the 100% coverage this resulted in the following graphs for the velocity of the wave front and the duration of the overtopping wave. Included is also the error bars of the standard deviation.

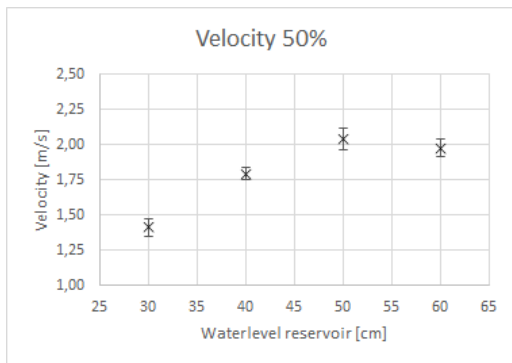


(a) Velocity of 100% coverage

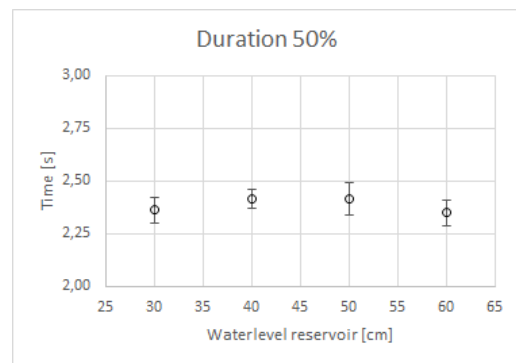


(b) Duration of 100% coverage

For the 50% coverage the following results are obtained:

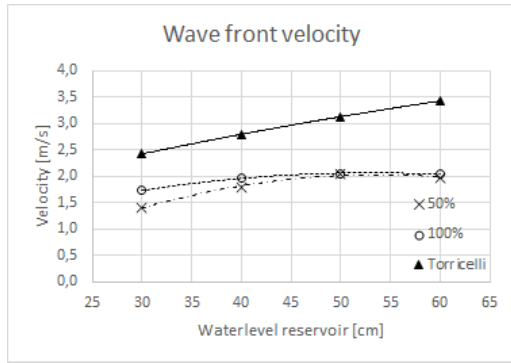


(a) Velocity of 50% coverage

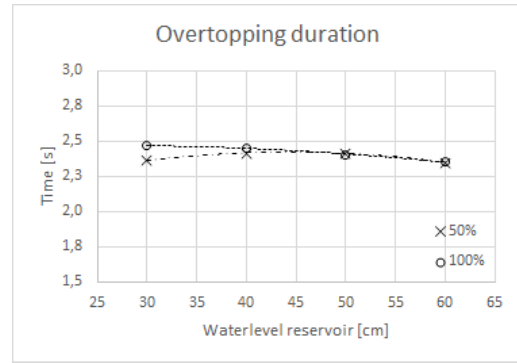


(b) Duration of 50% coverage

For both the 100% and the 50% coverage one can see that the error bars are small, meaning a small standard deviation. For test results this is a positive sign because it means that the performed tests are repeatable. For these tests the standard deviation did not exceed 4%. When these two observations are gathered and presented in the same figure the following figure is obtained as follows:



(a) Velocity overview



(b) Duration overview

The results of the video analysis show only a small difference in velocity between an impermeable crest with a 100% coverage and a partly covered crest with a coverage of 50%. Both velocities are below the velocity which is found when applying the equations found by Torricelli. Possible reasons and explanations will be discussed in the section 3.5.

3.4.2 Wave gauge measurements

Rietmeijer (2017) experienced a lot of noise during measurements using wave gauges and was not able to obtain data. In the present research the obtained noise is filtered using a Butterworth 3rd order low-pass digital filter with a cut-off frequency of 0.01. As can be seen in the following figure the filtered results give a correct representation of the results without the noise. The figure gives an overview of the several steps which are taken to obtain a velocity of the measured wave. As mentioned earlier in this report use is made of several wave gauges to measure accurately the velocity.

The maximum values of the specific discharge, wave layer thickness and velocity are gathered. In addition, the volume of the water leaving the reservoir is measured. And the volume of water passing the wave gauge is calculated by determining the surface of the specific discharge plot. This is done by applying trapezoidal numerical integration with the obtained data.

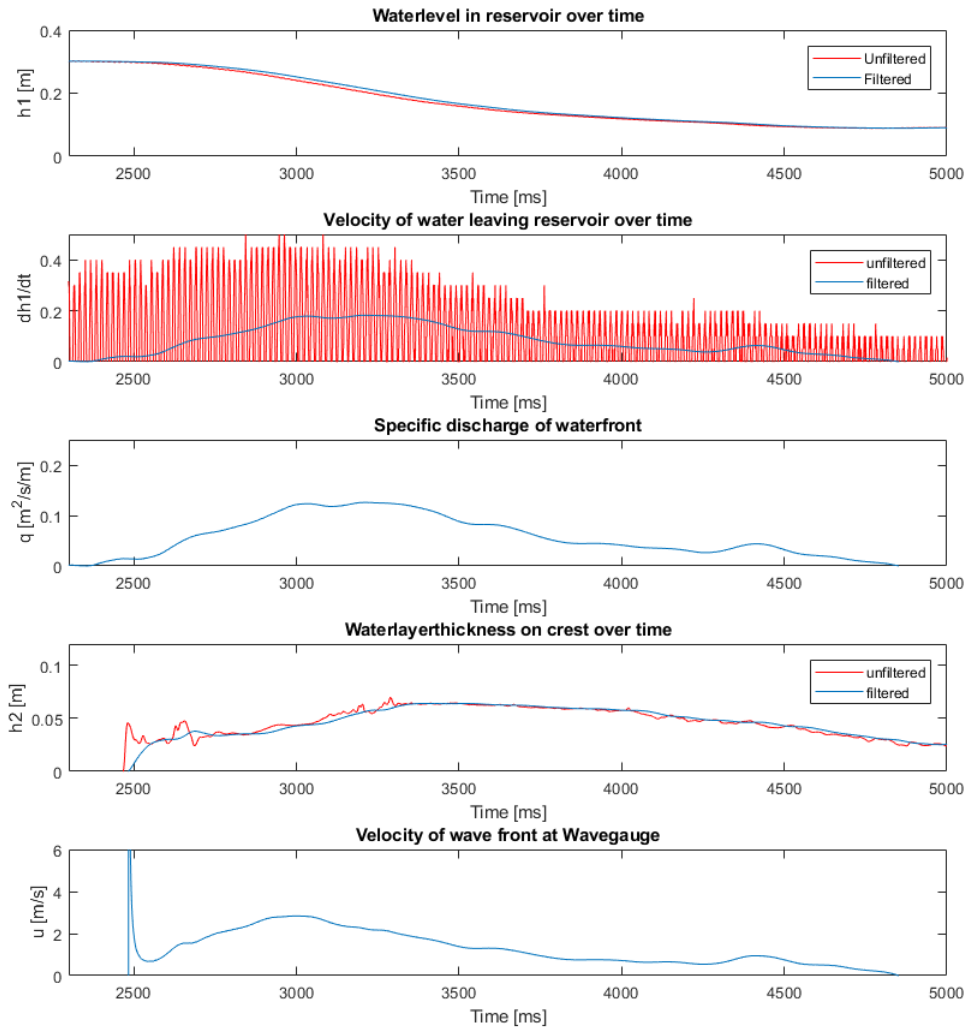


Figure 3.16: Overview of results obtained with wave gauges. 50% coverage, valve opening of 100mm and reservoir level of 30cm

For the example shown in Figure 3.16 the following results are obtained: The maximum specific discharge following from the derivative of the water surface in the reservoir and the surface area of the reservoir leads to a value of $q_{max} = 0.126m^3/s$. The maximum wave layer thickness measured is: $h_{max} = 0.064m$. When combined, these two findings lead to a measured maximum velocity of: $u_{max} = 2.839m/s$. When looking at the volume that leaves the reservoir, being the area of the reservoir multiplied with the difference in water level, and comparing this to the surface of the specific discharge multiplied with the width of the overtopping wave it can be seen that 102.88 liters leave the reservoir and 100.40 liters pass the wave gauge. These values are interesting because they are a check to see whether the measured and calculated values agree.

When we execute the same calculations and measurements for a wave with a coverage of the crest of 100% we obtain the following figure:

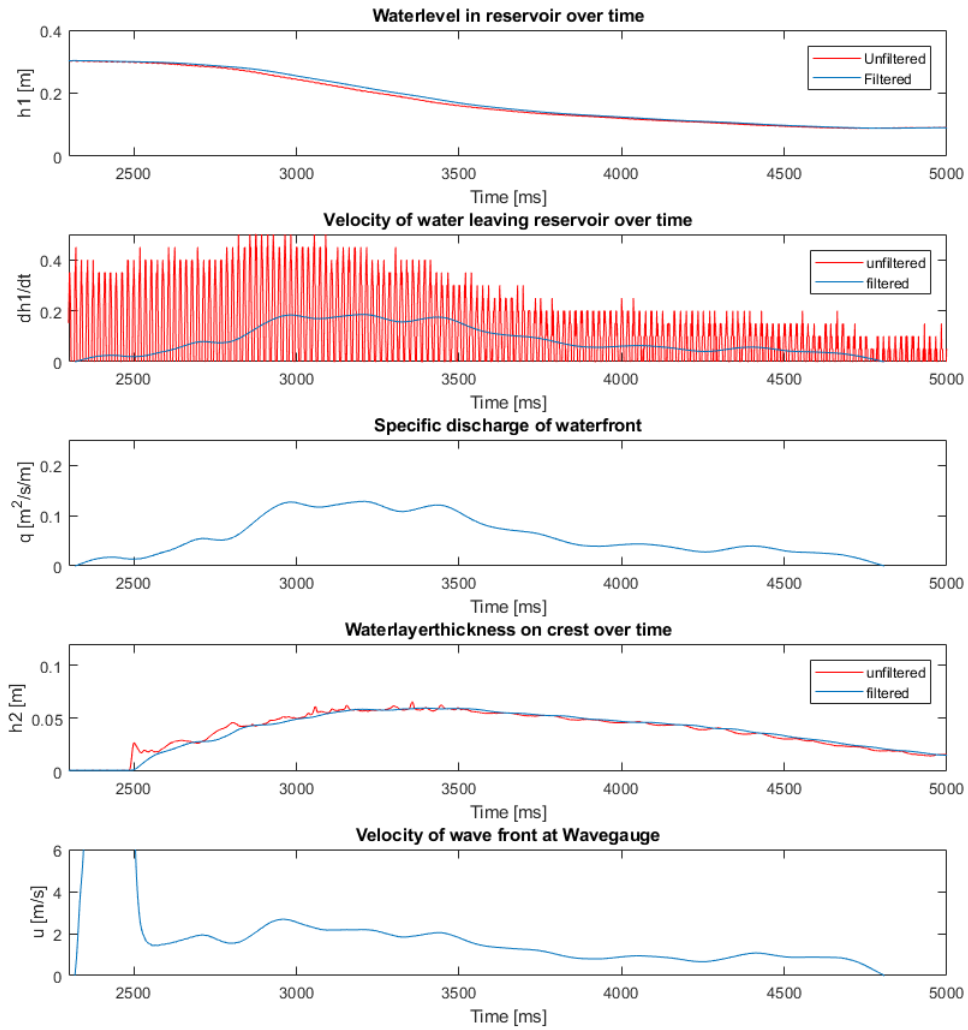
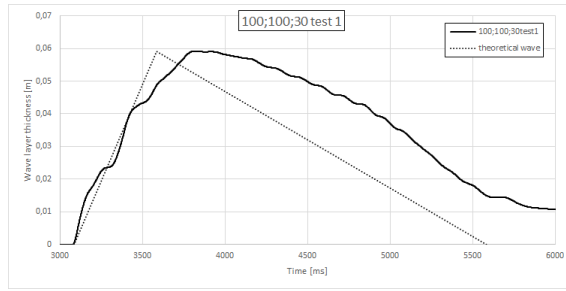


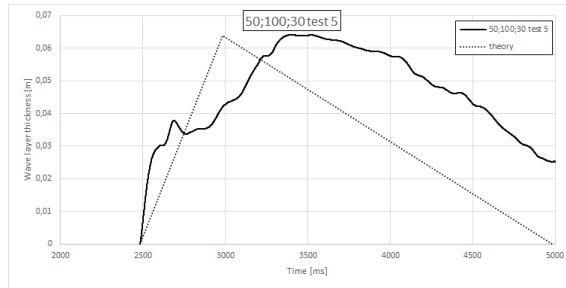
Figure 3.17: Overview of results obtained with wave gauges. 100% coverage, valve opening of 100mm and reservoir level of 30cm

The values found by Figure 3.17 are: $q_{max} = 0.128 \text{ m}^2/s$, $h_{max} = 0.060 \text{ m}$ and the maximum velocity $u_{max} = 2.682 \text{ m/s}$. The volume leaving the reservoir is 103.86 liters while the surface area of the specific discharge is 101.09 liters.

A closer look at the wave front steepness and the overtopping period, being the total time of the event, is taken in the following figure. In addition, the measured values are compared with the theoretical characteristics of a single overtopping wave in the following figure.



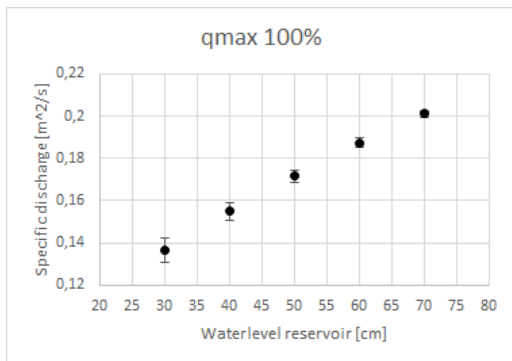
(a)



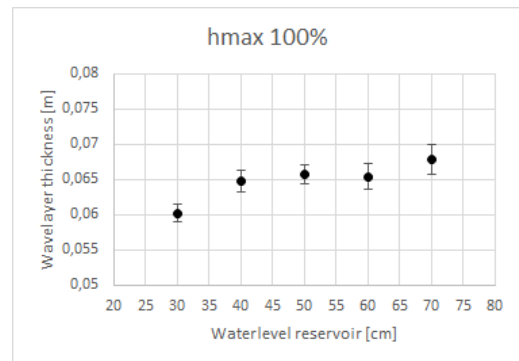
(b)

Figure 3.18: Measured wave steepness compared with theoretical wave steepness

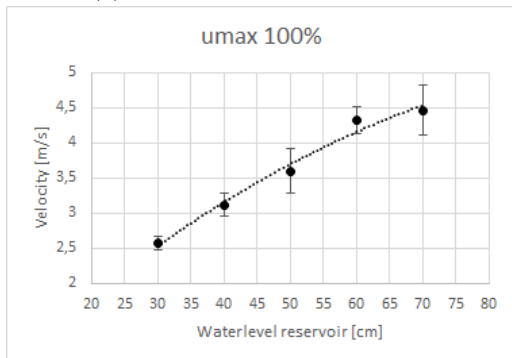
In Figure 3.18 an arbitrary wave has been chosen from the data set of the 50% coverage and the 100% coverage. Subsequently a theoretical wave has been added for comparison. This means; a wave with a time to reach h_{max} which is $1/5$ of the total overtopping time. In the figure the discontinues motion of the linear actuator is visible. This gives a delay in the peak value of the layer thickness. After the peak the slope of the theoretical wave and the actual wave are quite similar. The tests have been repeated ten times and the results are combined in the following graphs. For the case of 100% coverage:



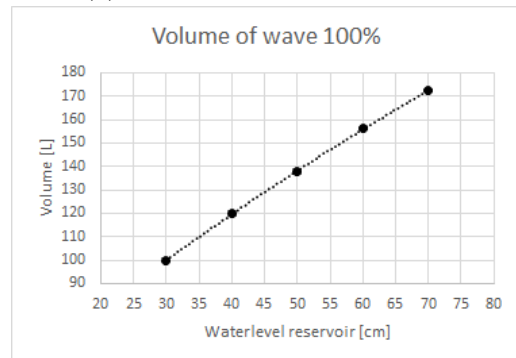
(a) Maximum specific discharge



(b) Maximum water layer thickness

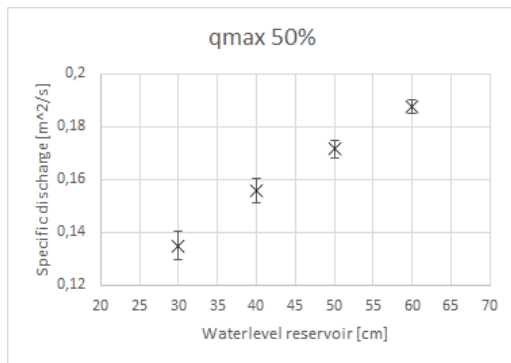


(c) Maximum velocity

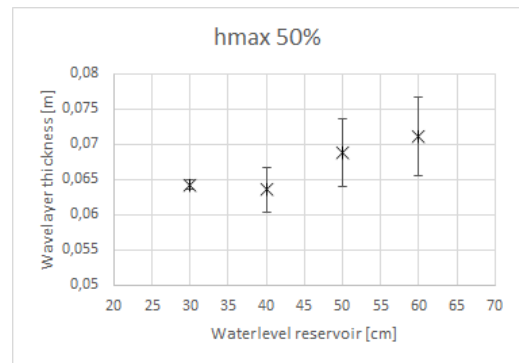


(d) Maximum volume

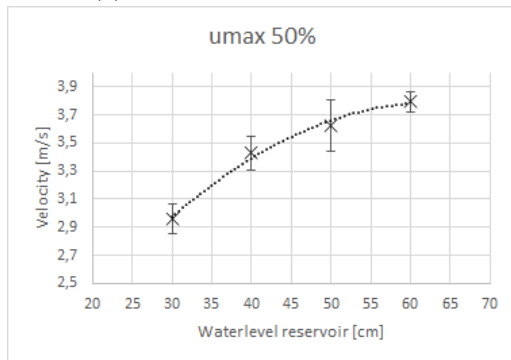
For the case of 50% coverage:



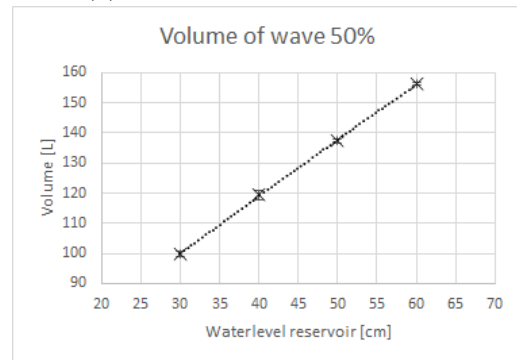
(a) Maximum specific discharge



(b) Maximum water layer thickness

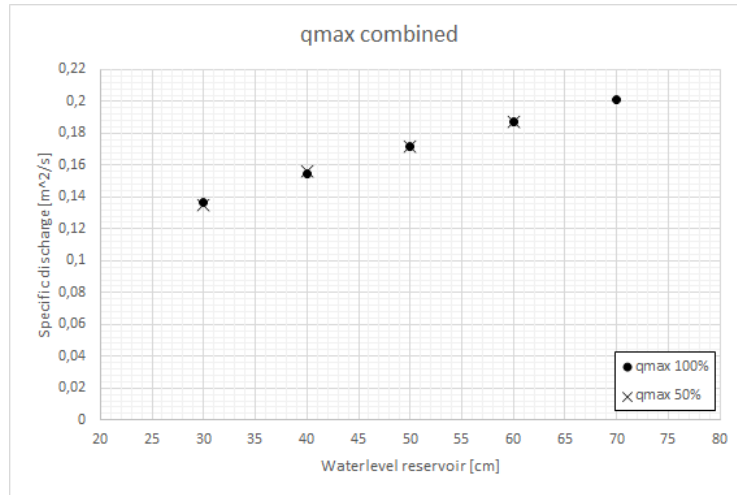


(c) Maximum velocity

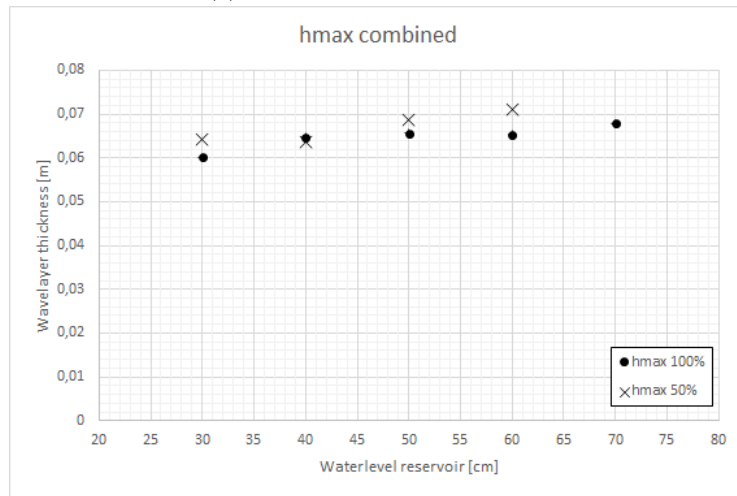


(d) Maximum volume

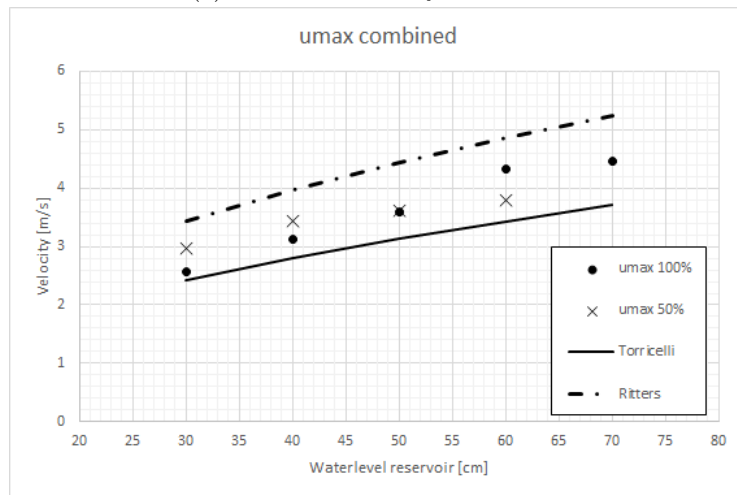
The error bars have been included to visualize the standard deviations of the ten measurements. In some cases, for example the volume, the error bars are so little they are not visible in the graph. Again the measurements of the coverage of 50% and the coverage of 100% have been joined together:



(a) Maximum specific discharge



(b) Maximum waterlayer thickness



(c) Maximum velocity

Figure 3.21: 50% and 100% coverage results of wave gauges combined

3.4.3 Combined results of the two measuring methods

The results of two different measuring techniques have been presented and will now be joined together to see if their values correspond to one another. The joined diagrams will then be discussed in section 3.5. In both measuring methods the velocity of the overtopping wave was

central because this research believes it plays an essential role in the process for rear slope stability. The results are combined in the following figure:

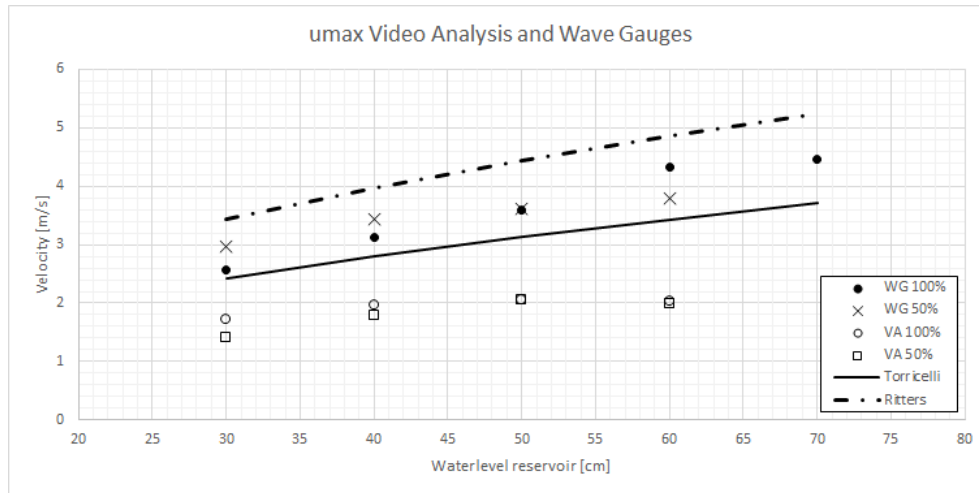


Figure 3.22: Velocity results of Video Analysis (VA) and Wave Gauges (WG) for both 50% and 100% coverage.

Tables and data used to produce the figures above are available in appendix B.

3.5 Conclusions

3.5.1 High-speed video measurements

Video analysis was thought to be difficult with available devices at the Waterlab of the Delft University of Technology. 25 frames per second produce to few frames per second. When shooting a video of a wave travelling at 2.5 m/s, between each frame the distance travelled is 10 centimeter. This distance is too large. By upgrading the video camera from 25 fps to 100 fps improvements are seen. The results of the video analysis show very little error bars. This means that the measurements are repeatable and consistent. Especially the measurements of the duration of the overtopping event have a very small percentage of standard deviations of no more than 1,6%. In addition the found values correspond to the set overtopping duration of 2,5 seconds which was very good for the lower reservoir water level and reasonable for the higher reservoir levels. This could be because the duration is harder to define or less accurate for higher wave velocities. For the velocities measured by video camera It was observed that the difference between 50% coverage and 100% coverage is small. Both velocities tend to be asymptotic for higher water levels in the reservoir of 2,0 m/s both for the duration and the velocity the difference in values between a coverage of 50% and 100% is small and it is concluded that this difference is negligible. Looking at the small error bars and the small difference between the percentages of coverage, it can be concluded that for further research the aspect of coverage ratio should not necessarily be taken into account for small crest widths. To sum up:

- Video analysis combined with frame stacking produces clear results as can be seen in Figures 3.10 and 3.11.
- The pre-defined duration of 2,5 seconds is a good measurement for smaller reservoir levels and reasonable one for higher reservoir levels.
- The measured velocity is lower than the values calculated by applying Torricelli. One should keep in mind that Torricelli is determined for stationer flow which is not the case here.
- The difference between a coverage of 50% and a coverage of 100% is insignificant in these tests.

- Video analysis is a good method for measuring overtopping duration per single overtopping wave event. Especially zoomed-in on the wave front valuable information is obtained on water velocity development over the crest.
- For velocity measurements video analysis might not be suitable as the camera is only able to measure the wave body which has a certain white value per pixel. Valuable information on front velocity is missed in this way.

3.5.2 Wave gauge measurements

The wave gauge measurements were analyzed using a matlab script and filtered by applying a Butterworth 3rd order low-pass digital filter with a cut-off frequency of 0.01. In this way clear wave forms were measured and the data was particularly useful for this research. As the wave gauges are very sensitive the most clearest measurement, taken from the meter inside the reservoir, gives a good indication of the specific discharge of the water leaving the reservoir. This combined with a wave gauge on the crest gives a clear representation of the wave at the beginning of the crest. The difference between 50% coverage and 100% coverage of the armour on the crest is very small at the position of the used wave gauge due to the fact that the possible friction of the crest has no influence on the wave. The wave layer thickness taken for several water levels in the reservoir for 100% coverage consistent results with low and constant standard variations of all the results around 2%. For the 50% coverage the measured wave layer thickness is of the same magnitude, but the standard deviation is bigger, and increases with increasing water level in the reservoir. This can be explained by the fact that the wave gets bigger and faster and the water gets more turbulent by interacting with the crest. The determination of the velocities over the crest has resulted in clear figures that show that the velocity increases for higher water levels in the reservoir. Comparing the velocities found with theoretical values obtained by applying Torricelli and the Ritter dambreak solution, one can see that the values lie in between them. Torricelli is actually designed for stationary flowing water, which is not the case here. So it is imaginable that the velocity is higher than this line. And the Ritter dambreak solution accounts for the very tip of a sudden released waterbody. The results of the velocity are low than this value due to friction with the surface of the crest, which causes the front end of the wave to bulge and so the front velocity decreases. It can be concluded that the measured velocities are in line with expectations and used literature. In conclusion:

- Wave gauges are suitable for measuring the volume which leaves the reservoir after the opening and closing sequence of the valve. Standard deviation is small and the increase in water level of the reservoir leads to a linear increase in specific discharge over the crest.
- For measuring wave layer thickness the wave gauges are suitable for 100% coverage, standard deviation around 2%, but less suitable for a coverage of 50%, standard deviation increasing from 1% for 30cm and 8% for 60cm.
- The velocity which is in this case calculated from the specific discharge and the wave layer thickness shows an increase for increasing water level in the reservoir. The standard deviations are within 9%, so they are believed to be acceptable. Due to friction with the underlayer the velocity is smaller than the Ritter dam break solution.
- By applying wave gauges for a 50% coverage and a 100% coverage both measurements are compared. For the specific discharge it is logical that the differences are small. For the wave layer thickness the differences in results are small, however the standard deviation and thus the certainty of the measurements is bigger for the 50% coverage tests.
- All standard deviations are well within ranges to conclude Wave Gauges can be applied in this research to measure specific characters of overtopping waves.

3.5.3 Conclusion on verification of Wave Overtopping Simulator

The system as built in the Waterlab of the University of Technology in Delft was designed to produce quasi-instantaneous waves which could model and overtopping wave event. By using different methods to measure wave characteristics it is concluded that the simulator is capable of producing an overtopping wave which can be coupled with a certain storm consisting of a

combination of significant wave height and peak period of waves. In addition it can produce certain waves which have a predefined probability of exceeding. In this way the simulator is believed to be use full in the research for overtopping waves and its effect on the stability of rear side cubes. A critical side note on the machine is that the opening mechanism needs improvement. This can clearly be seen in Figure 3.18a and Figure 3.18b by its chunks in the slope of the increasing wave layer thickness over time. Because of this, the wave reaches its maximum value later than theoretically. The slope of the decrease in wave layer thickness corresponds well to the theoretical value and it is believed that when the opening of the valve is improved the overall shape of the simulated wave corresponds well to the theoretical shape. In conclusion:

- The performed tests have shown that the Wave Overtopping Simulator as built in the Waterlab of the University of Technology Delft is capable of producing a single overtopping wave event which can affect rear slope stability.
- The difference between 50% coverage and 100% coverage is very small for both measuring techniques. Because of the lower standard deviation of the answers obtained when applying a coverage of 100% it is decided that 100% coverage is suitable for further research.
- The simulator is able to produce a quasi-instantaneous wave which is steep when the quasi-instantaneous wave is defined as a wave which reaches it maximum value within 20% of the total overtopping duration.

Chapter 4

Stability research

In this chapter the purpose of the model test will be described. A complete set of parameters as well as a complete set of dimensionless parameters will be provided that are of importance to the research. The scaling laws will be discussed as well as the mitigation of these effects. And a reference to previous research with a comparable set-up will be made and recommendation following these researches will be taken into account.

4.1 Methodology

The theoretical background of the physical model test, as described in chapter 2 is divided in three elements:

1. **Wave volume V , layer thickness h_{max} and velocity u_{max} .** These are the input parameters of the model. They are calculated and the volume, layer thickness and velocity can be adjusted by the operator. They are known and form the base of the overtopping wave event. The calculations are based on research performed by Zanuttigh et al. (2013) and Hughes (2015).
2. **Development over the crest.** For the development over the crest only empirical formulas are known which were developed by van Gent (2002) and Schüttrumpf and Oumeraci (2005). These formulas are empirical and are formulated for non-permeable slopes. These formulas have been used by Bosman et al. (2008) and Coticone (2015) to check if similarities were found. It was concluded that this was the case. For the validation of the overtopping simulator as developed by Rietmeijer (2017) these formulas will be used.
3. **Impinging wave.** The damaging element, the impinging wave, has been discussed in Kudale and Kobayashi (1996) and formulas have been provided to determine the position and velocity of this wave. In this research it is hypothesized that the impinging wave is the main element of damage and thus its position of impact is of importance. This is however not the only possibility. Other possibilities for contributions to damage to the rear slope are the quasi-steady flow or exfiltration. For the geometry of the set-up it is valuable to know where the impinging wave will strike the slope and its velocity. This knowledge will be used to try and link it to a damage parameter.

The work plan is based on these three elements and for each element preparatory calculations have been which are discussed in 2. In the following figure an overview is given of the design of the set-up:

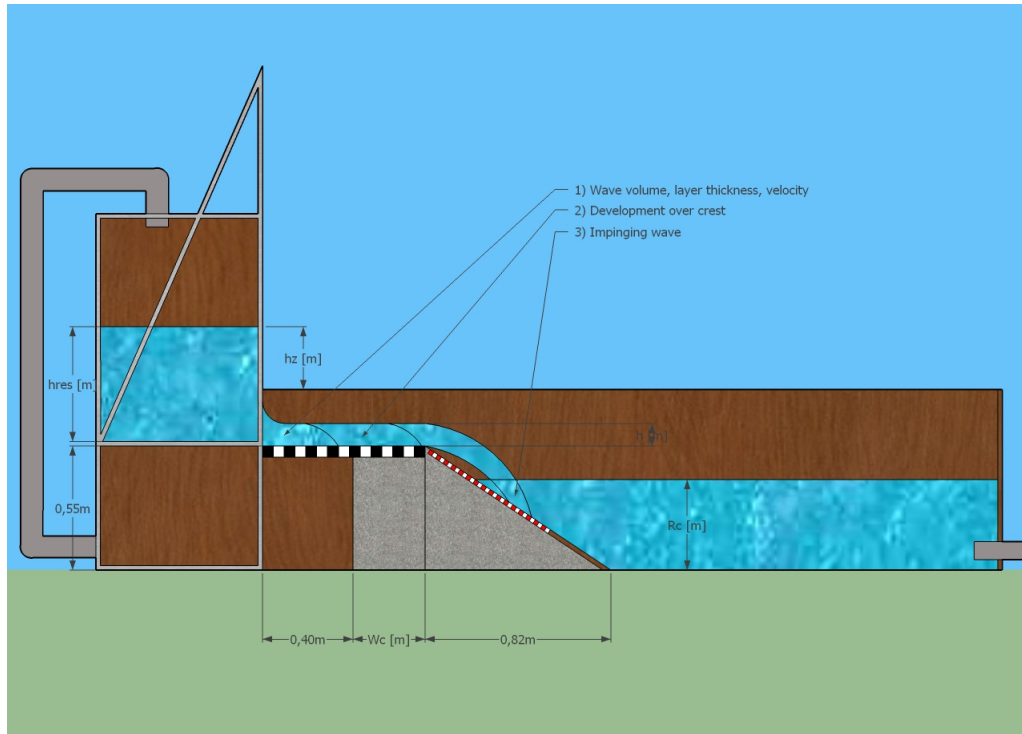


Figure 4.1: Design of the test set-up as built in the Fluid Mechanics Laboratory of Delft University of Technology

4.2 Breakwater geometry

This section will elaborate on the material dimensions and show technical drawings of all structural dimensions. Description of the material used in the model will also be given.

Model set-up

In the Waterlab at Delft University of Technology, room has been reserved to build a set-up which will be used to gather data on rear side stability of a cubic armour layer. Use is made of the wide flume which has a glass, see through window on one side which will be used to gather visual data. The floor of the flume is made of concrete and is strong enough to support the overtopping simulator and people working on the set-up. The reason why the tests for this research will not be conducted in a regular flume is that there is no need for a full length flume. The only requirement is that a supply of freshwater is available to fill the tank and a drainage for exceeding water. An overview of the set-up is given below:

The actual set-up used in this research is shown in figure 4.2



Figure 4.2: Set-up as built in Waterlab

The reason for using an overtopping simulator for physical model testing is that it has certain advantages over the use of a full flume. Firstly one has exact knowledge of the magnitude of hydraulic parameters which describe the overtopping wave. When using a flume, every spatial step, from offshore wave conditions to breaking on the breakwater, introduces new influencing factors on the propagating wave. It is extremely difficult to quantify these influences. Especially at the transition from the seaward slope to the crest, the scatter in simulated waves is big. By using a simulator the amount of deviation in the hydraulic parameters is minimized by excluding the factors before the start of the crest.

In addition, it is possible to test larger test scales without the requirement of a real wave. Real waves need 3-4 times the wave height as depth. Hence, only small waves can be tested. With a simulator this is not the case and the total dimensions of the set-up can be reduced, while increasing the maximum wave height which can be simulated. By increasing the scale of the waves scaling errors are decreased as well.

A disadvantage of using a simulator is that the link to an actual sea state is always solely based on theory and that the actual offshore wave conditions are merely an estimation of the real situation. Furthermore a simulator simplifies the reality and requires assumptions which are based on logical reasoning rather than on scientific facts. For instance the validation of the system needs to be done to ensure that when tests are executed using a simulator are compared with tests executed using a full length wave flume can be compared. However, in the stage the research and knowledge on the subject is now, a simulator is suitable to gain insight on the matter and make a big step in gathering data on overtopping waves. Subsequently the results can be compared to tests done in a wave flume

Wave Overtopping Simulator

As mentioned before for the collection of data, use will be made of an overtopping simulator in combination with a single breakwater configuration. A detailed technical overview of the simulator is given in appendix A.

The dimensions of the reservoir are, width x depth, $0.74 \times 0.70m$ and by adjusting the water level the speed of the out flowing water can be adjusted. The valve of the simulator can be opened up to a height of 20cm. The height of the reservoir and sliding door is 1m so a maximum of 500 liters can be simulated at once. To mimic the characteristics of an overtopping wave, the opening and closing of the valve should occur very precise. Hughes (2015) states that the flow can be schematized as being quasi-instantaneously. In order to simulate this, the valve has to open with a high velocity. This is achieved by using a linear actuator to operate the door. This is a Nitek linear motor that can deliver an instant force of more than 1100kN, depending on the opening distance this means an opening time of approximately 0.15s. The steering of the actuator is done by using a PC program called SoMove from Schneider Electronics. In this program the piston of the actuator can be steered by means of a written script. A detailed sheet of specs can be found

in appendix C

Breakwater model

For this research cubes are used which have a diameter of $d_n = 20mm$. The dimensions of these cubes are determined by analyzing the results obtained by Hellinga (2016) and Rietmeijer (2017). The cubes will be placed under an angle of 1V:1.5H and during placement wedges will be used to ensure a certain density of placement. In van Gent (2002) it is recommended to use a placement porosity of 20 – 25% for concrete elements placed on the front slope, in this research a porosity of $\approx 38\%$ is applied. As mentioned in Rietmeijer (2017) the transition from crest to rear slope is of great importance. It is chosen to make this a sharp transition as to make sure the failure will be on the rear slope instead of at the transition. In addition it is chosen to make use of a fixed toe.

To ensure that the requirements of stability are met while at the same time ensuring a regular placement of the cubes a ratio of cubes to filter layer of $\frac{D_n}{D_{n50, filter}} = 1,8$ is used, van Gent (2002). In this way a geometrically closed filter is applied to avoid erosion of the filter and core material. When applying cubes of 2 cm this results in a filter material: Marne jaune split 10-16 mm with $d_{n50} = 14mm$. A check is executed with the three stability guidelines posed in Schiereck and Verhagen (2012): Stability: $\frac{d_{15A}}{d_{85F}} < 5$; Internal stability: $\frac{d_{60}}{d_{10}} < 10$; and permeability: $\frac{d_{15A}}{d_{15F}} > 5$. By applying the Marne Jaune split the first two rules are obliged, the third rule is low. However this is compensated by using a high porosity of the armour layer so no build up of pressure can occur.

To induce sufficient turbulence in the overtopping wave tongue a certain length is reserved solely for the purpose of increasing the turbulence in the wave tongue. Previous research has indicated that a length of 40 cm seems sufficient from visual observation. A transect of the breakwater can be found in figure 4.3:

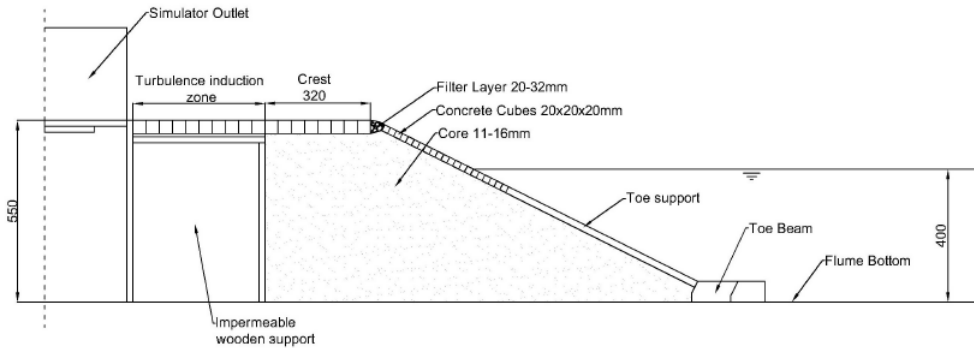


Figure 4.3: Transect of breakwater configuration, Rietmeijer (2017)

4.3 Instruments and measurements

The instruments used in this test set-up will be used to obtain wave heights and images to determine wave overtopping layer thickness and flow velocities. For each individual instrument the following points will be worked out:

- a Instrument type
- b Description calibration method
- c Selected sample frequency (Nyquist frequency)
- d Expected accuracy of measurement (of final engineering quantity after processing)
- e Range of measurement (usually between noise level and largest readable value)

f Discretization step / revolution

g Accuracy of the final answer

Depth meter in the box

The water in the reservoir can be monitored to determine the volume of water that exits the simulator. To determine the plunge, it is necessary to measure the development of the water-level over time. (ad.a) The water depth is measured using a fixed steel ball on a guidance rail. This, however, only gives accurate measurement until 4,5 cm above the bottom of the reservoir. For verification, a water gauge is placed which can measure even lower water heights. (ad.b) Both measuring equipment can be calibrated by a length scale which is fixed to the inner wall of the reservoir. (ad.c) It is believed that with a maximum emptying period of 5 seconds a frequency of 20 Hz will suffice. (ad.d) The expected accuracy will be 0.5mm. Close attention has to be paid that the water level in the simulator reservoir is stable and calm. (ad.e) For the steel ball it will be between 4.5cm - 1.0 m. With the wave gauge it will be 0.5 cm - 50cm. (ad.f) Discretization step will 1 mm. (ad.g) Due to the fact that not the length, but the volume of the reservoir is of importance for this experiment the magnitude of error will be $\sqrt[3]{E_{waterlevel}}$.

Side Video Camera

To measure the velocity of the water flowing over the crest in addition to wave gauges, a camera will be positioned on the side of the set-up. The camera used is a Sony FDR-AX33 digital 4K Video Camera Recorder. Through the glass window one will be able to photograph the development of the overtopping wave. A cross-section will be illuminated with lamps and the camera will film during an overtopping event. After analyzing the material, it is believed that the layer thickness and velocity of the wave tongue can be defined. (ad.a) 4K Video camera (ad.b) Calibrated using which checkered grid is placed inside of the glass wall to calibrate and minimize distortion.(ad.c) The Sony is able to shoot 4K, 3840x2160 in 25 frames per second or FullHD 1920x1080 in 50 frames per second. (ad.d)The accuracy of the video is influenced by the glass window giving an error of $\approx 1mm$. Furthermore the turbulence and fluctuation of the flow will give an additional $\approx 1mm$. For this measurement several repetitions are needed and a trend line should be fitted through the results. (ad.e)0.5-10cm. (ad.f) The film format in film mode of the video camera is 3840x2160 which is 8,3 megapixels. When fitted to the glass window the area filmed is 1246x700mm. These figures combined leads to 1 pixel $\approx 0.32mm$. For velocity measurements 50 frames per second is better. This results in 1920x1080 pixels meaning 1 pixel $\approx 0.65mm$. (ad.g)0.5cm.

Top camera for damage, horizontal displacement

To determine damage to the rear-side slope a camera will be positioned to monitor this process. This process includes the horizontal displacement of the cubes. A picture will be taken before and after to compare both moments in time. As mentioned in Hellinga (2016) it is necessary to enhance the contrast between the pores by installing two lights which illuminate the surface from the side. The pictures will be analyzed and damage number determined. (ad.a)Photo camera. (ad.b)-. (ad.c) Two photos per test. (ad.d) Width of flume is 76,5cm, using a camera of 6.1MP (3008x2008 pixels) results in 1 pixel equalling 0.25mm which is 0.5% of the flume width(ad.e) -. (ad.f) 0.25 cube size. (ad.g) -.

Laser scanner for vertical damage.

For the vertical displacement a laser will be used. This laser will make transects of the slope over a predetermined width to collect data on the elevation of cubes before and after a storm. After processing these transects a 3d model is made in matlab of the slope, before and after a storm. Trial transects have been made in the flume which is currently used for research of Beulink (2018) and the results obtained can be seen in the following images.

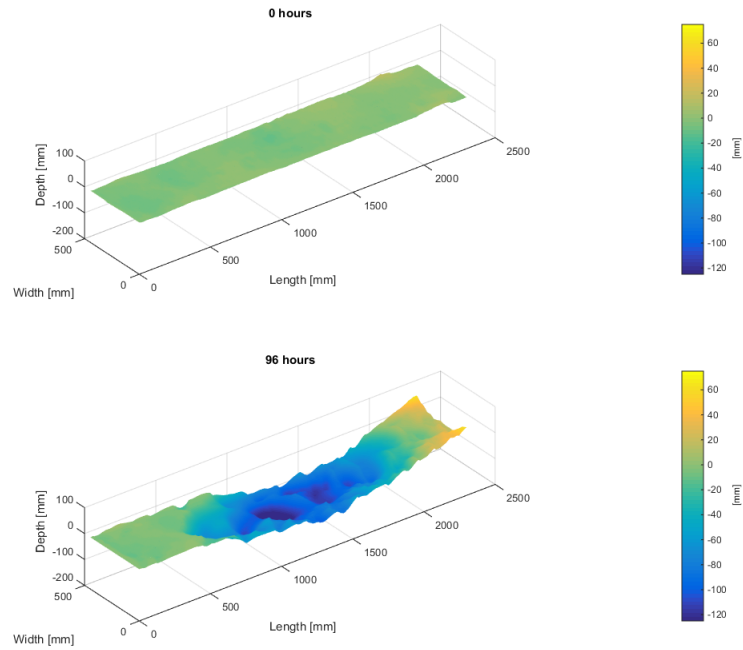


Figure 4.4: Transects made of a river bed at 0 hours and after 96 hours of flow

In this image the detail is very high which is positive. The laser used can read the elevation quite accurately and the plot looks representative of the development of the river bed in 96 hours. Another matlab script has been written which can calculate the difference in elevation between the transects. This can be seen in figure:

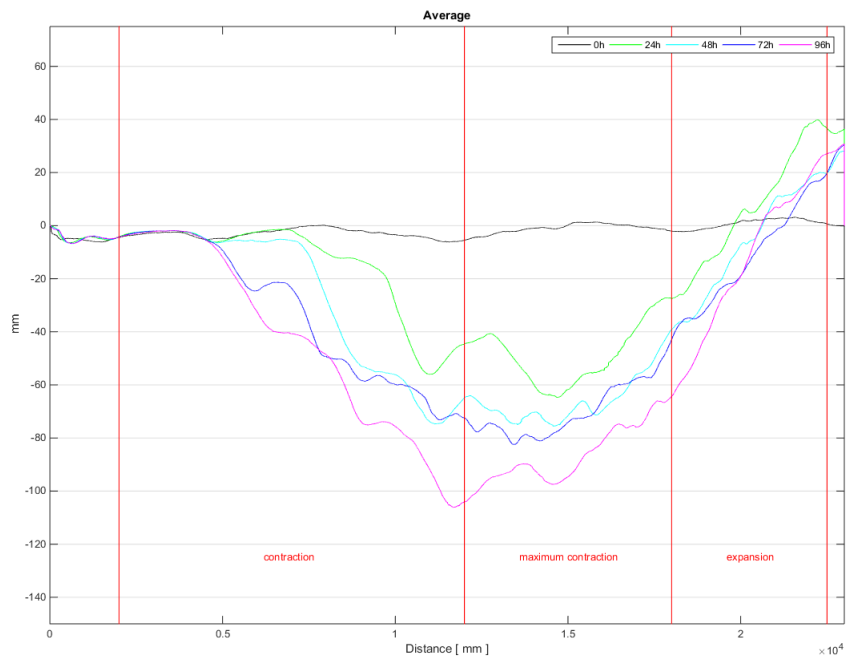


Figure 4.5: Difference for several time intervals of one transect

The laser which will be used during this research is an optoNCDT 1700 Intelligent sensor with integrated controller for industrial applications. With a start of 200mm and a end range of

950mm its measuring range is 750mm, which is sufficient for the height of the design breakwater used in this research. Its resolution at 2.5kHz without averaging is $50\mu\text{m}$. It is connected to a wheel which measures the distance of the laser travelled in horizontal direction. This is done to ensure that enough points are taken for high accuracy. It is set-up to take 1 point every 1/10m. The trajectory is 95cm and thus each file contains 95000 points in horizontal direction. This transect is taken every cm of the slope. In total 47 transects are taken for every storm damage measurement. An overview of the exact position of the instruments is given in figure 4.6 where the wave gauges are indicated by vertical stripes on the crest and the two cameras with their visual field on the set-up:

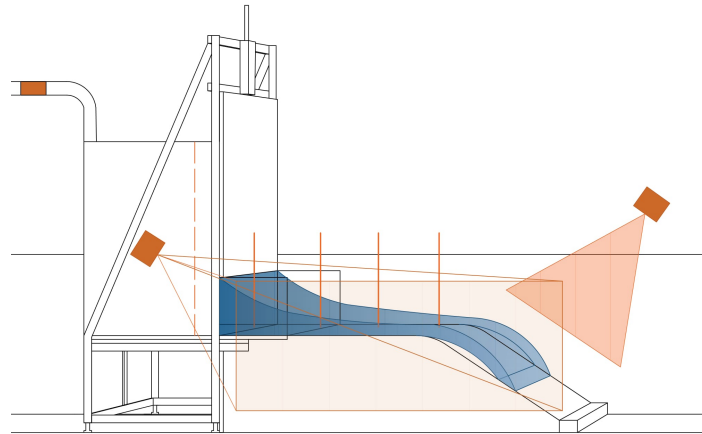


Figure 4.6: Positioning of measuring instruments

The physical model tests will be conducted in such a way as to find the point at which damage or failure occurs. At first the simulator must be calibrated and validated to determine if the simulator is capable of reproducing an overtopping wave event. Subsequently, a test series of irregular waves will be executed using a JONSWAP spectrum in which the significant wave height will be increased until failure of the rear-side slope. Before the actual test on failure and stability can be conducted, certain pre-tests must be done to take into account possible flaws and, where needed, adjust the simulator.

The measurements will be ordered in the following way. First the wave height metres in the box will be checked with the pre-calculated volumes. This will indicate whether the volume leaving the reservoir is representative for the storm which is tested. Subsequently the waterbody travels over the crest with a specific speed and wave layer thickness. These two parameters are measured by video camera and by wave gauges. These two methods of measuring must also be synchronized and compared to pre-calculated values. They measure the specific characteristics of the water body over the crest which will eventually create the impinging wave. The volume measured from the reservoir wave gauges together with the velocity of the wave front and the wave layer thickness on the crest following from video analysis and wave gauges, these two together are the input for the impinging wave and are synchronized. Next to this, the measurements of the camera on the slope and the laser determine the damage following from this 'storm'. The photo camera measures the horizontal displacement of the cubes, in the plane of the slope. The laser measures the vertical displacement, if cubes leave the plane of the slope. These two methods are synchronized as well to determine the amount of damage and to be able to conclude whether or not failure has occurred.

4.4 Recommendations from previous research

For the execution of the physical model tests a Wave Overtopping Simulator (WOS) will be used. This overtopping simulator is based on the simulator developed by van der Meer et al. (2006) and is built with dimensions based on the formulas of van Gent (2002) for modelling layer thickness and flow velocity of a wave tongue over the crest of a breakwater.

The actual simulator to be used in the present research is developed by Rietmeijer (2017) at the Delft University of Technology. This simulator has been designed to model overtopping waves to decrease uncertainties that arise when a breakwater is tested in a long flume as was done in the

research conducted by Hellinga (2016). Both studies gave more insight in the event of an overtopping wave however both experienced complications as well. As both papers describe similar subjects, their recommendations are summarized below:

Hellinga:

In this research due to a lack of data no clear relation could be found between the important hydraulic parameters, such as H_s and T_p , and rear slope stability. It is stated that smaller subsequent steps between significant wave height H_s values and more variations in parameters should be applied. This was done to give a clearer view of the start of damage. Less attention should be paid to the inner slope angle, since this parameter has almost no influence on rear slope stability. In addition, it was pointed out that the transition from crest to inner slope is an important aspect of the stability.

Rietmeijer:

During this research the wave overtopping simulator was designed and constructed and first tests were conducted with the device. Unfortunately no relation has been found between overtopping wave characteristics and stability of a single armour layer of cubes. In this report however, there are some valuable recommendations which should certainly be taken into account. To overcome the problem with the lack of knowledge regarding the exact volume in time inside the reservoir when the valve is opened, firstly, multiple floats should be installed next to each other in flume-axial direction in the reservoir. The devices should be placed next to each other with small intervals, an indication of 12 cm was given. This will significantly increase the accuracy of the water level measurement in time and consequently the applicability of the results.

Secondly, it is recommended to install 4,5 cm thick plexi-glass or perspex plates on both sides resulting in a decrease of the width downstream of the WOS. This adjustment helps to get a straight flow by cancelling the anomalies introduced by the difference of the simulators reservoir and the flume, such as eddies, deformed wave front and splashing of water up against the walls. Another result of this research is that a fixed toe should be applied as this is regarded to be less of a point of interest. To increase the range of layer thicknesses that the simulator can produce, improvements may be made to the valve in such a way that the door is more streamlined. From tests executed by Rietmeijer (2017) it was found that the orifice discharge coefficient is rather low, in the report set to $\mu = 0.5$.

In addition this report to conduct a full research into the velocities inside an overtopping wave volume and the turbulence of the wave front. This can either be done by improving the cameras used. In this specific research cameras have been used which are able to shoot 24 frames per second. This is considered by Rietmeijer (2017) to be insufficient for precise measurements. A second way to improve this aspect is to conduct Particle Imagery Velocimetry (PIV). This is an advanced techniques in which one can get clear data on velocities within a wave tongue, however, this is not in the scope of this research as the main concern is connecting wave volumes with rear slope stability. For future research the velocity development over the crest can most certainly be valuable.

A valuable recommendation about the rear slope stability is made in this report as well. This is also confirmed by reviewing current literature. Extrusion tests could be done to check if all cubes are well clamped. If the well clamped areas of a slope are clarified, a link may be made between the location of the found damage and the amount of clamping.

4.5 Scaling laws

When conducting physical model tests it is important to take into account scaling laws to guarantee similarity between a model and a prototype. The scaling laws discussed in Tirindelli and Lamberti (2000) are used as a base for this research. Three scaling laws are discussed:

Weber scaling

The Weber scaling describes the relative importance of the inertia of the fluid compared to the surface tension of the fluid. It is an indication of the dominance of either the surface tension keeping the water together as a droplet, or the fluids kinetic energy. Especially when the fluid contains entrapped air, the shape of the breaking wave can be influenced. A first rule for models with short waves is that the wave height should not be smaller than about 5 centimeter in order

to maintain similar breaking characteristics, van den Linde (2009).

$$We = \frac{Inertia}{Surfacetension} = \frac{\rho \cdot u^2 \cdot h}{\sigma} \quad (4.1)$$

In this equation the $\rho = 1000 \text{ kg/m}^3$, $u = \text{velocity m/s}$, $h = \text{water layer thickness}$ and $\sigma = \text{surface tension}$. The calculated value in this research is $We \approx 5 \cdot 10^3$.

Froude scaling

Froude scaling describes the flow of a waterbody by ordering it in three groups: Sub-critical, critical and super-critical flow, Schiereck and Verhagen (2012). It is the ratio of the kinetic versus potential flow; inertia and gravity forces.

$$Fr = \frac{U}{\sqrt{g \cdot h}} \quad (4.2)$$

In which u is the velocity of the fluid, g is gravitational acceleration and h is the layer thickness. In this study the calculated value is $Fr \approx 3.26$, which is super-critical flow.

Reynolds scaling

The Reynolds number describes the inertia versus the viscosity and indicates whether a flow is considered to be turbulent or laminar.

$$Re = \frac{u \cdot h}{\nu} \quad (4.3)$$

For normal circumstances $\nu = 10^{-6} \text{ m}^2/\text{s}$. And in hydraulic engineering practice the flow will always be turbulent, Schiereck and Verhagen (2012). In this study the calculated value is $Re \approx 1,5 \cdot 10^4$, turbulent flow.

Wave loads on rubble mound breakwaters have two main elements, impulsive load (peak load) and pulsating load (quasi-static), van den Linde (2009). The pulsating load is associated with a load of water travelling through the structure. Since the simulator does not account for wave action through the structure, as no use is made of a wave flume, the pulsating load is not taken into account. The calculated values for Weber and Reynolds exceed critical values and thus the scaling laws of Froude are applied. For the scaling rules the laws obtained by Froude will be used which gives the ratio between inertia and gravitation. When using this approach the following relationships can be derived:

Wave height	[m]	$n_h = n_L$
Time	[s]	$n_t = \sqrt{n_L}$
Velocity	[m/s]	$n_u = \sqrt{n_L}$
Acceleration	[m/s ²]	$n_a = 1$
Mass	[kg]	$n_M = n_\rho \cdot n_L^3$
Pressure	[kN/m ²]	$n_P = n_\rho \cdot n_L$
Force	[kN]	$n_F = n_\rho \cdot n_L^3$
Discharge	[l/s/m]	$n_q = n_L^{1.5}$

A list of dimensionless parameters which best characterize the research:

- Dimensionless stability parameter $N_s = H_s/(\Delta d_n)$
- Dimensionless crest height R_c/H_s
- Dimensionless instantaneous overtopping discharge $q/(g \cdot H^3)^{0.5}$
- Dimensionless time duration t/T_{ovt}

4.6 Test Program Stability Research

4.6.1 Fixed Toe

For the configuration with a fixed toe the wave series is used as presented in Table 4.1. This table is repeated here. As can be seen this test series exceeds the maximum value. This is done to ensure that the tail of overtopping waves does not account for any damage and to check the maximum value to be correct.

Rc = 0.15m										
Hs [m]	Tp [s]	$q/(g * Hs^3)^{0.5}$	Waves	Volume [L]	umax [m]	hmax [m]	qmax [m2/s/m]	To [s]	Hres [m]	Valve [m]
0.14	1.50	0.012	5	17	2.18	0.04	0.08	1.8	0.168	0.07
0.22	1.88	0.030	5	50	2.97	0.07	0.18	2.35	0.311	0.12
0.28	2.12	0.041	5	88	3.48	0.10	0.28	2.70	0.427	0.15
0.32	2.26	0.047	5	119	3.79	0.11	0.35	2.92	0.501	0.18
0.40	2.53	0.057	5	198	4.37	0.14	0.52	3.31	0.674	0.23
0.44	2.65	0.060	5	245	4.64	0.16	0.62	3.5	0.759	0.26

Table 4.1: Overview of the wave groups which correspond to storm conditions for Rc = 15 cm

For these waves the opening of the valve has been increased to simulate increasing waves. The water level in the reservoir has been kept constant in order to ensure that the wave hits the slope near the waterline. After repeating the wave 5 times the crest free board is changed and the following series are done:

Rc = 0.10m										
Hs [m]	Tp [s]	$q/(g * Hs^3)^{0.5}$	Waves	Volume [L]	umax [m]	hmax [m]	qmax [m2/s/m]	To [s]	Hres [m]	Valve [m]
0.14	1.50	0.028	7	20	2.35	0.05	0.09	1.87	0.195	0.07
0.22	1.88	0.049	6	57	3.16	0.08	0.20	2.43	0.352	0.12
0.28	2.12	0.058	6	98	3.68	0.10	0.31	2.78	0.477	0.16
0.32	2.26	0.063	5	132	4.00	0.12	0.39	3.00	0.563	0.19
0.40	2.53	0.070	5	216	4.57	0.15	0.57	3.39	0.736	0.24
0.44	2.65	0.073	5	266	4.83	0.17	0.67	3.57	0.823	0.27

Table 4.2: Overview of the wave groups which correspond to storm conditions for Rc = 10 cm

Rc = 0.20m										
Hs [m]	Tp [s]	$q/(g * Hs^3)^{0.5}$	Waves	Volume [L]	umax [m]	hmax [m]	qmax [m2/s/m]	To [s]	Hres [m]	Valve [m]
0.14	1.50	0.005	3	15	2.02	0.04	0.07	1.73	0.143	0.06
0.22	1.88	0.018	4	46	2.83	0.07	0.16	2.30	0.282	0.11
0.28	2.12	0.028	5	80	3.32	0.09	0.25	2.63	0.389	0.15
0.32	2.26	0.034	5	109	3.63	0.11	0.32	2.86	0.465	0.17
0.40	2.53	0.044	4	183	4.20	0.14	0.48	3.25	0.622	0.22
0.44	2.65	0.049	4	228	4.47	0.16	0.57	3.43	0.704	0.25

Table 4.3: Overview of the wave groups which correspond to storm conditions for Rc = 20 cm

As discussed in chapter 2 the wave intensity increases for decreasing crest height. In addition the amount of waves that occur for a high crest height decreases.

4.6.2 Non-fixed Toe

For these tests executed with a non-foxed toe, the fixed toe was replaced by a mass of filter material keeping the armour layer at the desired height. The tested wave heights have been lowered because it is hypothesized that the slope is significantly weaker. Furthermore the strength is decreased by applying a porosity of 38% as mentioned before to be able to initiate damage. In addition the configuration has been altered by increasing the amount of rows of cubic armour layer under water to see if there is a relation for the length of the armour layer and the stability of the slope. In these tests the crest height has been kept constant as well as the diameter of the cubes which have been used in the armour layer. The water level in the reservoir has been kept constant to ensure that the waves hit the slope just at the water level, the weakest point. This is not the ideal situation as sketched in theoretical approach. This was done to be able to perform as much tests as possible in the time frame. The following series is applied on a slope with a number of rows beneath the waterline ranging between 9 to 17.

Rc = 0.15m					
Hs [m]	Tp [s]	$H_s/(\Delta d_n)$	$q/\sqrt{g \cdot H_s^3}$	Waves	Valve
0.088	1.19	2.67	0.0021	2	0.035
0.100	1.27	3.03	0.0037	3	0.040
0.105	1.30	3.18	0.0046	3	0.045
0.110	1.33	3.33	0.0055	3	0.050
0.120	1.39	3.64	0.0074	4	0.055
0.130	1.44	3.94	0.0096	4	0.060
0.140	1.50	4.24	0.0118	5	0.065
0.150	1.55	4.55	0.0142	5	0.070
0.160	1.60	4.85	0.0165	5	0.075
0.165	1.63	5.00	0.0177	5	0.080
0.174	1.67	5.27	0.0199	5	0.085
0.184	1.72	5.58	0.0222	5	0.090
0.192	1.75	5.82	0.0240	5	0.095

Table 4.4: Wave series applied for Rc = 15 cm

By adjusting the valve height the wave height is increased leading to a more severe attack on the slope. The wave height is increased until failure of the slope occurs. A total of 50 test are done.

4.6.3 Crest Freeboard

To test the influence of the crest freeboard, laser technique will be used. A laser is able to measure the vertical and horizontal movement of a cube. A total of 47 transects will be made which start at the crest of the structure and measure a length of 95 centimeters along the axle of the set-up. where a data point will be measured every 1/10th of a millimeter. Between each transect 1 centimeter spacing is applied. This will results in a 3D surf plot of the slope with 9500 x 47 data points. During this test the wave series as presented in figure 4.4 are applied. Next to analyzing video results, the transects made with the laser are combined to form a 3D plot of the slope. This is done before the test and after the storm. The obtained difference plot can indicate if damage occurred and quantify this damage in order to obtain a damage parameter. The damage is quantified as a settlement s . This settlement is expressed as a factor of the nominal diameter after which different classes are defined for which settlement, damage, severe damage or failure occurs.

4.7 Data Analysis

This chapter discusses how the data will be analyzed and what outcome is expected. The calibration tests and wave tests must be analyzed before one can say something about the relevance of the different parameters. For both the calibration as for the overtopping waves test series the same measurement devices are used. This is in order to ensure consistency in the measurements. The objective of the test series is to determine the rear slope damage for different wave conditions. In order to find the desired parameters that influence the rear slope stability, several data processing routines are used which are discussed as well.

4.7.1 Wave characteristics

The wave gauges which are positioned on the breakwater measure the waves in voltages. The relevant parameters that are obtained from these measurements are the water level in the reservoir before and after testing, the layer thickness of the overtopping wave on the crest and the velocity of the wave front. The test series describe the expected outcome of these measurements. The accuracy and the way the waves are simulated by the Wave Overtopping simulator can be found in Chapter 3.4.

4.7.2 Rear slope damage

The rear slope damage is determined by a difference plot created by a matlab script with the use of two laser generated models of the rear slope before and after the overtopping wave event. In order to calculate the damage, 47 initial transects are made of the slope. Each transect contains 9500 data points that correspond to a voltage of the laser above the inner slope. A DasyLab script is used to set-up the link between laser and rotation wheel. After the waves, the transects are made again. By using the exact same reference point it is possible to compare both slopes by subtracting the former from the latter. In this way a difference plot is made which gives information on the movement of cubes.

The amount of damage can be expressed as the number of moved cubes relative to the the number of total cubes that fit in one row, the N_{od} . According to CIRIA (2007) start of damage for the outer-slope initiates for $N_{od} = 0.2 - 0.5$. For the present research start of damage amounts for $N_{od} = 0.3$, Hellinga (2016). However, N_{od} is a damage parameter designed for rubble mound structures where individual rocks leave the slope. In this research this may not occur and instead, settlement s is used. This can be both in vertical and horizontal direction. For example a settlement of 0.3 equals a distance of $0.3 \cdot 20 = 6mm$. For the vertical displacement the maximum displacement for a single cubes is $1.0 \cdot d_n$, meaning a complete removal of a cube from the rear slope. For the horizontal displacement failure occurs when the displacement exceeds the distance that the cubes overlay each other to comply with the 38% porosity. When the width of the flume is 78 cm and the porosity is 25% the amount of overlap between the rows of cubes is 9mm. If this overlap is exceeded, so $0.45 \cdot d_n$, then failure occurs. Due to the possible errors in the data processing, a displacement of less than $0.2 \cdot d_n$ is considered as no displacement. A visualization of the different types of displacement is shown in the following figures:

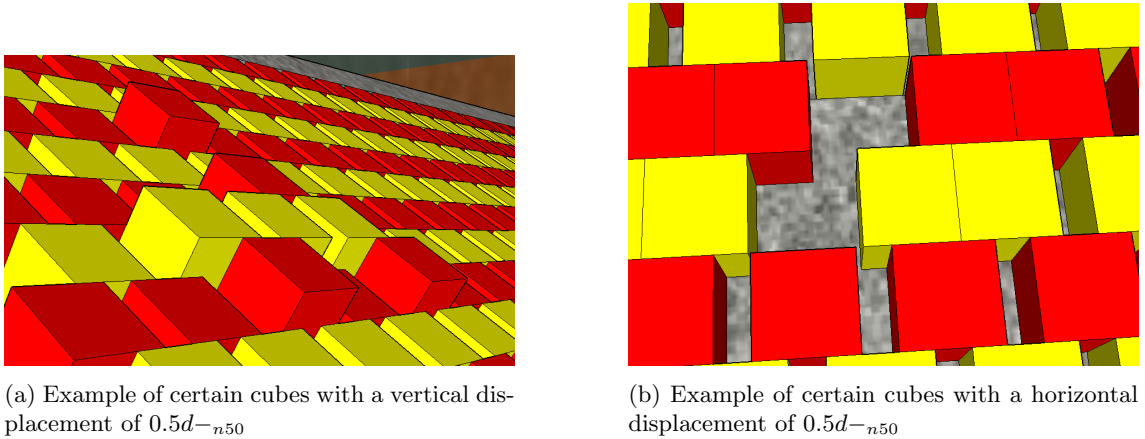


Figure 4.7: 2 degrees of freedom of the cubes

4.8 Results

4.8.1 Fixed toe

The first design of the set-up has a fixed toe to ensure that the damage occurs on the slope and is not a result of failure of the toe. This assumption is highly uncertain, and caution should be taken. The structure is built as can be seen in the following figure:



Figure 4.8: Test set-up built with a fixed toe

This set-up has a crest freeboard of 15 cm in combination with a 17 row counting single armour layer of cubes followed by a steel mesh roster with a high permeability. After execution of tests it was observed that no damage occurred. Increasing wave layer thickness, velocity and volume had no effect on the inner slope. The set-up was very strong and the cubes had a normal force which exceeded all expectations. Manually extracting a stone was difficult and clamping occurred evenly spread over the complete surface. It is observed that when the cubes are 'interlocked' in a certain pattern that the stability is fixed. No damage or movement of individual stones is observed. The wave series tested is shown in figure 2.3

When, after several hundreds of waves, suddenly failure occurs it is observed that erosion has taken place due to the fact that the metal roster does not have a tight fit with the sides of the basin. An interesting thing was observed; beneath the armour layer a hollow area had been created. Even with a hollow area under the armour layer still the center did not fail. The normal forces kept all the cubes perfectly in place. This can be seen in the following figure:



Figure 4.9: Photo's of the hollow space under the armour layer of the configuration with a fixed toe

This model effect led to the decision to change the toe. The fixed metal roster is replaced by a longer length of the armour layer, deeper under water. The stability of the toe was not part of this research, however failure of the toe results in failure of the complete armour layer, which indicates the high importance of a stable toe. However, this research focuses on the stability of units on the inner slope and so the fixed toe is replaced with a longer length of the armour layer.

4.8.2 Non-Fixed Toe

To initiate failure the set-up is adjusted by removing the fixed toe and by placing the cubes with a maximum porosity. This leads to an open space of $\approx 38\%$ per tested slope. Although it is common to apply an open space on the outer slope of 20 – 25%, the applied coverage ratio is significantly higher, however, it is justified taking into account the difficulties Hellinga (2016) and Rietmeijer (2017) had to initiate failure. As mentioned in 4.6 the Test Program, for the following tests a reservoir level of 30 cm was applied, to ensure the water hits the slope just at the water line which was believed to be its weakest point. Subsequently the opening distance of the valve is increased from 35mm until 95mm, to simulate waves ranging from 0.088m to 0.192m as can be seen in figure 4.4. This deviates from the plan presented in 2, however this pragmatic solution is applied since the time frame did not allow for further perfection of the simulated waves A couple of examples of the failure which was observed is presented in the following figures. For the corresponding codes of the specific test mentioned in the captions of the figures, please consult appendix D.

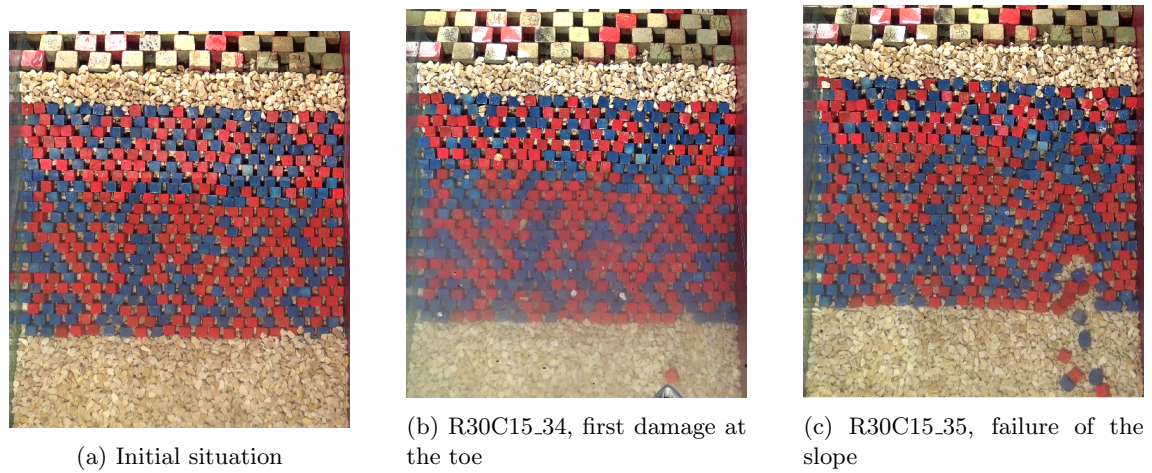


Figure 4.10: Example A

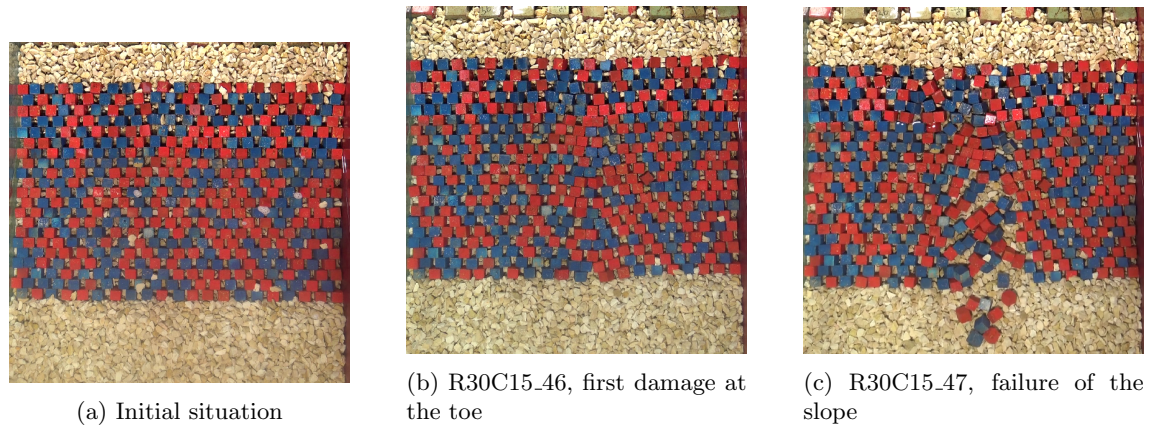


Figure 4.11: Example B

Both in example A and example B cube movement initiates at the toe. Both examples have 14 rows of armour layer beneath the water line and both have a crest freeboard of 15 cm, or a $R_c/(\Delta dn) = 4.55$. The failure mechanism in both tests agree. First the toe is attacked by the wave which impinges on the armour layer and flows underwater to reach the toe. Subsequently after several storms the wave was able to remove cubes from the first row above the toe. After initiation of 1 cube subsequently, during the next storm the slope fails. Individual extraction of a single cube in the slope, or especially in the first four rows beneath the water line, considered the weakest section Hellinga (2016), is not observed. As can be seen in appendix D, a total of 49 tests have been done and table D.1 gives an overview of the tested configuration with the stability parameter at

which failure occurred combined with the number of rows of cubes beneath the water line. Next to the table with an overview, in appendix D more photos have been added of examples of failure cases.

As stated before individual cubes drawn from the slope is not observed. To confirm the visual observation, laser transects have been made to see whether this technique is useful for these tests. And if it is possible to quantify this movement.

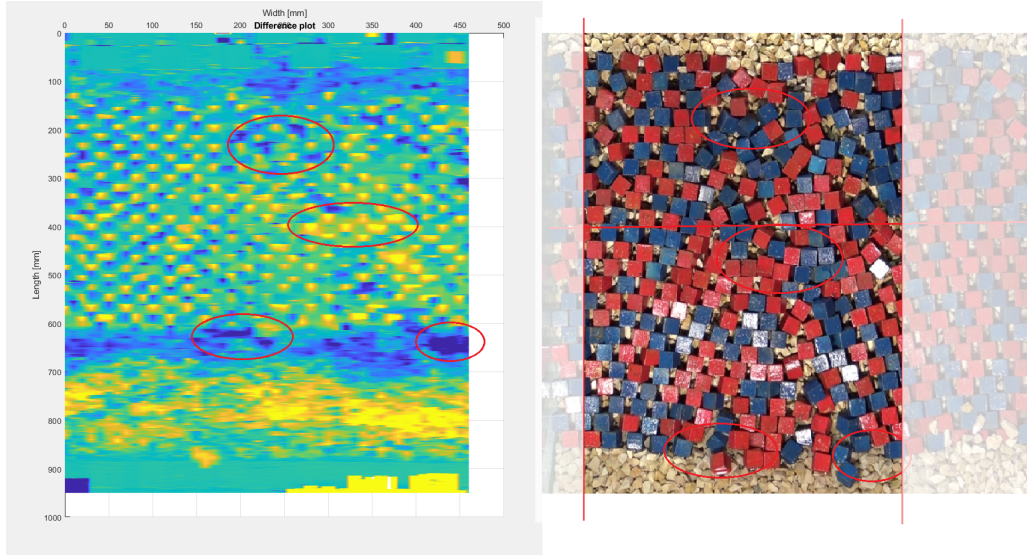
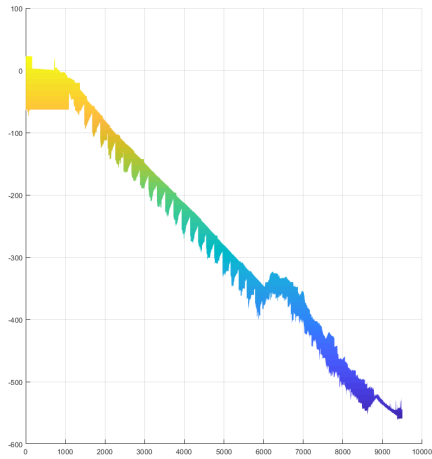
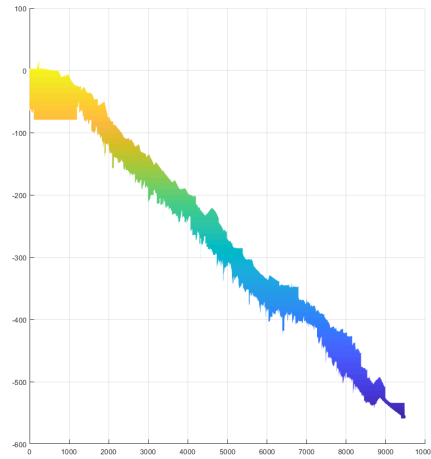


Figure 4.12: Analysis of failure R30C15.43

The right-hand photo of figure 4.12 indicates the area which is measured by laser. The laser equipment had a protective housing which limited the horizontal range. For this specific test the occurred damage lies within the measurable range. In the left figure the area where damage corresponds to the right picture are circled. Dark blue spots give a negative difference in height. Yellow areas give a positive difference in height. Negative difference in height in this case means missing cubes or erosion of material. Erosion was observed at the toe over the full width of the configuration. The eroded material seems to be transported slightly downstream to a yellow area which was also more or less evenly distributed over the width of the set-up. From the laser image, it is possible to identify the areas where damage occurs, however no good distinction can be made between the rows and no individual movement of the cubes can be distinguished. The erosion of the toe was also visible when the transects are viewed from the side:



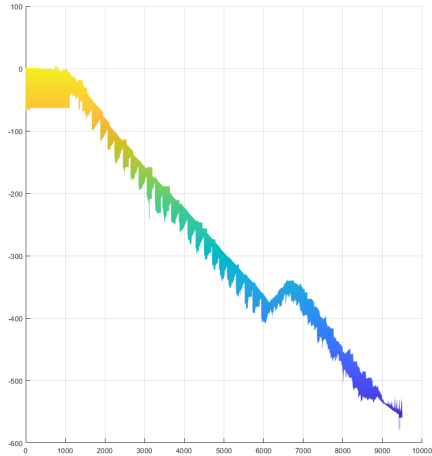
(a) Initial slope, side-view



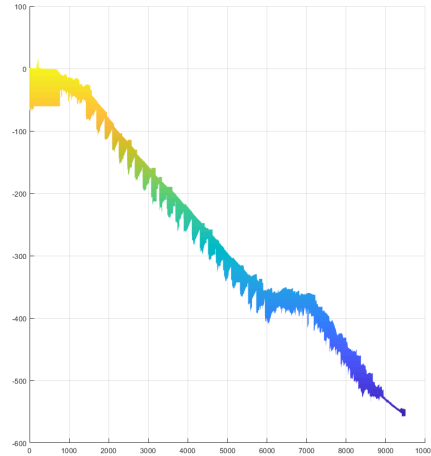
(b) Failed slope, side-view

Figure 4.13: Analysis of failure R30C15_43, before and after storm

This figure shows the erosion which takes place at the toe. The wave force acts on the filter material functioning at the toe and after the storm the toe was damaged resulting in the failure of the slope. Together with damage at the toe, it was observed that the ordered placement of the cube is disturbed. To see the influence of an increased length of armour layer when loaded by an impinging wave, the configuration was changed by increasing the armour length beneath the water line, of which the result is shown in the following figure:



(a) Initial slope R30C15_39, side-view



(b) After R30C15_39, side-view

Figure 4.14: Analysis of R30C15_39, after same storm conditions as figure 4.13 during test R30C15_43

For this configuration the attack on the toe was less severe. There was erosion at the toe but not enough to disrupt the ordered placement of the cubes, and no failure was observed. This indicates a first relation between the impinging wave attack and the erosion of the toe. In appendix D more side-views are provided which show the development (erosion) of the toe as the result of different storm conditions with different breakwater configurations. A single overview of all the 49 tests is given in figure 4.15. In this figure the stability parameter has been set out against the number of rows beneath the water line. The values used for the figure can be found in appendix D:

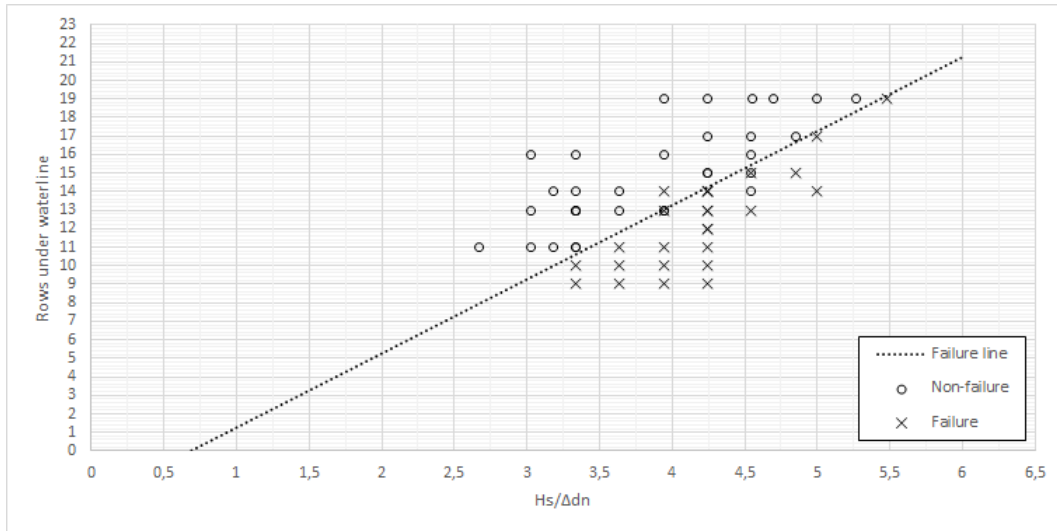


Figure 4.15: Overview of the correlation between dimensionless stability parameter and number of rows beneath the waterline

This figure shows a possible relation between the stability of the slope expressed in the stability parameter $N_s = H_s / (\Delta d_n)$ and the number of rows which are applied beneath the water line. These results only hold for a toe which has been constructed to support the armour layer in dry conditions. There has to be a force balance between the self-weight of the armour layer and the mass of the toe. During several tests the slope seems to 'dig in' the toe. This is a result of a armour layer mass which is too big for the toe to be supported. This is a different failure mechanism than is discussed above. In these test the erosion of the toe is the failure mechanism which leads to the extraction of a cube in the first row above the toe of the construction.

4.8.3 Crest Freeboard

To investigate the importance of the crest freeboard tests have been executed with varying heights of the crest freeboard. To find correlation between the settlement and the stability parameter of the slope laser transects have been made and the horizontal displacement of the cubes has been measured. A result of 4 arbitrary chosen transects can be found in the following figure:

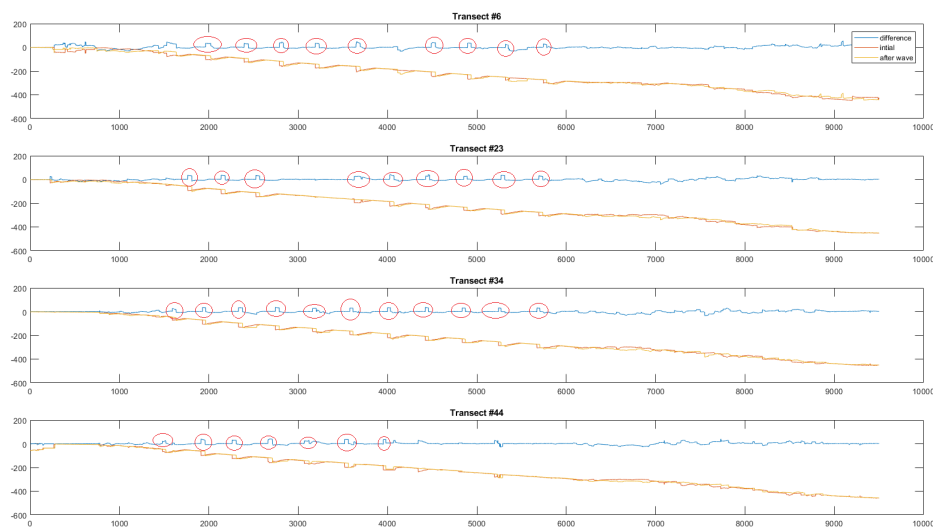


Figure 4.16: Settlement of the slope with a freeboard of 10 cm quantified

In figure 4.16 settlement is indicated by the red circles. These red circles show characteristic movement of a slope. Comparing the initial slope with the slope after a wave series shows that there is movement in the direction downward of the slope. The peaks in the difference correspond to a distance settled. For the crest freeboard of 10 cm no visual movement of the slope is observed. However, movement, settlement, is observed looking at individual transects. When 4 arbitrary transects are taken from the data and the average of all the peaks is taken it appears that for $R_c = 10$ cm the settlement equals $0.25 \cdot d_n$ with d_n the nominal diameter of the cubes applied as single armour layer.

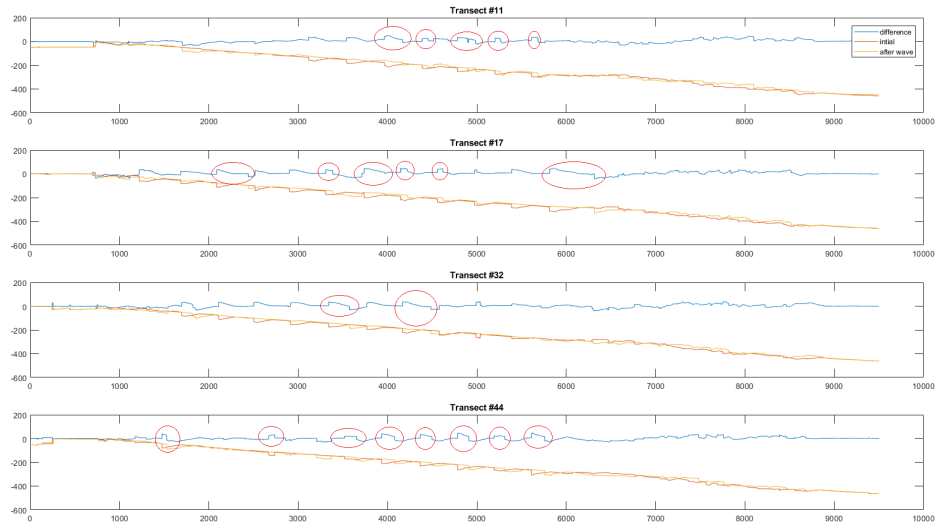


Figure 4.17: Settlement of the slope with a freeboard of 15 cm quantified

For figure 4.17 the settlement seems to be larger and the deviation of the settlement between the transects has increased. This analysis is done for all the tests executed and the results are gathered in the following figure. Figures 4.16 and 4.17 are taken from all the tests and can be summarized in the following figure:

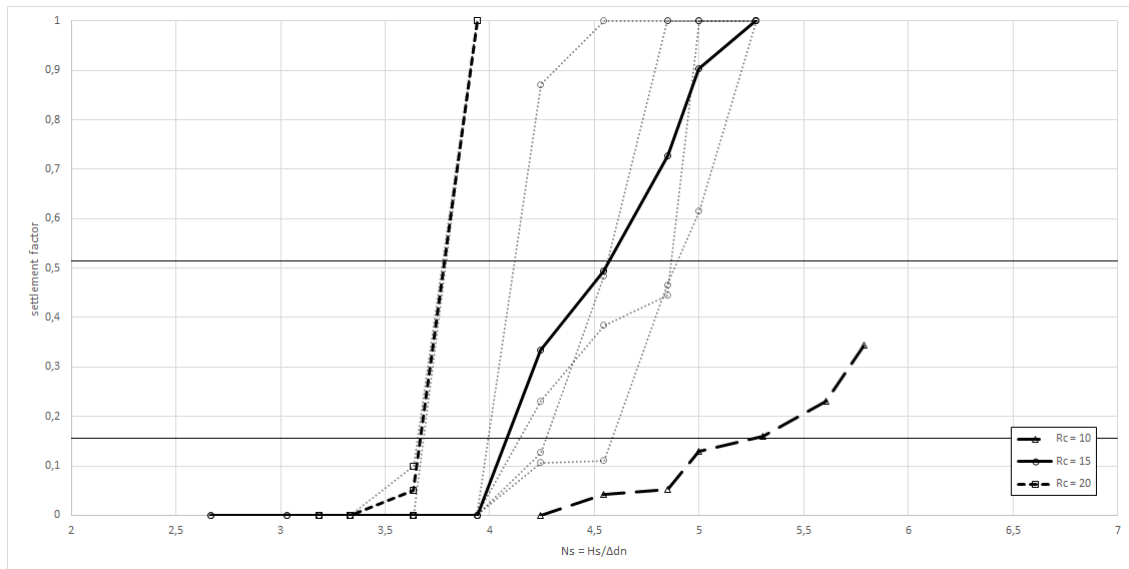


Figure 4.18: Stability parameter over settlement observed

In this figure the gradient of the settlement with increasing storm conditions is visible. At first settlement occurs up until $s = 0.15$. Cross-reference with video analysis results that at this

value no damage is observed and that the cubes are still in an ordered grid. Values higher than 0.15 show signs of damage to severe damage. All the tests which have a settlement higher than $0.5 \cdot d_n$ are observed to have failed. A value of $s = 1$ corresponds to a cube which has left the ordered grid and is observed to be instant failure or collapse of the structure. To give a visual representation of the correlation between the dimensionless stability parameter and the dimensionless relative crest freeboard the results of the tests have been combined in the following figure:

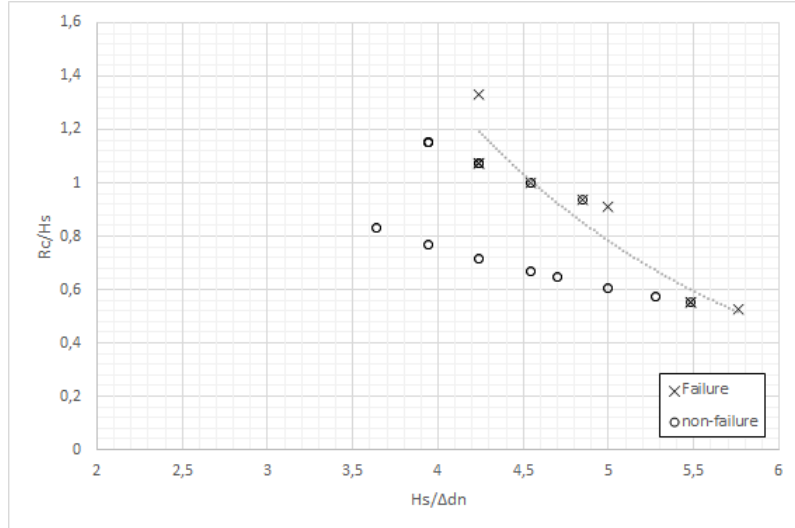


Figure 4.19: Overview of the relation between dimensionless stability parameter and the dimensionless crest height

This figure shows a possible relation between the crest height and the damage of the armour layer. An increased relative crest freeboard means that the distance, height, over which the waterbody accelerates increases. This results in a velocity of the water jet being larger which causes the structure to fail. When the relative crest freeboard is lowered the overtopping wave will increase in size do to a higher percentage of overtopping waves, however it will accelerate less and result in a higher dimensionless stability parameter.

These results only apply for a configuration where the toe is constructed by means of a mass of filter material at the toe in order to create an equilibrium between the self-weight due to gravity and the counteracting force of the toe. If this is not in equilibrium, an other failure mechanism will occur being a 'dig-in' of the armour layer into the toe. This failure mechanism differs from the one observed in this research as is shown in figure 4.10 and 4.11.

4.9 Conclusions

4.9.1 Fixed Toe

The initial purpose of this research was to build a configuration which contained a fixed toe with the armour layer placed only over the length of the slope that was thought to be most vulnerable. Yet, after numerous tests using a fixed toe, the structure showed no signs of either damage or failure. Manually extracting cubes to mimic protrusion or to decrease the stability of the structure resulted in neither damage nor failure. It is believed that the structure with a fixed toe is extremely strong as was also observed by Rietmeijer (2017). It can be concluded that by creating a fixed toe the structure is unrealistically strong due to the fact that the waves which are needed to initiate damage and eventually failure are storm conditions which would already cause failure either on the outer part of the breakwater or the layer of cubes on the crest of the breakwater. In addition, these waves exceed the dimensions of the Wave Overtopping Simulator and so it is not possible to continue performing research on a fixed toe. It was found that the normal forces between the cubes is vital in the stability of the armour layer as a whole. Once there is sufficient overlap between the cubes, being either a 20% or a 40% porosity, for these tests this showed no significant difference.

That is why it is concluded that for the remainder of this research the cubes will be placed without a fixed toe and with a porosity which is as high as practically is possible. In conclusion:

- No damage nor failure was observed for the tests executed with a fixed toe.
- Manually extracting cubes did not decrease the stability of the structure.
- The toe stability is a fundamental part of the research and should not be considered infinitely strong in the research.
- The porosity of the inner slope of a breakwater containing a cubic armour layer should be taken as high as possible. It is believed that a minimal amount of interlocking is sufficient to ensure stability and enough clamping between the cube rows.
- A single layer of cubes is again, stronger than initially thought and continuous research is needed to understand the process of damage and failure to the rear slope of a breakwater containing an cubic armour layer.

4.9.2 Non-fixed Toe

After the removal of the fixed toe, it was unclear what the starting point of the damage / failure of the structure would be. Individual cube rocking and vertical movement is not observed thus far and so it is believed that this failure mechanism is not governing in this test-up. The test executed with the aimed configuration showed interesting results. Almost in all the cases the damage was initiated by a cube which was washed out of the lowest row, most near to the toe. This means that the plunging wave is absorbed by the armour layer and a flow of turbulent water flows over the armour layer over a certain length. This length of armour layer underneath the water layer determines how this flow is diminished. This can be seen by the shape of the toe which is observed after several overtopping wave events, where the bulge of filter material at the toe is distributed down the slope.

The laser measuring equipment was thought to be valuable to identify areas where movement of cubes has taken place as can be seen in figure 4.12. The scour at the toe is visible and the cubes extracted from the lowest row as well as holes in the armour layer are clear. However it is found that the laser equipment lacks the ability to identify individual movement of cubes and to quantify the damage, when analyzing a complete slope made up of singular transects. These individual transects have been found to be helpful to quantify the settlement of the slope which occur after a storm event.

The reaction of the slope on a plunging wave has been found to be different than initially thought. When looking at the situation of the outer slope, the built-up pressure can lead to a difference in pressure beneath and above the armour layer. This built up pressure can also lead to cubes being pushed out. This vertical 'pushing out' does not occur on the inner slope. Due to normal forces and friction between the cubes, no individual cube failed, as was stated in former research. For example, a conclusion by Hellinga (2016) states that only the first 4 rows below the surface of the water level should be armoured by cubes. When the porosity of the armour configuration allows for enough interface between the rows, the slope acts as a rigid body. Two failure mechanisms have occurred: weakening of the toe by wave impact with subsequently cubes being removed at the first row above the toe, or an imbalance between the mass of the armour and the mass of the toe. In this case the slope will slide down and 'dig in' the toe. The first failure mechanism can be solved by increasing the strength of the toe by applying either cubes or a specially designed concrete element toe increase the mass of the toe. The erosion of the toe can be diminished by increasing the length of the armour layer so that the toe is situated deeper beneath the water line. In this way the waterbody which can absorb the energy of the impinging wave increases and the turbulent movement of the wave over the armour layer is diminished resulting in less erosion of the toe.

4.9.3 Crest Freeboard

When varying the height of the crest it is believed that by the increased height of water the wave does not accelerate over a big distance and so the plunging wave is easily dissipated. Very large

waves with a big volume and velocity over the crest are absorbed by the water prior to plunging onto the armour layer. In this way no damage is caused to the rear slope. On the other side, small waves which overtop the structure with a high freeboard, have a long distance to accelerate by means of gravitation and it's velocity has increased significantly when hitting the armour layer thus causing severe damage. Because of this phenomenon it is thought that instead of the significant wave height, the crest freeboard is a more appropriate parameter to describe the stability of the rear slope. When cross referencing the video analysis with the found values for settlement the settlement can be categorized in four groups:

- $0 - 0.15 \cdot d_n =$ settlement
- $0.15 - 0.5 \cdot d_n =$ damage
- $0.5 - 1.0 \cdot d_n =$ failure
- $> 1.0 \cdot d_n =$ instant failure / collapse

For the stability of the armour layer as a result of the erosion of the toe, a relation has been found between the number of rows applied in the construction beneath the water line. It is proven that an increased number of armour layer increases the stability of the armour layer. It has to be mentioned that by increasing the length of the armour layer the toe has to increase in mass to balance the increased self-weight of the armour layer. These categories are not a general guideline and they only appeal for this specific toe configuration.

Chapter 5

Conclusions

In this chapter the summary bullet points of each chapter will be repeated after which the conclusion of the whole research will be given. In this last part of this thesis also the research questions will be answered which were mentioned in Chapter 1.

5.1 Theoretical Approach

In chapter 2 a clear elaboration has been given of the theoretical approach to simulate storm conditions which can be applied in a simulator to test the rear stability of a single cubic armour layer on a rubble mound breakwater. A table has been presented as input parameters for the Wave Overtopping Simulator and their link to characteristic storm conditions, being: significant wave height H_s and peak period T_p .

5.2 Verification of the Wave Overtopping Simulator

- Video analysis combined with frame stacking produces clear results as presented in figures 3.10 and 3.11.
- The pre-defined duration of 2,5 seconds is measured good for reservoir levels ranging from $0.3m < H_{res} < 0.6m$.
- Due to the bulging of the wave front the measured front wave velocity is lower than the values calculated by applying Ritter (1892). The measured velocity was higher than the velocity calculated by applying Torricelli's law, this is due to the fact that this law applies to stationary flow which is not the case when a certain volume is released quasi-instantaneous.
- The difference in measured front velocity and overtopping duration between tests executed with a crest porosity of 50% and 0% is insignificant.
- Video analysis is a good method for measuring overtopping duration per single wave event.
- An improvement of the Wave Overtopping Simulator has been made by controlling the duration of the valve opening. Where in the research of Rietmeijer (2017) only a sudden opening is considered, this research applied a sudden opening and closure of the valve.

5.3 Stability Research

- In total 49 tests with varying configurations in number of rows beneath the waterline have been tested and the relation between the dimensionless stability parameter and the number of rows of single cubic armour layer beneath the water line has been presented. The range of dimensionless parameter is $2.5 < H_s/(\Delta d_n) < 5.5$. The number of rows of cubic armour layer ranges from 9 until 19.
- In total 35 tests have been executed with a crest freeboard of $R_c = 0.1m$, $R_c = 0.15m$ and $R_c = 0.20m$. The relative crest height range tested is: $0.52 < R_c/H_s < 1.43$.

- Erosion of the toe of the inner slope of a single cubic armour layer can be reduced by applying more rows of cubes beneath the water line. In addition the strength of the toe has to be increased to compensate for the larger force applied by the self-weight of the armour layer.
- An exponential relation has been presented between the stability parameter and the relative crest freeboard. A higher crest freeboard results in more acceleration of the water body and an increased jet, impinging on the armour layer.

5.4 Overall Conclusion

The presented report of the study on the stability of a cubic armour layer, can be seen as a tour through all the phases of the research. A research in which the problem definition was quite clear and straight forward, due to the fact that not a lot research has been done and results are hard to reproduce. By approaching the problem as is explained in Chapter 2 I aimed to make a clear distinction between real wave conditions which occur during storms and the wave conditions which are characterized using a simulator. After which the simulator is then tested to see whether it is possible to simulate waves and how well these waves are simulated. Subsequently the stability is tested using a simplified version of the test program due to the time-consuming buildup of the slope and test set-up. Much has been learned and this new knowledge can be used to improve the theory and to gain more data on rear slope stability.

In the introduction it has been stated that several sub-questions were posed to guide the work and help to answer the main question. These sub-questions will be answered first:

What elements of an overtopping wave characterize the flow of the water body?

The elements which characterize an overtopping wave are it's overtopping front velocity u_{max} , the water layer thickness h_{max} , the specific discharge q_{max} and the duration of the overtopping event T_{ovt} .

What percentage of overtopping waves is defined as extreme?

In order to be able to test a range of waves one has to keep in mind; the maximum allowable values which are limited by the simulator and a practical amount of waves which can be executed in a short time frame. This resulted in a percentage of 0.1%, one in thousand, of the overtopping waves in storm with a duration of 3 hours. In this way the characteristics fit the dimensions of the simulator and the amount of waves, average of 5 waves per storm, are practical for testing in a laboratory.

What are the input parameters of the Wave Overtopping Simulator?

Input parameters of the Wave Overtopping Simulator are the water level h_{res} , the valve height h_{valve} the opening acceleration and deceleration of the valve and the total opening time of the simulator.

Does the newly developed wave overtopping simulator provide reliable results compared to theoretical values with regard to front wave velocity, water layer thickness and overtopping period?

The waves which result from the Wave Overtopping Simulator have a certain velocity, layer thickness, steepness of the wave front and duration. For these characteristics the simulator proves to be able to simulate overtopping wave events. The linear motor has shown to struggle with very short opening times and immediately afterwards short closing times. This results in a faltering opening and closing sequence. Still affects the steepness of the wave front. However, in this research the error is acceptable.

How does the velocity of an overtopping wave develop over the crest of a rubble mound breakwater?

The slope of the framestacks result in a velocity of the wave over the crest. The gradient of these images was constant over time. This is based on measurements with the naked eye. In van Gent and Pozueta (2004) the velocity of the wave front is believed to decrease where in Vitulli (2017) generally larger values of the velocity are found at the transition from crest to inner-slope then

at the seaward side of the crest. In this research due to the constant gradient observed in the framestacks the velocity over the crest is assumed constant. The front velocity of the water body is measured to be smaller than values found by applying Ritter (1892). This is due to the friction with the crest and the bulging of the wave front.

What failure mechanisms play a significant role in the quantitative description of the stability of a single armour layer of cubes on the rear slope of breakwaters?

Two main failure mechanisms have been observed during the stability research. The first being an insufficient strength of the toe which results in 'sliding' of the complete armour layer as a rigid body. The second being erosion of the toe after which from the first row above the toe the first cube initiates in movement. Single extraction of cubes in the first 4 rows beneath the water line, as observed during research of Hellinga (2016) was not observed. In addition it argued that the stability of the rear slope is correlated to the relative crest height. With a relatively low crest freeboard, very large wave have a significant velocity over the crest. When this velocity reaches the transition from crest to rear slope of a breakwater it can either be dissipated by a waterbody, in the case of a small crest freeboard. Or it accelerates by means of gravitation. And this aspect plays a significant role. Small waves which top over have a lower velocity. However, when they reach the transition of crest to slope, when this transition is constructed in a sharp transition, the gravitational acceleration can increase this velocity to be higher than the waves with a higher significant wave height. The water-jet impinging on the armour layer is guided over the armour layer towards the toe. Over the distance it travels over the toe it is dampened by the water, and so it is shown that when increasing this length until 19 rows beneath the water line, the stability increases significantly. These failure mechanisms are found for a construction where the toe is made from a volume of filter material applied to the toe. When a different construction of the toe is applied these values of stability may differ.

Can the failure mechanisms be quantitatively assessed?

The sliding of the armour layer as a rigid body has been quantified by applying laser technique which is able to identify settlement of the armour layer. By executing 37 tests where for each test 47 transects of 9500 points are made the difference of the slope compared to the initial position can be determined. After analysis it followed that the following classes can be identified from settlement:

- $0 - 0.15 \cdot d_n =$ settlement
- $0.15 - 0.5 \cdot d_n =$ damage
- $0.5 - 1.0 \cdot d_n =$ failure
- $> 1.0 \cdot d_n =$ instant failure / collapse

Main research question

How can the stability of a single cubic armour layer on the rear-slope of breakwaters quantitatively be assessed using a Wave Overtopping Simulator?

By applying the theoretical approach, input parameters for the Wave Overtopping Simulator have been found. By verification of the Wave Overtopping Simulator and it's measuring equipment it is concluded that waves with specified characteristics can be simulated. These waves have been used to simulate storm conditions which result in damage in the inner slope of the structure. The damage has been expressed in certain classes of settlement and correlation has been found between the stability of the structure and the amount of rows beneath the waterline. A concrete design formula for the rear slope blocks has not been found during this research.

Chapter 6

Recommendations

Although a big step has been made in the improvement of prediction methods for damage and failure of the rear side of breakwaters during storm events, this has not resulted in an actual design tool which can be applied. In the last couple of years research has been done improving the knowledge on the subject. Unfortunately the results are hard to reproduce. This means that more research is needed to design such a tool and to validate it. One of the most important recommendations of this study is that Witteveen+Bos should continue supporting research on the subject of cubic armour layers on the rear slope as much can still be learned. The following is recommended:

Validation of Simulator

In this report the Wave Overtopping Simulator built by Rietmeijer (2017) was verified. The characteristics of the wave can be measured. To ensure this simulator is valid, research has to be done in which the simulator is tested and compared to tests executed in a wave flume in which actual propagating waves are used in stead of a sudden release of a volume of water. Subsequently the waves should be measured as well as the response of the rear slope.

Crest freeboard in stead of Significant Wave Height in the stability parameter

The main conclusion which can be drawn from this report is the fact that the significant wave height might not directly be the most important parameter to describe the stability of the rear slope. The tests have shown that the damage profile between the different heights of the crest freeboard is significantly different and the study is close to finding the tipping point at which ratio of crest freeboard and the length of the armour layer underneath the water layer stability will occur. This parameter has not been applied before and so, additional research should be done to confirm whether this is a valuable parameter for the description of rear slope damage.

Toe stability

Tests on the stability of toe for a construction using a single cubic armour layer should be performed. The test series used in this report should be used to execute different configurations in which the toe made up of filter material is replaced by rocks or other material to test toe stability.

Velocity of impinging wave

This research has argued the influence of the relative crest freeboard on the stability of the armour layer. A parameter which was discussed is the velocity of the wave front. Further research should be executed in the quantification of this velocity at which damage or failure of the armour layer occurs. Protrusion of the blocks also plays a significant role which can be assessed.

Constant velocity of overtopping wave event

In this research, looking at the results of framestacks, the velocity of the wave front is constant over the crest. This is not in accordance with known literature. Other studies have performed tests using PIV (Particle Image Velocimetry). This method of tracing individual particles and

calculating their velocity is more accurate than using a high speed camera. In this research it is not applied due to time restriction. However, in the future the test set-up as built in the Waterlab of the Technical University of Delft should be expanded with this technology since it has been proven to be of added value to determine the development of the velocity over the crest. Still, the magnitude of the velocity at the transition from crest to rear slope has to be defined.

Movement of individual cubes

In this research the movement of the slope has been observed as a rigid body and only individual stones at the lowest rows left the ordered grid. In further research, attempts have to be made to identify individual stones and track their movement along the slope. Often the failure of one stone initiates failure for the whole slope. When the whole system is implemented in a real project it can be helpful to be able to identify these singular cubes which will fail and to repair on these locations.

Linear actuator

The Wave Overtopping Simulator used in this research is a very helpful system to reproduce specific overtopping waves and will keep on helping research in the future. However an essential aspect of an overtopping wave is its steepness at the front. This steepness results from the instantaneous release of water and it is for a great deal responsible for the plunge on the slope surface. Still the linear actuator seems to have some issues with the transition of an upward motion to a downward motion. Serious attention should be given to this fact because it can improve the simulated waves in a major way. A better simulation of these waves leads to a more accurate damage profile of the inner slope. In addition, an improvement of the linear actuator can enable the system to simulate more waves in a smaller time frame, making the whole test program less time consuming.

Constant overtopping volume over the crest

In the current research the volume has been assumed to be constant over the crest and all the water leaving the reservoir ends in a plunge on the rear slope. This might not be the case. Since we are looking at permeable structures it is very likely that water will infiltrate into the crest and rear slope itself, meaning less water that will attack the rear slope. The results obtained in this research should therefore be seen as a conservative approach. It is recommended to conduct research in the infiltration of these overtopping waves into the crest in order to be able to design an even more economical armor layer by applying cubes of a smaller diameter.

Test program

The test program and methodology of the current research is a logical way of attacking this problem. However, still a great many of assumptions were made in order to come to this approach, assumptions which were often based on research specified in other areas of the breakwater such as the outer slope. This outer slope has different loads than the inner slope and therefore will also need different assumptions. As time passes more research on this side of the breakwater will be done and an improved methodology can be applied.

Bibliography

- L. Beulink. Influence of Hard-wood Tree Trunks on Erosion of Riverbed. *Msc. Thesis*, 2018.
- G. Bosman, J. van der Meer, G. Hoffmans, H. Schüttrumpf, and H. J. Verhagen. Individual Overtopping Events at Dikes. *Coastal Engineering*, pages 1–13, 2008.
- O. Castro-Orgaz and H. Chanson. Ritter’s dry bed dan-break flows: positive and negative wave dynamics. *Environmental Fluid Mechanics*, 17:665–694, 2017.
- CIRIA. *The Rock Manual. The use of rock in hydraulic engineering (2nd edition)*. C683, CIRIA, London, 2007.
- R. Coticone. Reconstruction of Flow Characteristics over the Crest of a Breakwater with PIV Technique. *Msc. Thesis*, 2015.
- J. de Rouck. CLASH - D46: Final Report. *Ghent University, Belgium*, 2005.
- T. Hai. Velocity and water-layer thickness of overtopping flows on sea dikes. *Report of measurements and formulas development*, February, 2014.
- L. Hellinga. Stability of Single Layer Cubes on Breakwater Rear Slopes. *Msc. Thesis*, 2016.
- S. Hughes. Adaptation of the Levee Erosional Equivalent Method for the Hurricane Storm Damage Risk Reduction System. *US Army Corps of Engineers*, May, 2001.
- S. Hughes. Improvements in Describing Wave Overtopping Processes. *Coastal Engineering*, 1, 2012.
- S. Hughes. Hydraulic Parameters of Overtopping Wave Volumes. *Colorado State University, Engineering Research Center*, February, 2015.
- M. Kudale and N. Kobayashi. Hydraulic Stability Analysis of Leaside Slopes of overtopped Breakwaters. *Coastal Engineering Proceedings*, pages 1721–1734, 1996.
- J. Möller, R. Weissmann, H. Schüttrumpf, J. Grüne, H. Oumeraci, W. Richwein, and M. Kudella. Interaction of Wave Overtopping and Clay Properties for Seadikes. *ICCE*, 2003.
- A. Rietmeijer. Rear-slope Revetment Stability Approached by the Wave Overtopping Simulator. *Msc. Thesis*, 2017.
- A. Ritter. Die Fortpflanzung von Wasserwellen. *Zeitschrift Verein Deutscher Ingenieure*, 36(2): 947–954, 1892.
- G. Schiereck and H.-J. Verhagen. *Introduction to Bed, Bank and Shore Protection*. VSSD, Leegwaterstraat 42, 2628 CA Delft, The Netherlands, 2012.
- H. Schüttrumpf and H. Oumeraci. Layer Thicknesses and velocities of wave overtopping flow at seadikes. *Coastal Engineering*, 52:473–495, 2005.
- M. Tirindelli and A. Lamberti. Wave Action on Rubble Mound Breakwaters: the Problem of Scale Effects. *Delos*, 2000.
- P. van den Linde. Stability of single layer armour units on low-crested structures. *Msc. Thesis*, 2009.

- J. van der Meer. Conceptual Design of Rubble Mound Breakwaters. *International Conference on Coastal Engineering*, pages 447–510, 1992.
- J. van der Meer, P. Bernardini, W. Snijders, and E. Regeling. The Wave Overtopping Simulator. *ICCE*, 2006.
- J. van der Meer, N. Allsop, T. Bruce, J. de Rouck, A. Kortenhuis, T. Pullen, H. Schüttrumpf, P. Troch, and B. Zanuttigh. *EurOtop - Manual on wave overtopping of sea defences and related structures*. Environment Agency, ENW, KFKI, 2016.
- J. van der Meer et al. *Technisch Rapport Golfploop en Golfoverslag bij Dijken*. NIVO, Delft, 2002.
- B. van Dijk. The rear slope stability of rubble mound breakwaters. *Msc Thesis*, 2001.
- M. van Gent. Wave Overtopping Events at Dikes. *World Scientific, ICCE*, 2002.
- M. van Gent and B. Pozueta. Rear-side Stability of Rubble Mound Structures. *Coastal Engineering Conference*, 29(4):1–13, 2004.
- M. van Gent, H. van den Boogaard, B. Pozueta, and J. Medina. Neural Network Modelling of Wave Overtopping at Coastal Structures. *Coastal Engineering*, 54:586–593, 2007.
- H.-J. Verhagen. Infiltration of Overtopping Water in a Breakwater Crest. *Proceedings of the Coastal Engineering Conference*, 2005.
- M. Vitulli. Quantification of Wave Overtopping Hydraulic Parameters. *Msc. Thesis*, 2017.
- B. Zanuttigh, J. van der Meer, T. Bruce, and S. Hughes. Statistical Characterisation of Extreme Overtopping Wave Volumes. *Institution of Civil Engineers Conference Paper*, 2013.

Appendix A

Theoretical Approach

A.1 Crest freeboard $R_c = 0,10\text{m}$

Results of calculations with a crest freeboard of 0,10m:

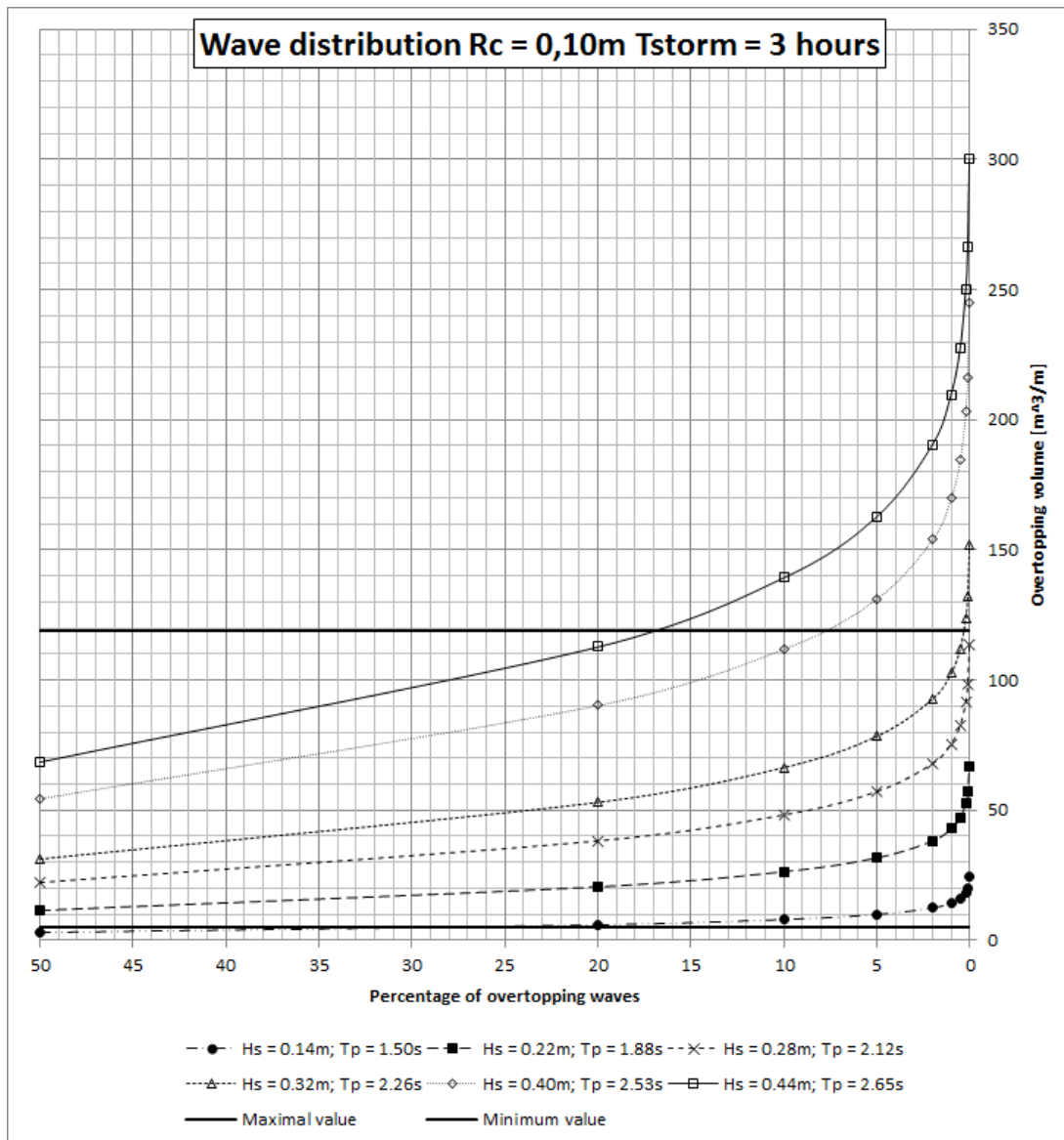


Figure A.1: Two-parameter Weibull distribution for crest height of 10 cm with increasing wave heights

Rc = 0.10m										
Hs [m]	Tp [s]	$q/(g * Hs^3)^{0.5}$	Waves	Volume [L]	umax [m]	hmax [m]	qmax [m2/s/m]	To [s]	Hres [m]	Valve [m]
0.14	1.50	0.028	7	20	2.35	0.05	0.09	1.87	0.195	0.07
0.22	1.88	0.049	6	57	3.16	0.08	0.20	2.43	0.352	0.12
0.28	2.12	0.058	6	98	3.68	0.10	0.31	2.78	0.477	0.16
0.32	2.26	0.063	5	132	4.00	0.12	0.39	3.00	0.563	0.19
0.40	2.53	0.070	5	216	4.57	0.15	0.57	3.39	0.736	0.24
0.44	2.65	0.073	5	266	4.83	0.17	0.67	3.57	0.823	0.27

Table A.1: Overview of the wave groups which correspond to storm conditions for Rc = 10 cm

A.2 Crest freeboard Rc = 0,20m

Results of calculations with a relative crest freeboard of 0,20m:

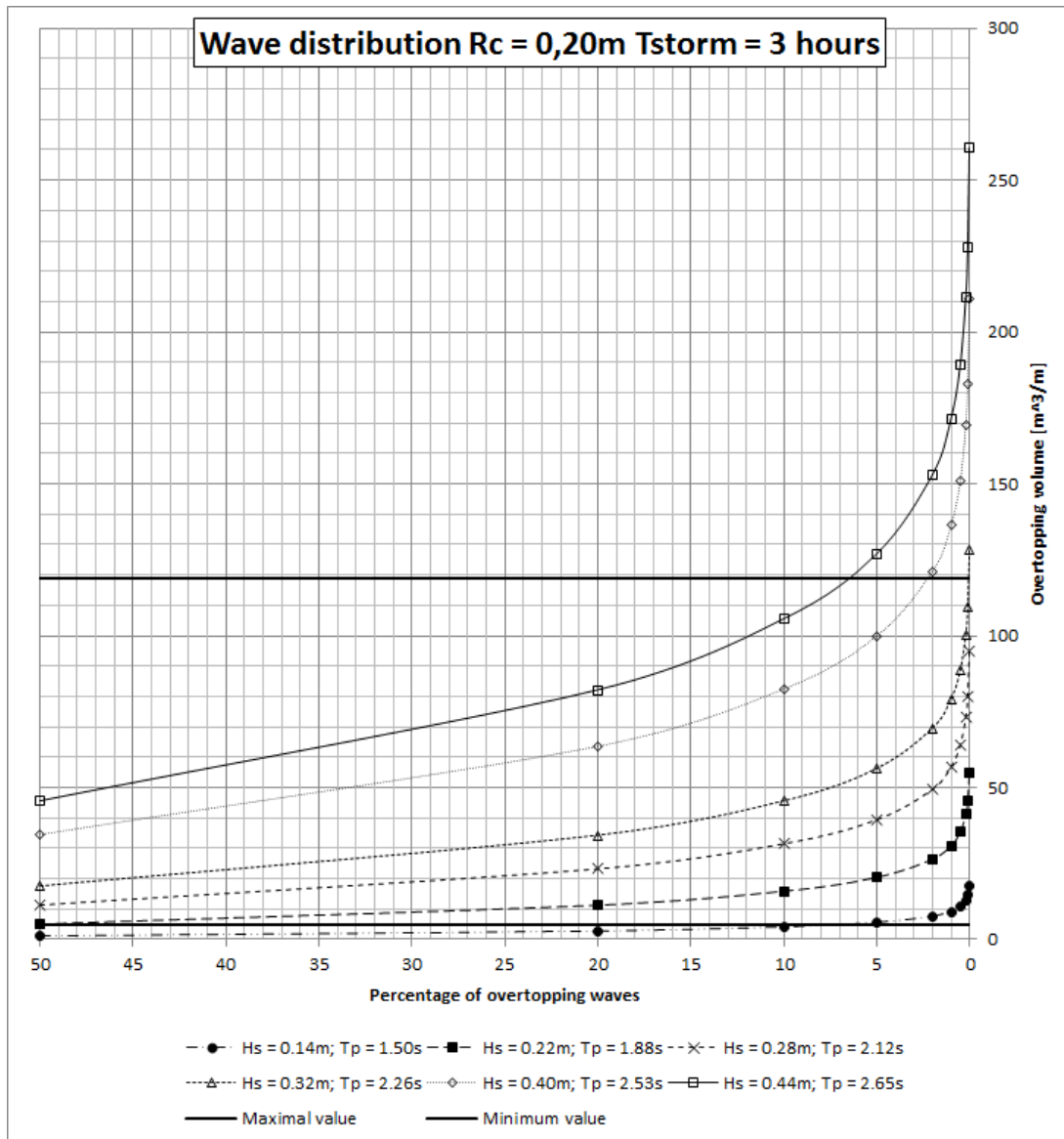


Figure A.2: Two-parameter Weibull distribution for crest height of 20 cm with increasing wave heights

Rc = 0.20m										
Hs [m]	Tp [s]	$q/(g * Hs^3)^{0.5}$	Waves	Volume [L]	umax [m]	hmax [m]	qmax [m2/s/m]	To [s]	Hres [m]	Valve [m]
0.14	1.50	0.005	3	15	2.02	0.04	0.07	1.73	0.143	0.06
0.22	1.88	0.018	4	46	2.83	0.07	0.16	2.30	0.282	0.11
0.28	2.12	0.028	5	80	3.32	0.09	0.25	2.63	0.389	0.15
0.32	2.26	0.034	5	109	3.63	0.11	0.32	2.86	0.465	0.17
0.40	2.53	0.044	4	183	4.20	0.14	0.48	3.25	0.622	0.22
0.44	2.65	0.049	4	228	4.47	0.16	0.57	3.43	0.704	0.25

Table A.2: Overview of the wave groups which correspond to storm conditions for Rc = 20 cm

Appendix B

Results of Verification Wave Overtopping Simulator

B.1 Wave gauge measurements

Here the tables with the results of the measurements done for the verification of the Wave Overtopping Simulator are presented.

50:100:30						100:100:30					
	qmax [$m^2/s/m$]	hmax [m]	umax [m/s]	vol.wave [L]	vol.res [L]		qmax [$m^2/s/m$]	hmax [m]	umax [m/s]	vol.wave [L]	vol.res [L]
1	0.135	0.064	3.024	99.23	100.55	1	0.128	0.059	2.518	100.66	103.61
2	0.135	0.065	2.883	98.91	99.84	2	0.141	0.061	2.554	99.74	101.97
3	0.14	0.064	3.052	99.84	101.63	3	0.136	0.061	2.556	100.79	103.59
4	0.128	0.064	2.873	100.57	103.39	4	0.137	0.06	2.466	100.55	102.95
5	0.126	0.064	2.839	99.54	100.99	5	0.145	0.059	2.735	99.58	100.7
6	0.134	0.065	2.877	100.38	102.7	6	0.141	0.06	2.479	100.38	102.73
7	0.132	0.063	2.86	100.46	102.98	7	0.137	0.063	2.549	98.47	99.67
8	0.142	0.064	3.084	97.79	99.2	8	0.128	0.06	2.682	101.09	103.86
9	0.143	0.065	3.076	100.97	103.27	9	0.131	0.059	2.498	100.21	102.05
10	0.135	0.065	3.042	100.24	101.14	10	0.142	0.06	2.664	98.6	99.69
avg	0.14	0.06	2.96	99.79	101.57	avg	0.14	0.06	2.57	100.01	102.08
stdev	0.01	0.00	0.10	0.95	1.48	stdev	0.01	0.00	0.09	0.90	1.58

Table B.1: hres = 30 cm

50:100:40						100:100:40					
	qmax [$m^2/s/m$]	hmax [m]	umax [m/s]	vol.wave [L]	vol.res [L]		qmax [$m^2/s/m$]	hmax [m]	umax [m/s]	vol.wave [L]	vol.res [L]
1	0.149	0.061	3.449	117.05	118.8	1	0.161	0.064	3.398	120.86	124.14
2	0.158	0.063	3.172	121.16	122.6	2	0.152	0.066	3.262	118.6	120.12
3	0.154	0.062	3.337	119.98	121.57	3	0.159	0.064	2.867	119.35	120.69
4	0.157	0.061	3.424	118.93	120.2	4	0.151	0.062	2.954	118.77	121.01
5	0.165	0.063	3.582	120.58	121.5	5	0.148	0.067	3.09	120.72	122.6
6	0.151	0.063	3.39	118.76	120.56	6	0.156	0.066	3.114	121.68	123.97
7	0.155	0.063	3.436	121.31	123.26	7	0.153	0.066	3.265	120.11	121.4
8	0.157	0.072	3.529	117.34	119.12	8	0.156	0.064	3.138	119.33	120.64
9	0.154	0.065	3.384	119.26	121.32	9	0.158	0.064	2.997	118.13	120.64
10	0.16	0.063	3.581	120.33	122.55	10					
avg	0.16	0.06	3.43	119.47	121.15	avg	0.15	0.06	3.12	119.73	121.69
stdev	0.00	0.00	0.12	1.48	1.48	stdev	0.00	0.00	0.17	1.19	1.51

Table B.2: hres = 40 cm

50:100:50						100:100:50					
	qmax [$m^2/s/m$]	hmax [m]	umax [m/s]	vol.wave [L]	vol.res [L]		qmax [$m^2/s/m$]	hmax [m]	umax [m/s]	vol.wave [L]	vol.res [L]
1	0.176	0.065	3.617	137.25	140.77	1	0.168	0.068	3.641	137.88	140.63
2	0.173	0.063	3.546	137.23	140.85	2	0.169	0.067	3.354	137.91	142.34
3	0.17	0.063	3.717	136.61	139.72	3	0.171	0.065	3.351	136.6	140.53
4	0.171	0.078	3.837	138.56	141.58	4	0.175	0.065	4.373	139.68	142.88
5	0.168	0.07	3.424	136.75	140.6	5	0.17	0.065	3.521	137.74	140.01
6	0.167	0.071	3.574	137.66	142	6	0.173	0.066	3.526	137	140.8
7	0.173	0.067	3.589	136.96	140.21	7	0.178	0.066	3.834	139.74	142.59
8	0.174	0.073	3.489	136.28	139.52	8	0.171	0.063	3.66	136.83	140.53
9	0.167	0.072	3.449	138.04	141.46	9	0.17	0.066	3.324	137.23	140.04
10	0.176	0.066	4	138.2	140.04	10	0.172	0.066	3.437	135.88	139.92
avg	0.17	0.07	3.62	137.35	140.68	avg	0.17	0.07	3.60	137.65	141.03
stdev	0.00	0.00	0.18	0.74	0.82	stdev	0.00	0.00	0.32	1.25	1.13

Table B.3: hres = 50 cm

50:100:60					100:100:60						
	qmax [$m^2/s/m$]	hmax [m]	umax [m/s]	vol.wave [L]	vol.res [L]		qmax [$m^2/s/m$]	hmax [m]	umax [m/s]	vol.wave [L]	vol.res [L]
1	0,184	0,065	3,88	155,53	159,32	1	0,189	0,064	4,115	157,01	161,81
2	0,192	0,08	3,793	156,33	160,79	2	0,188	0,067	4,486	156,61	161,03
3	0,191	0,064	3,762	155,75	159,76	3	0,185	0,066	4,095	156,33	161,3
4	0,187	0,072	3,75	156,54	160,3	4	0,186	0,067	4,328	156,56	161,5
5	0,184	0,067	3,639	156,58	162,3	5	0,186	0,065	4,446	156,32	160,79
6	0,187	0,07	3,807	156,35	161,08	6	0,189	0,069	4,643	155,55	160,86
7	0,187	0,068	3,892	156,18	160,81	7	0,189	0,064	4,437	156,79	161,79
8	0,189	0,071	3,792	155,94	161,23	8	0,185	0,065	4,322	157,09	162,28
9	0,189	0,079	3,816	156,49	160,17	9	0,191	0,064	4,048	156,57	161,32
10	0,186	0,076	3,835	156,72	160,59	10	0,187	0,063	4,374	155,74	159,56
avg	0,19	0,07	3,80	156,24	160,64	avg	0,19	0,07	4,33	156,46	161,22
stdev	0,00	0,01	0,07	0,39	0,83	stdev	0,00	0,00	0,19	0,50	0,75

Table B.4: hres = 60 cm

50:100:70					100:100:70						
	qmax [$m^2/s/m$]	hmax [m]	umax [m/s]	vol.wave [L]	vol.res [L]		qmax [$m^2/s/m$]	hmax [m]	umax [m/s]	vol.wave [L]	vol.res [L]
1						1	0,2	0,068	4,414	173	178,42
2						2	0,2	0,068	4,76	171,13	175,92
3						3	0,203	0,067	4,93	172,4	178,86
4						4	0,2	0,068	4,297	172,73	177,78
5						5	0,201	0,066	4,789	172,46	177,49
6						6	0,201	0,066	4,783	172,22	176,22
7						7	0,201	0,072	4,621	172,4	178,45
8						8	0,202	0,066	4,072	172,08	176,58
9						9	0,199	0,071	3,96	172,26	176,61
10						10	0,204	0,067	4,069	173,04	176,66
avg						avg	0,20	0,07	4,47	172,37	177,30
stdev						stdev	0,00	0,00	0,35	0,54	1,04

Table B.5: hres = 70 cm

No tests have been done with a porosity of the crest of 50% and a reservoir water level of 70 centimeters.

B.2 Video measurements

For the tables of the video measurements for each tested wave a figure as figure 3.10 was produced and analyzed. The p1,p2,p3 and p4 are the data points taken between which the period or the velocity is calculated. To increase the accuracy, the waves tested on a crest with a porosity of 0%, 4 points have been taken.

50;100;30										
wave #	P1		P2		P3		v [m/s]	TOVT [s]		
1	1	73	1264	104	1264	338	1,31	2,34		
2	7	42	1264	70	1264	308	1,45	2,38		
3	1	122	1264	149	1264	383	1,51	2,34		
4	1	34	1264	65	1264	298	1,31	2,33		
5	1	91	1264	121	1264	355	1,36	2,34		
6	1	91	1264	121	1259	356	1,36	2,35		
7	10	64	1264	92	1264	329	1,44	2,37		
8	6	55	1264	83	1263	321	1,45	2,38		
9	10	92	1254	119	1264	359	1,49	2,4		
10	10	96	1264	124	1264	364	1,44	2,4		
							1,41	2,363		
						avg	1,42	2,37		
						stdev	0,06	0,03		
						%	4,32	1,06		
50;100;40										
wave #	P1		P2		P3		v [m/s]	TOVT [s]		
1	33	107	1258	131	1264	365	1,65	2,34		
2	42	14	1250	35	1264	278	1,86	2,43		
3	22	72	1223	93	1264	330	1,84	2,37		
4	32	48	1226	70	1264	302	1,75	2,32		
5	5	75	1258	97	1264	339	1,84	2,42		
6	19	17	1228	39	1262	285	1,77	2,46		
7	10	86	1261	107	1258	353	1,92	2,46		
8	1	90	1243	113	1263	357	1,74	2,44		
9	15	70	1240	92	1263	335	1,80	2,43		
10	13	48	1221	70	1264	313	1,77	2,43		
11							1,79	2,41		
						avg	1,79	2,42		
						stdev	0,06	0,04		
						%	3,11	1,77		
50;100;50										
wave #	P1		P2		P3		v [m/s]	TOVT [s]		
1	125	91	1189	107	1263	343	2,15	2,36		
2	18	130	1245	149	1264	389	2,08	2,4		
3	35	97	1246	117	1262	360	1,95	2,43		
4	18	88	1208	108	1262	349	1,92	2,41		
5	32	32	1234	50	1263	292	2,15	2,42		
6	11	89	1176	108	1262	348	1,98	2,4		
7	1	79	1196	96	1264	339	2,27	2,43		
8	78	71	1237	90	1262	331	1,97	2,41		
9	38	44	1230	63	1263	306	2,02	2,43		
10	26	24	1236	43	1258	289	2,05	2,46		
11	46	35	1236	54	1264	292	2,02	2,38		
							2,05	2,42		
							0,10	0,02		
							5,10	0,92		
50;100;60										
wave #	p1		p2		p3		p4	v	t	
1	64	38	1247	58	792	48	792	284	1,91	2,36
2	87	104	1252	123	488	108	488	344	1,98	2,36
3	189	74	1158	90	738	82	738	316	1,95	2,34
4	166	100	1195	116	796	109	796	338	2,07	2,29
5	240	83	1241	99	688	90	688	325	2,02	2,35
6	223	26	1258	43	724	34	724	269	1,96	2,35
7	200	61	1222	78	621	67	621	303	1,94	2,36
8	277	69	1234	85	743	78	743	311	1,93	2,33
9	139	64	1238	81	522	69	522	307	2,09	2,38
10	285	40	1248	56	753	49	753	287	1,94	2,38
									1,98	2,35
									0,06	0,03
									3,07	1,12

100;100;30										
wave #	V1	V2	T1	T2	v [m/s]	t [s]				
1	64	55	977	75	843	70	843	317	1,47	2,47
2	42	77	1081	96	828	90	828	339	1,76	2,49
3	25	57	1222	79	845	72	845	315	1,76	2,43
4	95	54	1208	76	844	69	844	315	1,63	2,46
5	33	90	1162	111	864	103	864	351	1,73	2,48
6	35	103	1234	125	805	116	805	363	1,76	2,47
7	23	13	1034	31	866	26	866	273	1,81	2,47
8	38	95	1208	116	807	109	807	355	1,80	2,46
9	39	126	1208	148	873	141	873	387	1,71	2,46
10	38	45	1243	68	804	58	804	306	1,69	2,48
								avg	1,71	2,47
								stdev	0,10	0,02
								%	5,79	0,66

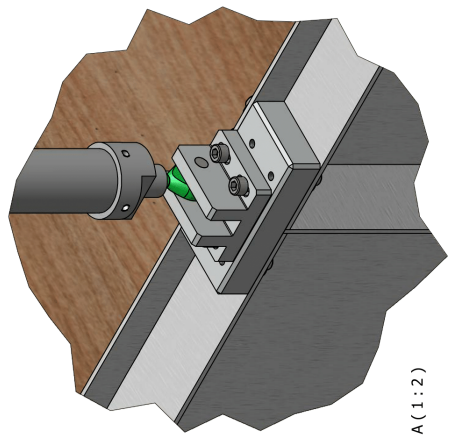
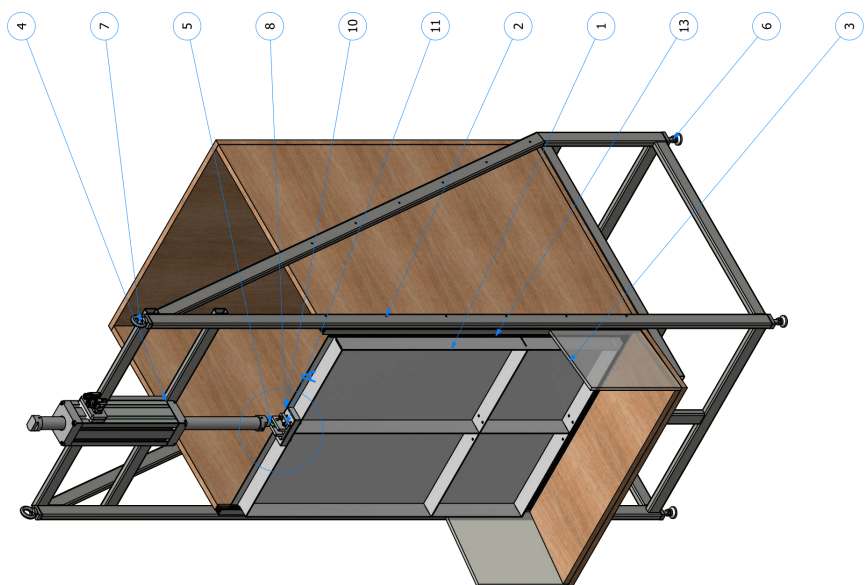
100;100;40										
wave #	Vpunt1	Vpunt2	Tpunt1	Tpunt2	v	t				
1	37	92	1215	112	411	97	411	337	1,90	2,40
2	19	70	1214	89	490	75	490	323	2,03	2,48
3	9	62	1205	82	509	68	509	318	1,93	2,50
4	45	20	1240	40	907	35	907	280	1,93	2,45
5	54	91	1225	110	793	103	793	349	1,99	2,46
6	10	115	1228	134	413	119	413	354	2,07	2,35
7	41	121	1226	141	814	135	814	382	1,91	2,47
8	52	13	1227	32	844	27	844	277	1,99	2,50
9	92	102	1238	121	435	106	435	355	1,95	2,49
10	42	55	1217	73	422	58	422	297	2,11	2,39
									1,98	2,45
									0,07	0,05
									3,53	2,11

100;100;50										
wave #	Vpunt1	Vpunt2	Tpunt1	Tpunt2	v	t				
1	137	78	1188	96	808	90	808	336	1,88	2,46
2	173	75	1212	91	541	80	541	321	2,09	2,41
3	189	125	1196	141	568	131	568	372	2,03	2,41
4	236	64	1205	79	411	67	411	305	2,08	2,38
5	213	136	1219	151	517	139	517	377	2,16	2,38
6	99	86	1224	103	566	92	566	335	2,13	2,43
7	159	47	1169	63	808	59	808	296	2,04	2,37
8	171	83	1179	99	505	86	505	329	2,03	2,43
9	192	31	1215	47	578	38	578	278	2,06	2,40
10	82	110	1200	128	520	117	520	355	2,00	2,38
									2,05	2,41
									0,08	0,03
									3,78	1,20

100;100;60										
wave #	Vpunt1	Vpunt2	Tpunt1	Tpunt2	v	t				
1	97	49	1245	68	771	61	771	297	1,95	2,36
2	125	58	1241	76	803	70	803	307	2,00	2,37
3	130	69	1224	86	754	79	754	316	2,08	2,37
4	132	37	1227	54	764	48	764	280	2,08	2,32
5	139	72	1203	89	782	83	782	318	2,02	2,35
6	161	82	1205	99	792	93	792	322	1,98	2,29
7	154	11	1224	28	756	24	756	262	2,03	2,38
8	211	68	1234	84	800	78	800	314	2,06	2,36
9	94	50	1207	67	763	61	763	296	2,11	2,35
10	96	88	1198	105	515	93	515	330	2,09	2,37
									2,04	2,35
									0,05	0,03
									2,58	1,17

Appendix C

Technical drawings WOS



A (1 : 2)

14	1	Bk. Stelschroef ISO4026 - M3 x 8	RVS A2-70	Factory nummer: 51240.030.008	
13	10	Laagcilinder Binnensteekant DIN7984 - M3 x 10	RVS A2-70	Factory nummer: 51040.030.010	
12	17	Laagcilinder Binnensteekant DIN7984 - M3 x 8	RVS A2-70	Factory nummer: 51040.030.008	
11	4	Binnensteekant DIN912 - M6 x 20	RVS A2-70	Factory nummer: 51050.060.020	
10	8	Binnensteekant DIN912 - M6 x 16	RVS A2-70	Factory nummer: 51050.060.016	
9	4	Binnensteekant DIN912 - M6 x 12	RVS A2-70	Factory nummer: 51050.060.012	
8	8	Sluifring 3rd ISO7093 - M6	RVS A2-70	Factory nummer: 51530.060.001	
7	2	Opglobout_gesmeed DIN580_A2_M10	RVS A2-70	Factory nummer: 51941.100.001	
6	4	Leveling_Pads_2259_NH_M10	Stainless Steel	Masfeller nummer: 65521.091	
5	1	Rod_ends_GT-R_DIN_12240-4_K_M10	Stainless Steel	Masfeller nummer: 63295808	
4	1	Linear actuator	Niobk: GD350MS-350-S		
3	1	Overtopping_Hout	GEL709-5004		
2	1	Overtopping_Frame	GEL709-5003		
1	1	Overtopping_Deur	GEL709-5002		
Stnr. Aant.		Benaming	Nummer	Material	Opmetingen
Gefabed		Tom Phillips	Overtopping_Simulator_Assembly		
Controle			Project		
Datum		26-10-2016	Overtopping simulator		
Status		Concept	Tekening nummer		
Material			GEL709-5001		
Aantal		1	Schaal		
			Eenheid		
			mm		
			1:10		
			Ra		
			Alle vlakken level		
			Ruwbled volgens NEN-EN ISO 1302:2002 en NEN-ISO 2768-mH		
			Functiebereik verarbeiden volgens de VwE		
			Blad nr.		
			1 / 1		
			Formaat		
			A3		



Appendix D

Stability research

D.1 Overview test series

In this appendix the table with results of the 49 tests of the stability research are presented.

Test number #	$H_s/\Delta dn$		Rows under waterline
	Stable	Failure	
R30C15.01	2,67		11
R30C15.02	3,03		11
R30C15.03	3,18		11
R30C15.04	3,33		11
R30C15.05	3,33		11
R30C15.06		3,64	11
R30C15.07		3,94	11
R30C15.08		4,24	11
R30C15.09		3,33	10
R30C15.10		3,64	10
R30C15.11		3,94	10
R30C15.12		4,24	10
R30C15.13		3,33	9
R30C15.14		3,64	9
R30C15.15		3,94	9
R30C15.16		4,24	9
R30C15.17	3,33		13
R30C15.18	3,64		13
R30C15.19	3,94		13
R30C15.20		4,24	13
R30C15.21	3,33		13
R30C15.22		3,94	13
R30C15.23	4,55		14
R30C15.24		5,00	14
R30C15.25	3,03		13
R30C15.26	3,33		13
R30C15.27	3,94		13
R30C15.28		4,24	13
R30C15.29		4,55	13
R30C15.30	3,03		16
R30C15.31	3,33		16
R30C15.32	3,94		16
R30C15.33	4,55		16
R30C15.34	4,24		15
R30C15.35		4,55	15
R30C15.36	4,24		15
R30C15.37	4,55		15
R30C15.38		4,85	15
R30C15.39	4,24		17
R30C15.40	4,55		17
R30C15.41	4,85		17
R30C15.42		5,00	17
R30C15.43		4,24	14
R30C15.44	3,18		14
R30C15.45	3,33		14
R30C15.46		3,64	14
R30C15.47		3,94	14
R30C15.48		4,24	14
R30C15.49		4,24	14

Table D.1: Overview of dimensionless stability parameters at which failure occurs

D.2 Failure overviews per test

More examples of failure that occurred during the 49 tests can be found below:



Figure D.1: 15 rows beneath water line

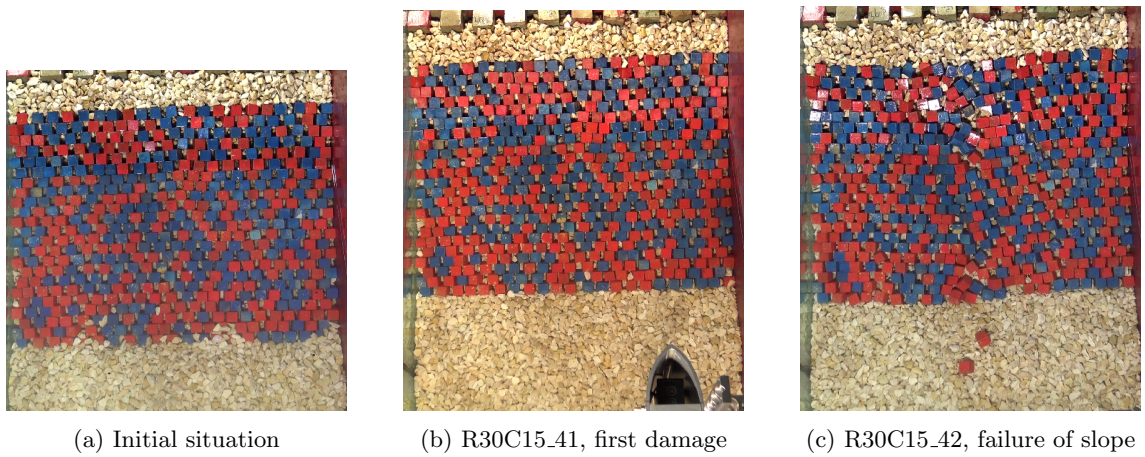


Figure D.2: 17 rows beneath waterline

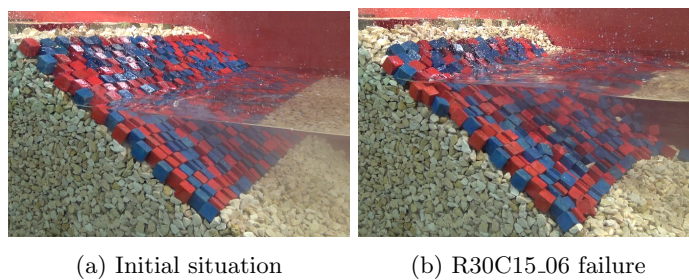
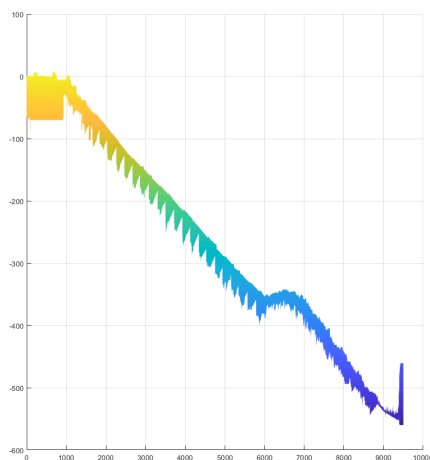
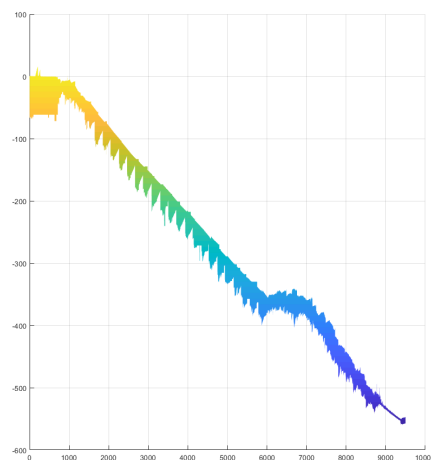


Figure D.3: 11 rows beneath the waterline

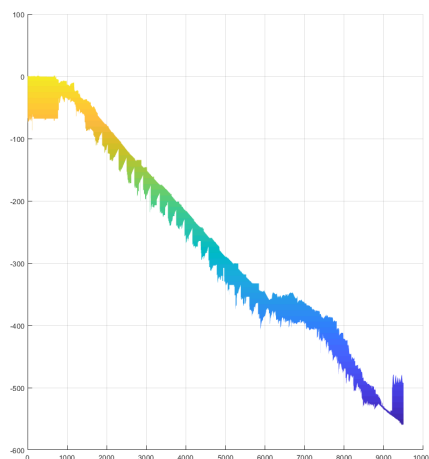
D.3 Transect side-views



(a) Initial

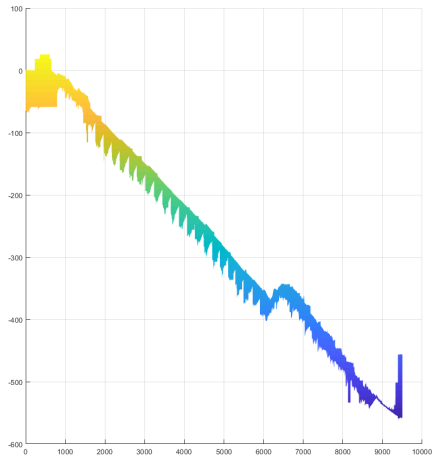


(b) R30C15_34

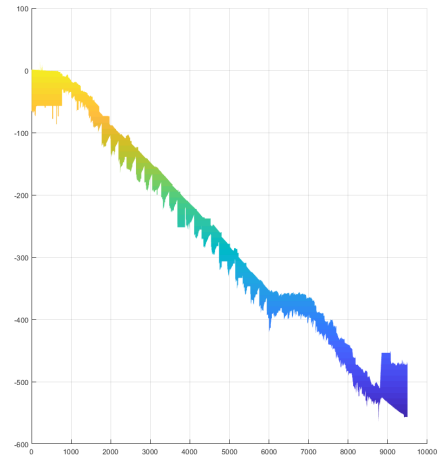


(c) R30C15_35, failure

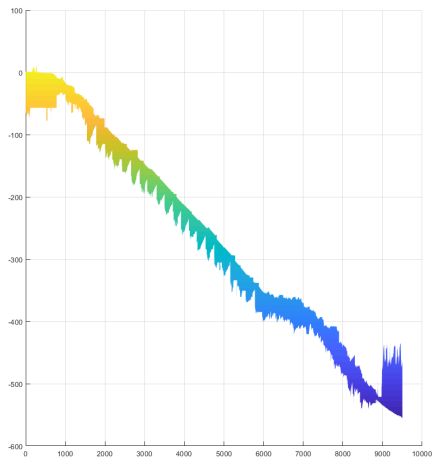
Figure D.4: Test R30C15_34 and 35. Configuration with 15 rows beneath the water line



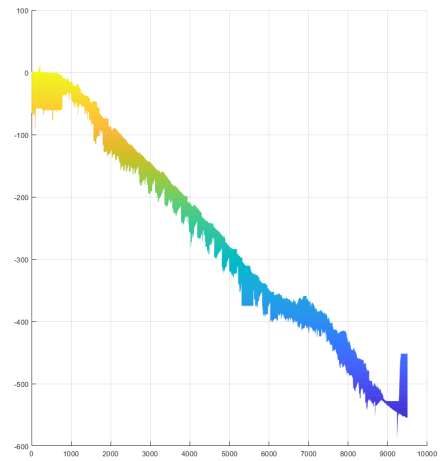
(a) Initial



(b) R30C15_36



(c) R30C15_37



(d) R30C15_38, failure

Figure D.5: Test R30C15_36, 37 and 38. Configuration with 15 rows beneath the water line

Appendix E

Matlab codes

E.1 Wave gauge meters

```
close all;
clear all;
clc;

xmin          = 2900;
xmax          = xmin + 2700;

%% data GHM's in het reservoir

file          = ('50;100;40test_7.asc');
delimiter     = ',';
R             = 7;
C             = 1;
data          = dlmread(file,delimiter,R,C);
h1            = (data(:,5) + data(:,6)) / 200;
[B1,A1]       = butter(3,0.01);
volume        = (h1(xmin)-h1(xmax))*0.68*0.69*1000;

%% specific discharge of water leaving reservoir

dh1_dt        = diff(h1) * -1000;
dh1_filter_dt = diff(h1_filter) * -1000;
depth         = 0.69;
q             = (depth*dh1_filter_dt);
qmax          = max(q(xmin:xmax));
Liter         = trapz(q(xmin:xmax))*0.69;

%% laagdikte meting over de kruin, golfhoogtemeter het dichtsbij de valve

h2            = ((data(1:(end-1),4) + 3.35) / 100);
[B2,A2]       = butter(2,0.009);
h2_filter     = filter(B2,A2,h2);
hmax          = max(h2_filter(xmin+500:xmax));

%% velocity of wave front

u             = q./h2_filter;
umax          = max(u(xmin+300:xmax));

%% figuren maken
```

```

figure;

subplot(511);
plot(h1, '-r');
hold on
plot(h1_filter);
xlabel('Time [ms]');
xlim([xmin xmax]);
ylabel('h1 [m]');
ylim([0 0.8]);
legend('Unfiltered', 'Filtered');
title('Waterlevel in reservoir over time');

subplot(512);

plot(dh1_dt, '-r');
hold on
plot(dh1_filter_dt);
xlabel('Time [ms]');
xlim([xmin xmax]);
ylabel('dh1/dt');
ylim([0 0.6]);
legend('unfiltered', 'filtered');
title('Velocity of water leaving reservoir over time');

subplot(513);

plot(q);
xlabel('Time [ms]');
xlim([xmin xmax]);
ylabel('q [m^2/s/m]');
ylim([0 0.3]);
title('Specific discharge of waterfront');

subplot(514);

plot(h2, '-r');
hold on
plot(h2_filter);
xlabel('Time [ms]');
xlim([xmin xmax]);
ylabel('h2 [m]');
ylim([0 0.12]);
legend('unfiltered', 'filtered');
title('Waterlayerthickness on crest over time');

subplot(515);

plot(u);
xlabel('Time [ms]');
xlim([xmin xmax]);
ylabel('u [m/s]');
ylim([0 6]);
title('Velocity of wave front at Wavegauge');

%% Maximale waarden printen

file

```

```

fprintf('qmax: %.3f m^2/s \n', qmax);
fprintf('hmax: %.3f m \n', hmax);
fprintf('umax: %.3f m/s \n', umax);
fprintf('Volume of overtopping wave: %.2f liters \n', Liter);
fprintf('Volume of water leaving res: %.2f liters \n', volume);

```

E.2 Framestack plotting

```

close all; clear all; clc;
%%

obj = VideoReader('100;100;30test_10.mp4');

list_of_frames = [];

for k = 1 : 400 %fill in the appropriate number, all movies used are 400 frames (4 sec)
    this_frame = readFrame(obj);
    list_of_frames = [list_of_frames;this_frame(256,3:1266,:)];
end

sizes = size(list_of_frames)
yl = zeros(sizes(1),1)+1;

imagesc(list_of_frames);
xticklabels = 0:5:40;
xticks = linspace(1, size(list_of_frames, 2), numel(xticklabels));
set(gca, 'XTick', xticks, 'XTickLabel', xticklabels)
xlabel('Crest width [cm]')
yticklabels = 0:0.1:4;
yticks = linspace(1,size(list_of_frames, 1), numel(yticklabels));
set(gca, 'YTick', yticks, 'YTickLabel', yticklabels)
ylabel('Time [s]')

```

E.3 3d profile plotter

```

close all;
clear all;
clc;

transects      = 47;
d               = 45; % allowd error margin
l_tr           = 9500;

%% Import je initial data

for j=1:transects;
    file        = (['test023_',num2str(j),'.asc']);
    delimiter    = ','; %Delimiter used in the asc files between the columns
    R           = 7;    %Start at R+1
    C           = 0;    %Start at column C+1
    data        = dlmread(file,delimiter,R,C);
    if length(data)~= l_tr;
        error('Een profiel heeft niet de goeie lengte');
    end
end

```

```

        if data(1,3) == 10
            error('Meetfout aan begin van transect 1');
        end
        P1(:,j)      = (data(:,3)*-1)*63.512+48.028;
    end;

F1 = P1; % F is filtered data

for i = 1 :(size(F1,1) -1);
    for j = 1:size(F1,2)
        if abs(F1(i+1,j)-F1(i,j)) > d;
            F1(i+1,j) = F1(i,j);
        end
    end
end

%% Import je profielen na de schade

for j=1:transects;
    file      = (['test024_',num2str(j),'.asc']);
    delimiter = ',';
    R          = 7; %Start at R+1
    C          = 0; %Start at column C+1
    data       = dlmread(file,delimiter,R,C);
    if length(data)~= l_tr;
        error('Transect in data of insufficient length');
    end
    if data(1,3) == 10
        error('Error at start of transect');
    end
    P2(:,j)    = (data(:,3)*-1)*63.512+48.028; %P is je rauwe data
end;

F2 = P2; % F is filtered data.

for i = 1 :(size(F2,1) -1);
    for j = 1:size(F2,2)
        if abs(F2(i+1,j)-F2(i,j)) > d;
            F2(i+1,j) = F2(i,j);
        end
    end
end

%% Verschil

D = (F1 - F2)*-1;

[B,A]      = butter(3,0.01);          %Butterworth digital filter design. 3rd order lowpass digi
D_filter   = filter(B,A,D);

%% figuren maken
figure;
surf(F1);
xlim([1 size(F1,2)])
view([118 32]);
shading('interp');

figure;

```

```

surf(F2);
xlim([1 size(F2,2)])
view([118 32]);
shading('interp');

figure;
surf(D);
shading('interp');
view([-180 90]);
xlabel('Crest width [cm]');
xlim([1 size(D,2)])
ylabel('Cross sectional length [cm]');
title('Difference of profile before and after storm');

subplot(411);
plot(D(:,11));
hold on
plot(F1(:,11));
plot(F2(:,11));
title('Transect #11');
legend('difference','intial','after wave');

subplot(412);
plot(D(:,17));
hold on
plot(F1(:,17));
plot(F2(:,17));
title('Transect #17');

subplot(413);
plot(D(:,32));
hold on
plot(F1(:,32));
plot(F2(:,32));
title('Transect #32');

subplot(414);
plot(D(:,44));
hold on
plot(F1(:,44));
plot(F2(:,44));
title('Transect #44');

```

Appendix F

Specifications of Linear Motor



Motor Specification

GD350ES		
Peak Force ⁽¹⁾	N	1161
Peak Force @ C/s increase	N	--
Continuous stall force (passive cooling)	N	259,7
Max. velocity ⁽¹⁾⁽³⁾	m/s	8,28
Max. acceleration ⁽²⁾⁽³⁾	m/s ²	310,5
Continuous stall force (with heatsink plate)	N	--
Continuous stall force (fan cooling)	N	--
Continuous stall force (liquid cooling) ⁽⁷⁾	N	493,4

Electrical Specification

GD350ES		
Nominal DC-Link Voltage	V _{dc}	560
Maximum DC-Link Voltage	V _{dc}	610
Peak current ⁽⁶⁾	A _{pk}	23,4
Peak current ⁽⁶⁾	A _{rms}	16,55
Continuous stall current (passive cooling)	A _{rms}	3,7
Continuous stall current (with heatsink plate)	A _{rms}	--
Continuous stall current (fan cooling)	A _{rms}	--
Continuous stall current (liquid cooling) ⁽⁷⁾	A _{rms}	7,03
Force constant	N/A _{rms}	70,18
Back EMF constant (ph-ph) ⁽⁴⁾	V _{pk} /(m/s)	57,30
Back EMF constant (ph-ph)	V _{rms} /(m/s)	40,52
Resistance @ 25 C (ph-ph) ⁽⁴⁾	Ohm	5,03
Resistance @ 135 C (ph-ph) ⁽⁴⁾	Ohm	7,2
Inductance (ph-ph) ⁽⁴⁾	mH	5,68
Electrical time constant	ms	1,129
Motor constant	N/?W	0,000

Thermal Specification IC40

GD350ES		
Max. winding temperature	C	180
Max. Duration with peak current	s	1
Max. Power dissipation ⁽⁵⁾	W	147,94
Thermal resistance (case-ambient)	C/W	0,42
Thermal resistance (winding-case)	C/W	0,31
Thermal resistance (winding-ambient) ⁽⁵⁾	C/W	0,73
Thermal time constant ⁽⁵⁾	s	2373

Mechanical Specification

GD350ES		
Stator length	mm	502
Stator diameter	mm	88x88
Stator mass	kg	3,45
Slider length (min/max)	mm	536 / 2302
Slider diameter	mm	35
Slider mass	kg/m	7,1
Magnetic Period (Polar pitch)	mm	60

Encoder Specification

GD350ES		
Encoder Type		SIN/COS 1 Vpp
Encoder power supply		5 V
Resolution		1 sine period per polar pitch

(1) Based on triangular move over 360mm stroke without payload and without taking in account voltage limits - (2) Based on a 30 mm stroke, without payload - (3) The specifications and data may be subject to change depending of the load (4) Manufacturing data - 10% - (5) In compliance with IEC 60034-1 (6) Service type S3, duty cycle 5% - (7) Estimated value